# C-H BOND ACTIVATION OF HYDROCARBONS BY A TUNGSTEN ALLENE COMPLEX

by

STEPHEN H. K. NG

B.Sc., The University of British Columbia, 2000

A THESIS SUBMITTED IN PARTIAL FULFILMENT OF

THE REQUIREMENTS FOR THE DEGREE OF

MASTER OF SCIENCE

in

THE FACULTY OF GRADUATE STUDIES

(Department of Chemistry)

We accept this thesis as conforming

to the required standard

THE UNIVERSITY OF BRITISH COLUMBIA

July 2002

Department of Chemistry

The University of British Columbia
Vancouver, Canada

Date 29 July 2002

## Abstract

Gentle thermolysis of the 18e alkyl-allyl complex, $Cp^*W(NO)(CH_2CMe_3)(\eta^3$-1,1-$Me_2C_3H_3$) (**1.1**), generates a reactive 16e allene intermediate, $Cp^*W(NO)(\eta^2$-$H_2C{=}C{=}CMe_2$) (**A**), by a first-order process with concomitant evolution of neopentane via hydrogen abstraction from the dimethylallyl ligand. Intermediate **A** has been structurally characterized as its $PMe_3$ adduct, and is capable of effecting both single and multiple intermolecular C-H bond activations of hydrocarbon solvents to form alkyl-allyl and allyl-hydrido complexes.

The products of reactions of **A** with methyl-substituted arenes (i.e. $sp^2$ C-H vs $sp^3$ C-H) indicate an inherent preference for the activation of stronger arene C-H bonds, however steric effects are also relevant as indicated by the exclusive formation of benzylic C-H activation products in mesitylene.

Thermolyses of **1.1** in alkane solvents generate products resulting from three successive C-H bond-activation reactions. Preliminary studies suggest that allyl-hydrido complexes are formed along with an organic product; for example, in cyclohexane, 1,1-dimethylpropylcyclohexane results from coupling of a solvent molecule and a fragment derived from the precursor dimethylallyl ligand. The allyl-hydrido complexes have potential synthetic utility, since studies conducted on structurally and electronically related CpMo complexes show that they may be capable of ultimately producing homoallylic alcohols.

## Table of Contents

---

## List of Tables

## List of Figures

## List of Abbreviations

The following abbreviations are employed in this Thesis.

| | |
|---|---|
| ° | degree (of angle or temperature) |
| α | the position once removed from a reference point (i.e. a metal center) |
| I(t) | integral at time t |
| I(0) | initial integral |
| Å | angstrom, $10^{-10}$ m |
| anal. | analysis |
| atm | atmosphere(s) |
| β | the position twice removed from a reference point |
| br | broad (spectral) |
| $^t$Bu | tert-butyl |
| Bzl | benzyl, $CH_2C_6H_5$ |
| °C | degrees Celsius |
| $^{13}$C | carbon-13 |
| $^{13}C\{^1H\}$ | proton-decoupled $^{13}$C |
| cal | calorie |
| calcd. | calculated |
| cm | centimetre(s) |
| $cm^{-1}$ | wavenumbers |
| COSY | correlation spectroscopy |
| Cp | $\eta^5$-$C_5H_5$, cyclopentadienyl |
| Cp* | $\eta^5$-$C_5Me_5$, pentamethyl Cp |
| Cp' | Cp or Cp* |
| δ | chemical shift in ppm |
| d | doublet or day(s) |
| D, *d* | $^2$H |
| Δ | heat |
| e | electron |
| ee | enantiomeric excess |
| η | hapto, denotes ligand hapticity |
| $Et_2O$ | diethyl ether |
| g | gram |
| γ | the position thrice removed from a reference point |
| h | hour(s) |
| $^1$H | proton |
| $^2$H | deuterium |
| $^2H\{^1H\}$ | proton-decoupled $^2$H |
| HMBC | heteronuclear multiple bond coherence |
| HMQC | heteronuclear multiple quantum coherence |
| *h*ν | irradiation |
| Hz | hertz ($s^{-1}$) |
| Irrad. | irradiate |
| IR | infrared |
| *J* | coupling constant |
| $^nJ_{AB}$ | n-bond J between atoms A and B |
| $k_{obs}$ | observed rate constant |
| kcal | kilocalorie(s) |

| | |
|---|---|
| K | degrees Kelvin |
| L | litre(s) |
| LREI | low resolution electron impact |
| LUMO | lowest unoccupied molecular orbital |
| m | multiplet |
| *m* | meta |
| *m/z* | mass-to-charge ratio |
| Me | methyl, $CH_3$ |
| Mes | mesityl, $CH_2C_6H_3$-3,5-$Me_2$ |
| mg | milligram(s) |
| mL | millilitre(s) |
| mmol | millimole(s) |
| mol | mole(s) |
| MS | mass spectrum |
| Mxyl | 3-Me-benzyl, $CH_2C_6H_4$-3-Me |
| NMR | nuclear magnetic resonance |
| NOE | nuclear Overhauser effect |
| Npt | neopentyl, $CH_2CMe_3$ |
| ν | stretching frequency |
| *o* | ortho |
| obs | obscured (spectral) |
| ORTEP | Oak Ridge Thermal Ellipsoid Plot |
| Oxl | 2-Me-benzyl, $CH_2C_6H_4$-2-Me |
| $^{31}P$ | phosphorous-31 |
| $^{31}P\{^1H\}$ | proton-decoupled $^{31}P$ |
| $P^+$ | parent molecular ion |
| *p* | para |
| Ph | phenyl, $C_6H_5$ |
| ppm | parts per million |
| Pxyl | 4-Me-benzyl, $CH_2C_6H_4$-4-Me |
| R | hydrocarbyl ligand |
| $R^2$, R1 | residuals (statistics) |
| s | singlet, strong (spectral) or second(s) |
| selNOE | selective NOE |
| t | triplet or time |
| $t_{1/2}$ | half-life |
| T | temperature |
| TLC | thin-layer chromatography |
| THF | tetrahydrofuran |
| TMS | tetramethylsilane |
| Tol | tolyl, $C_6H_4$-Me |
| w | weak (spectral) |
| Xyl | dimethyl aryl ligand, $C_6H_3$-$Me_2$ |

## Acknowledgements

First and most importantly, I would like to thank my family who have supported me during my various endeavours over the past 25 years. Mom and Dad, thanks so much for being there for me when I needed you, and kudos to you two for being such great parents and keeping me out of trouble. To my big brother Dave, thanks for being my initial musical influence and not listening to garbage. My little sister Emily, thanks for allowing me to bug you to no end. Kate, thanks for keeping me amused with your foosball talents. To the newest addition to my family, my dear little Hannah, I know you can't read this right now, and you probably will never bother reading this Thesis, but thank you for brightening my days over the past 10 months or so.

To the Big-Kahuna, a.k.a. Peter, my deepest thanks for taking me into your research group and letting me do my own thing around the lab. It has been a most enjoyable and satisfying experience. I appreciate the time you took to sit and chat with me when I had questions, worries, beefs and stories and I thank you for all your help and advice.

Trevor, where do I start? You've been an amazing mentor, musical companion, lab partner and friend. I cannot begin to tell you how much fun you've made this whole research thing. Coffee breaks, hockey games, poking fun at people who have no business being made fun of... the list goes on. It has all been a huge part of my existence for the past two years of my life, and consequently I am greatly indebted to you.

Big Swede, a.k.a Dr. Pamplin, thanks for all the help and advice you've given me during the final stretch of my degree. You have also been a vital part of my lab-sanity. Big thanks to you for ensuring that Trevor won nothing at golf.

I must also express my gratitude to former members of the Legzdins group, namely Brett Sharp and Craig Adams, who showed me the ropes around the lab and addressed my teething-pain questions and concerns. Dr. Adams, thank you SO much for handing this project to me on a silver platter and acting as a consultant throughout the past two years. More thanks go out to you for putting up with me as a desk partner during those first eight months.

Nick Burlinson, Liane Darge, Marietta Austria, Peter Borda, Brian Patrick, Marshall Lapawa, Bob Bau, Natalie Thompson and Judy Wrinskelle also deserve recognition for their invaluable assistance throughout the duration of this study.

Last but not least, my thanks go out to Dennis Lefebvre who has given me a ride to and from the lab everyday in "l'autobus" and for being a constant source of laughter.

*"Life moves pretty fast. If you don't*

*stop and look around once in a while,*

*you could miss it."*

Ferris Bueller

# Chapter 1

## *Homogenous Intermolecular C-H Bond-Activation Reactions of Hydrocarbons by Organometallic Species*

---



---

## 1.1 Introduction

The results of investigations performed on the thermal C-H bond-activating chemistry of a novel system is presented in this Thesis. To gain a better understanding of the significance of this discovery, it is essential to commence with a brief discussion regarding organometallic chemistry and the sub-field of C-H bond activation by transition metal complexes.

### 1.1.1 Synopsis of Organometallic C-H Bond-Activation Chemistry

Organometallic chemistry, in its most succinct definition, encompasses the study of complexes that contain at least one direct bond between a metal and a carbon atom. The inception of this scientific domain[1] in 1760 with the preparation of "Cadet's fuming liquid"[2] has led to the development of a wide variety of new compounds, many of which play key roles in commercially important processes such as the polymerization of alkenes into polyethylene and polypropylene. The catalytic component of this reaction, active at 25 $^{o}$C and 1 atm, is in stark contrast to the conditions required for thermal polymerization (200 $^{o}$C and 1000 atm) and is just one example of the benefits reaped through the study of organometallics.[3] That this dominion is effectively the link between the two broad fields of organic and inorganic chemistry serves as a means of developing novel methods for tackling age-old problems. One such quandary is the activation of C-H bonds of hydrocarbons in a selective manner, followed by functionalization in an overall effort to

produce valuable materials starting from widely available and relatively inexpensive hydrocarbon feedstocks.[4] The former transformation is the subject of interest in this Thesis and involves the scission of a carbon-hydrogen (C-H) bond of a hydrocarbon substrate by an organometallic fragment.

One of the ultimate goals is the activation of methane C-H bonds due to its large constituency in natural gas.[5] Being the most simple, stable hydrocarbon subunit, it could potentially be used as a building block to generate larger, more commercially useful products via breakage of its C-H links. Thus, one impetus for investigating the area of C-H bond activation is the notoriously stable behaviour exhibited by alkanes, manifested by the low polarity of the C-H bond and the high bond energies of 90 - 110 kcal/mol.[6] Alkanes are not, however, completely unreactive as activation in the absence of metallic fragments has been known for quite some time. Thermal and photolytic reactions that require large amounts of energy are capable of cleaving C-H bonds, but do so in a typically non-selective manner, usually via free radical mechanisms.[7]

Hence, there continues to be active research conducted in this field towards the discovery and evolution of metal-based systems that effect C-H bond activation of hydrocarbon substrates selectively and under relatively mild conditions.

### 1.1.2 Homogenous Intermolecular C-H Activations by Organometallic Complexes

Metal-mediated C-H bond activation using soluble organometallic compounds ordinarily occurs in one of four fashions, namely oxidative addition, σ-bond metathesis, metalloradical activation, and 1,2-addition.[8]

#### 1.1.2.1 Oxidative Addition

Investigations involving the direct stoichiometric interaction of metal centers with C-H bonds provided the first essential pieces of data regarding the C-H activation process. Oxidative addition, the formal two-electron oxidation of the electronically unsaturated metal center via addition of R-H, leads to the formation of alkyl-hydrido complexes (eq. 1.1).

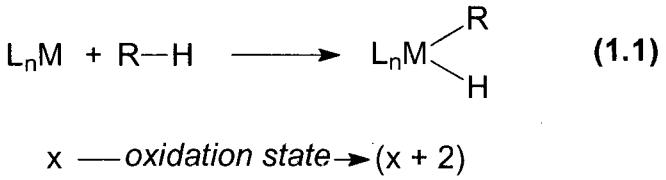


As such, the metal center must fit certain criteria in order to be a viable host for oxidative addition. These criteria basically encompass the ability of the metal center to possess a d-electron configuration such that an (n+2) oxidation state exists and is accessible to accommodate the addition of 2e from the hydrocarbon C-H scission product.[3] Typically, as a result of its coordinative unsaturation, the reactive intermediate

must be formed *in situ* via decomposition of a precursor species. One of the first examples of an organometallic species capable of effecting homogenous intermolecular oxidative addition to single C-H bonds involves the generation of the reactive intermediate, $Cp^*Ir^{I}(PMe_3)$ from its precursor $Cp^*Ir^{III}(PMe_3)H_2$ which is then able to activate C-H bonds of benzene, cyclohexane and neopentane (e.g. eq. 1.2).[9]

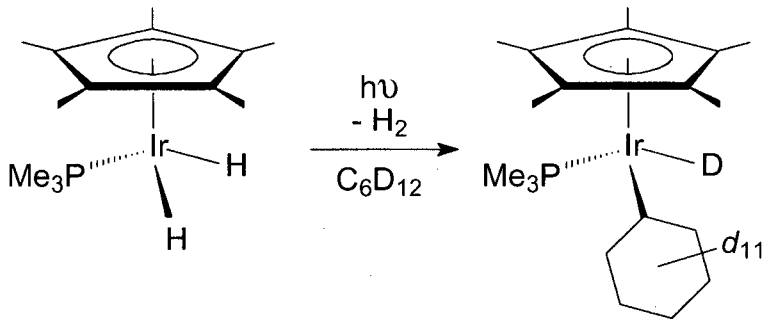


**(1.2)**

### 1.1.2.2 Sigma-Bond Metathesis

Another common mechanism of C-H activation involves the exchange of alkyl groups R and R' of M-R and R'-H (Scheme 1.1). The exchange process typically occurs at formally $d^0$ or $f^n d^0$ metal centers,[10-13] suggesting that an oxidative-addition type mechanism is not feasible because of the absence of an accessible (n+2) oxidation state.[14]

**Scheme 1.1**

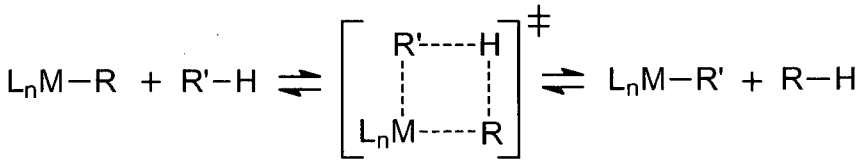

Mechanistic data[15] collected for such systems provide evidence for a 2 + 2 σ-bond metathesis pathway containing a four-center transition state (Scheme 1.1). The large primary kinetic isotope effects ($k_H/k_D$ ~ 3-6) support scission of the C-H linkage in the transition state. Additionally, kinetic studies showing first-order dependence on the concentrations of both metal complex and alkane substrate and negative entropies of activation are indicative of an associative mechanism and a highly ordered transition state.

Analogous to Scheme 1.1, the metathesis of a metal-hydride and an alkane to reversibly yield the corresponding metal-alkyl and dihydrogen gas has also been established (e.g. eq. 1.3).[16,17]

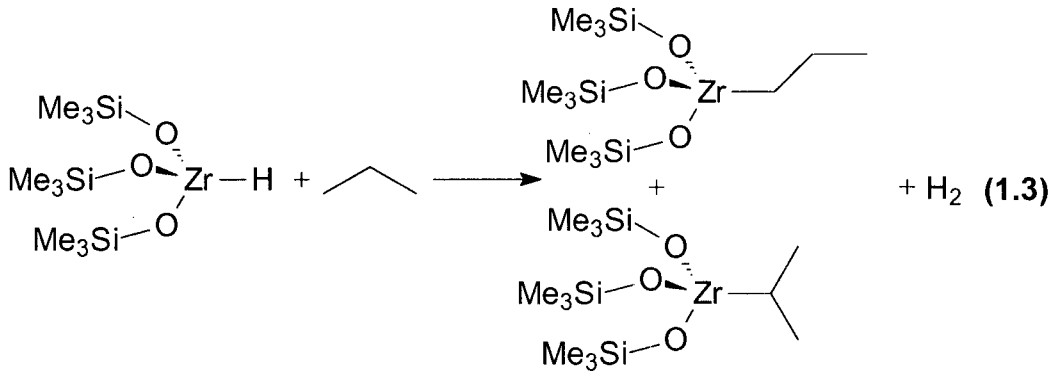


**(1.3)**

### 1.1.2.3 Metalloradical Activation

The exclusive activation of methane in benzene by paramagnetic substituted porphyrin Rh (II) complexes yield equimolar amounts of Rh-$CH_3$ and Rh-H species.[18,19] Mechanistic studies conducted on (tetramesitylporphyrinato)rhodium(II) monomer,

(TMP)Rh· and (tetraxylylporphyrinato)rhodium(II) dimer, $[(TXP)Rh]_2$ provide evidence for a transition state involving a four-centered linear complex (Scheme 1.2).

**Scheme 1.2**

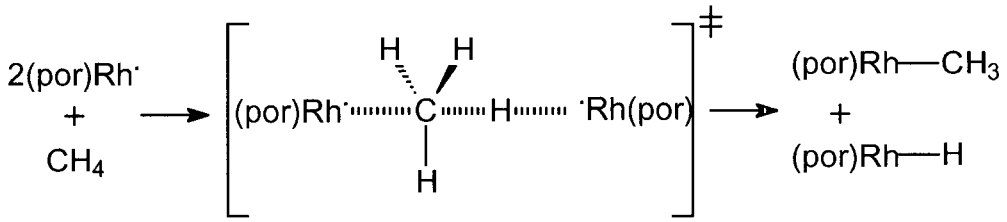


(por) = (TMP), (TXP)

### 1.1.2.4 1,2-Addition

Until quite recently, the identification of metal-alkylidenes that exhibit intermolecular C-H activation remained elusive.[14] The proposed pathway involves the addition of an alkane C-H bond across the metal-carbon double bond. The microscopic reverse reaction, the α-hydrogen elimination of hydrocarbon, has been well documented,[20] as have many examples of intramolecular C-H activation.[15,21-23] At present there are four reported systems that effect intermolecular C-H bond activation via generation of transient reactive alkylidene complexes from thermal decomposition of precursor bis(alkyl) species and one of these is given as an example in Scheme 1.3.[24-27]

**Scheme 1.3**

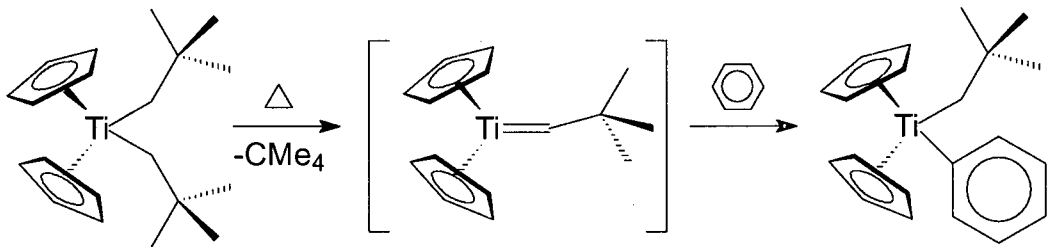


This method of C-H activation also includes the addition of a hydrocarbon C-H linkage across a metal-nitrogen[28-31] double bond resulting in the formation of a new metal-carbon bond (Scheme 1.4).

**Scheme 1.4**

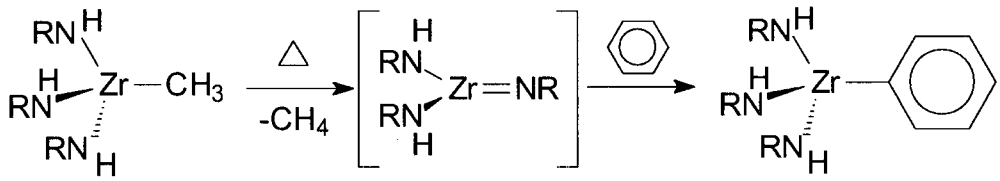


R = $^{t}Bu_3$-Si

## 1.2 The Legzdins C-H Bond-Activating Family of Compounds

### 1.2.1 Tungsten Acetylene System

The alkyl-vinyl complex, Cp*W(NO)(CPh=$CH_2$)($CH_2SiMe_3$), has been thoroughly studied and is capable of effecting dual C-H bond activation of alkane substrates under mild conditions (45 °C, 48 h) to yield metallocyclic-allyl complexes as a result of coupling between the vinyl ligand and the activated substrate (e.g. eq. 1.4).[32]

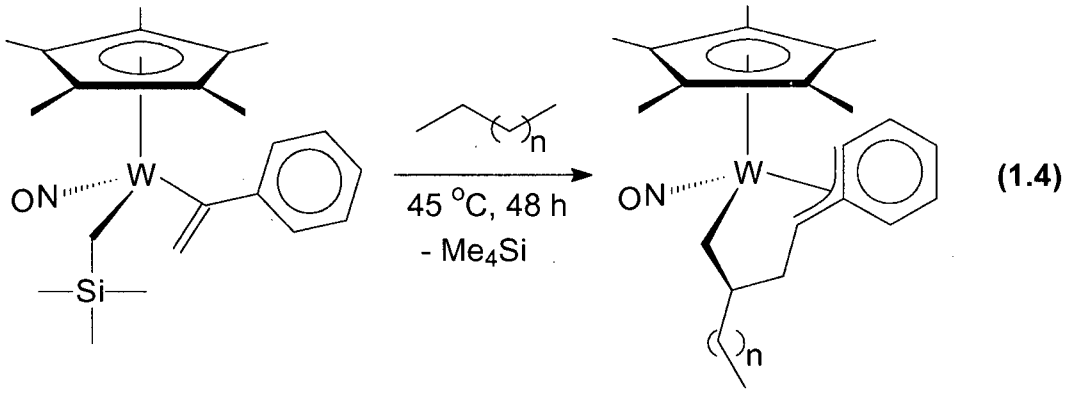


**(1.4)**

Deuterium labelling studies in benzene-$d_6$ yield the C-D activated phenyl-vinyl analog with deuterium incorporation at the β-position of the alkenyl ligand. This result implies the transient existence of a $\eta^2$-acetylene complex that is responsible for the C-H activating properties of the precursor alkyl-vinyl species. Further evidence for the generation of an intermediate acetylene is gained from the thermal reaction of Cp*W(NO)(CPh=$CH_2$)($CH_2SiMe_3$) in ethylacetate (Scheme 1.5).[33] Attempts to trap the proposed acetylene intermediate with trimethylphosphine have been unsuccessful.

**Scheme 1.5**

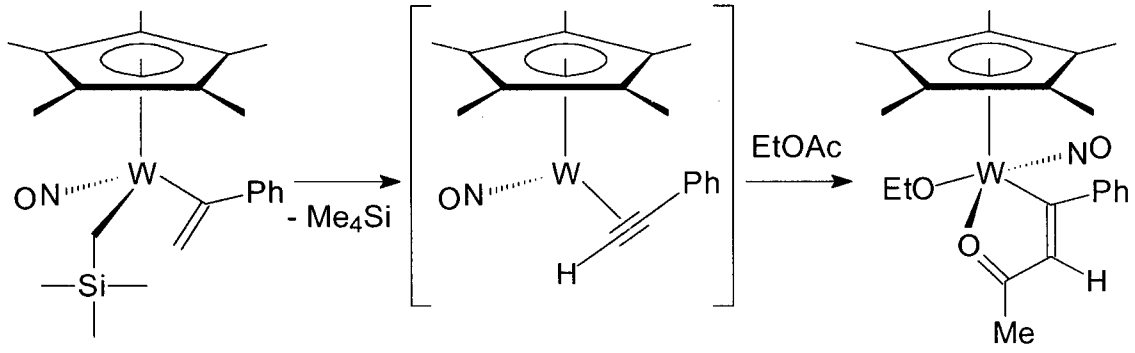


Mechanistic and kinetic studies show that the generation of the purported acetylene intermediate is rate-determining and that it is formed by elimination of tetramethylsilane from the precursor alkyl-vinyl complex. The reactive intermediate generated *in situ* is then capable of effecting C-H bond activations of methyl-substituted arenes to form mixtures of benzyl- and aryl-vinyl organometallic compounds.

### 1.2.2 Tungsten Alkylidene Systems

In 1997, members of the Legzdins research group reported the formation of a reactive neopentylidene species, Cp*W(NO)(=CHCMe$_3$), upon thermal decomposition of Cp*W(NO)(CH$_2$CMe$_3$)$_2$ under moderate conditions (70 °C, 40-48 h). The generation of the alkylidene species *in situ* leads to C-H activation of arene and alkane substrates (Scheme 1.6).[27]

**Scheme 1.6**

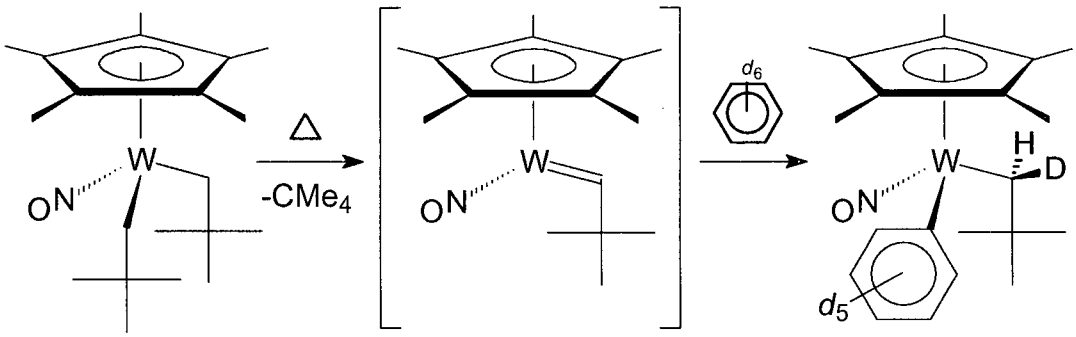


Deuterium labelling studies show exclusive incorporation of deuterium into the synclinal position relative to the newly formed M-C(aryl) linkage. This stereoselectivity is consistent with a 1,2-addition mechanism across the M=C bond of a reactive alkylidene intermediate. Moreover, thermolysis of the precursor bis(neopentyl) species in neat $PMe_3$ yields the base-stabilized adduct of the neopentilydene complex, namely $Cp^*W(NO)(PMe_3)(=CHCMe_3)$. Mechanistic studies show that the bis(alkyl) complex decomposes and eliminates neopentane in a first-order process with a rate constant of $4.6(1) \times 10^{-5}\ s^{-1}$ at 72 °C.[34]

Interestingly, the thermolysis of $Cp^*W(NO)(CH_2CMe_3)_2$ in methyl substituted arenes affords more than one product.[34,35] The formation of benzylic C-H activated products can subsequently eliminate neopentane to form a reactive benzylidene species, which has also been shown to activate C-H bonds (Scheme 1.7).

**Scheme 1.7**

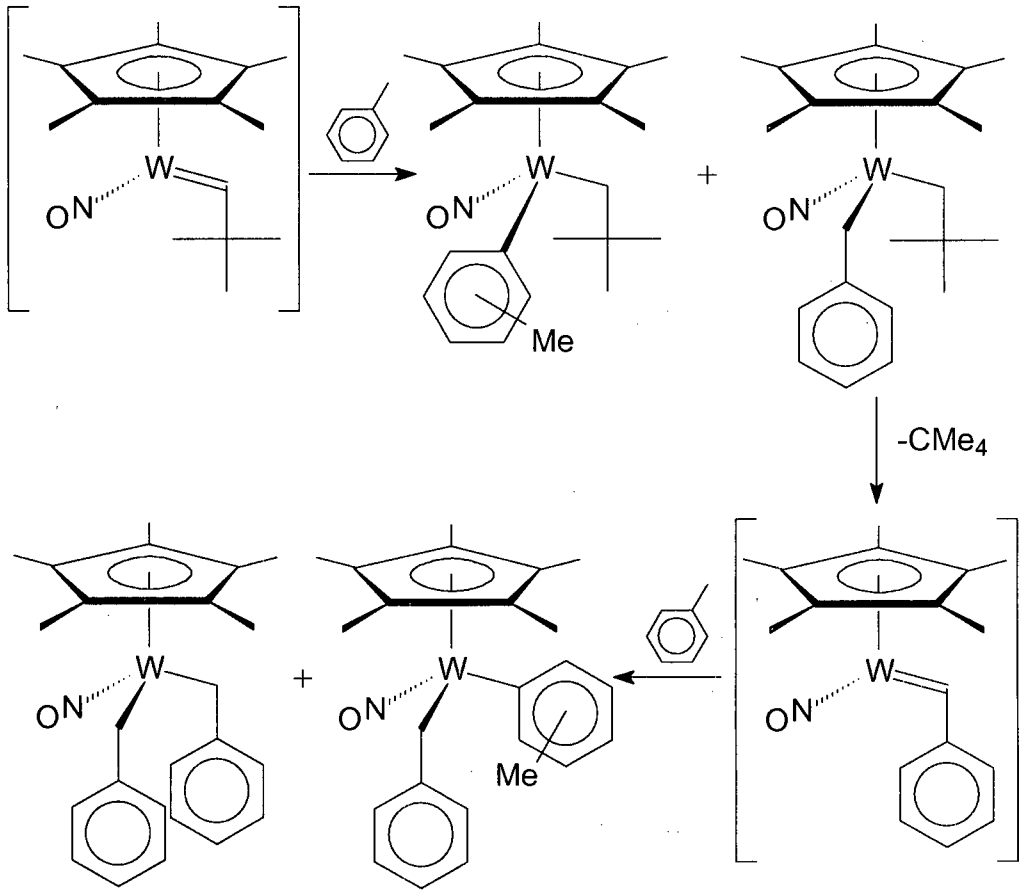


Surprisingly, the thermolysis of Cp*W(NO)($CH_2CMe_3$)$_2$ in cyclohexane in the presence of excess $PMe_3$ yields two products, the aforementioned base-stabilized neopentylidene complex, and a phosphine-trapped cyclohexene adduct (eq. 1.5).[27] The formation of the latter complex indicates the sequential activation of two C-H bonds of cyclohexane.

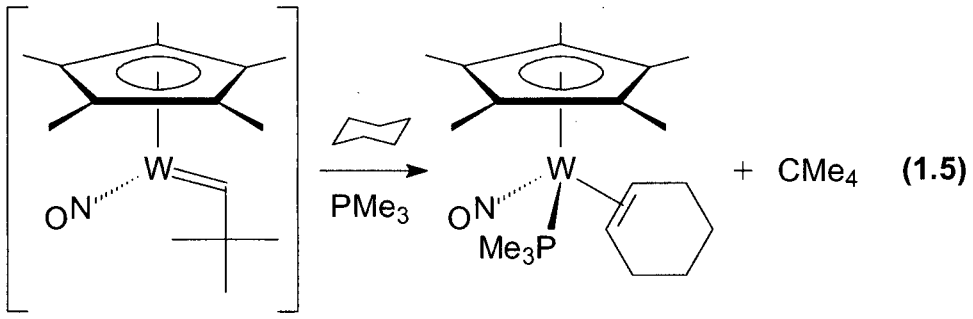


(1.5)

### 1.2.2 Molybdenum Alkylidene and Benzyne Systems

Most recently, other members of the Legzdins group have reported the preparation of the molybdenum congener of the tungsten alkylidene species that is capable of effecting C-H activations of benzene and tetramethylsilane at room-temperature in an analogous fashion.[36] Remarkably, the thermolysis of $Cp^*Mo(NO)(CH_2CMe_3)_2$ in benzene yields not only the anticipated neopentyl-phenyl species, but also a bis(phenyl) complex (eq. 1.6).

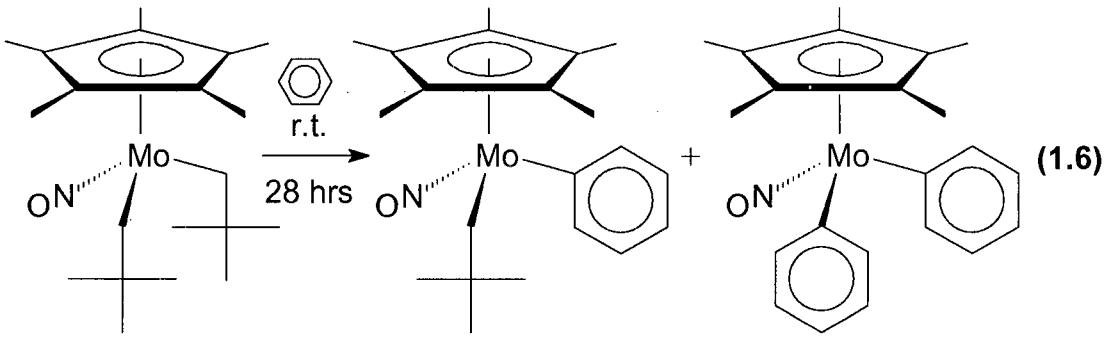


(1.6)

Trapping experiments utilizing pyridine generate two organometallic species, namely the pyridine adducts $Cp^*Mo(NO)(NC_5H_5)(=CHCMe_3)$, and $Cp^*Mo(NO)(NC_5H_5)(C_6H_4)$ (eq. 1.7).

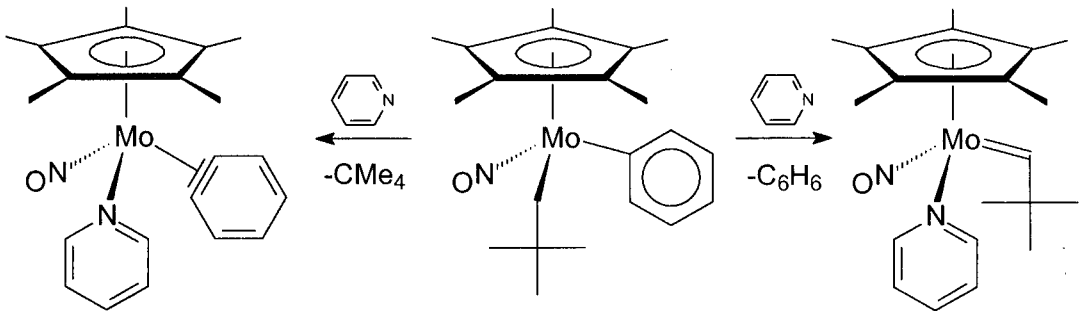


(1.7)

## 1.3 The Idea Behind Cp*W(NO)($CH_2CMe_3$)($\eta^3$-1,1-$Me_2C_3H_3$) (1.1)

During the course of studies conducted on the reactivity of the tungsten neopentylidene system, an interesting result arose from one of the experiments. The thermolysis of Cp*W(NO)($CH_2CMe_3$)$_2$ in 2-methyl-2-butene results in the formation of a number of products as an exclusive result of C-H activation *and* the generation of a metallocyclic species comprised of two coupled substrate molecules, whose identity has been confirmed by single-crystal x-ray diffraction analysis (eq. 1.8).[37]

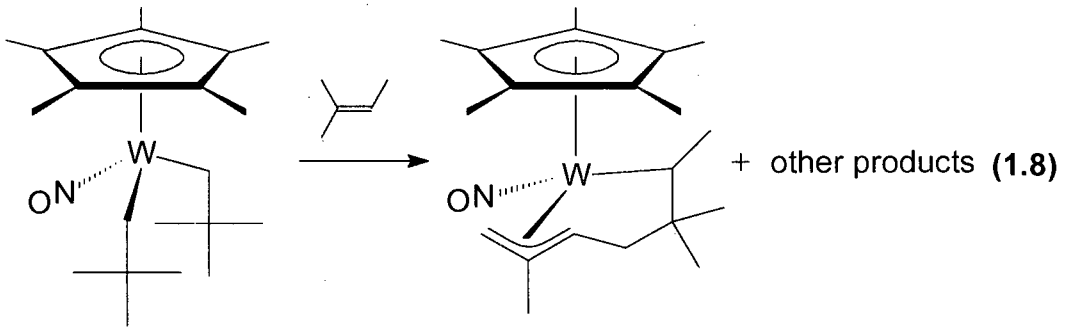

**(1.8)**

The only viable rationale for the formation of this product involves the activation of one solvent molecule to give an intermediate neopentyl-allyl complex that subsequently eliminates another equivalent of neopentane to give a diene species that can then couple to a second molecule of the alkene to ultimately yield the product observed (Scheme 1.8).

**Scheme 1.8**

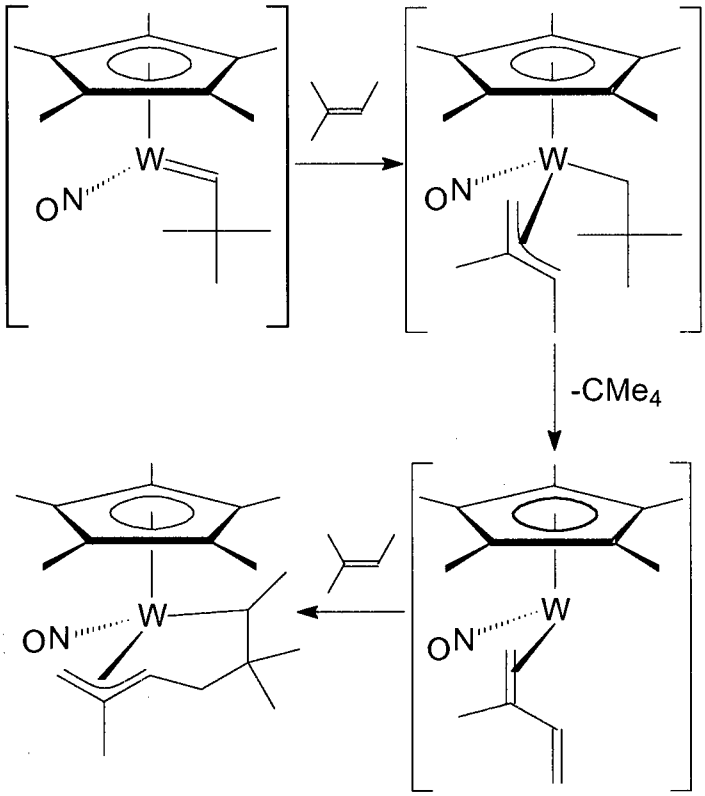


Consequently, the initial target was to synthesize a neopentyl-allyl complex that might thermally generate a diene intermediate via the elimination of neopentane. Presumably, if the diene is successfully formed *in situ* under thermal conditions in benzene-$d_6$ (for purposes of monitoring via $^1$H NMR spectroscopy), and if it is indeed a reactive intermediate, then the thermolysis of the alkyl-allyl in 2-methyl-2-butene would result in a similar coupled product. Hence, the synthesis of the neopentyl-dimethylallyl complex, namely Cp*W(NO)($CH_2CMe_3$)($\eta^3$-1,1-$Me_2C_3H_3$) (**1.1**) which is the principal precursor of the chemistry described in this Thesis, has been performed (Figure 1.1).

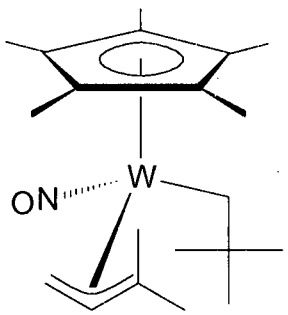


**1.1**

**Figure 1.1 The neopentyl-dimethylallyl complex, Cp*W(NO)($CH_2CMe_3$)($\eta^3$-1,1-$Me_2C_3H_3$) (1.1)**

The solution structure of **1.1** with the dimethylallyl terminus situated trans to the NO ligand as expected for this class of compound, has been established.[38] The allyl moiety of **1.1** also displays features indicative of $\sigma$-$\pi$ distortion as evinced by its $^{13}C\{^1H\}$ NMR spectrum ($C_6D_6$) which exhibits a resonance at 101.7 ppm (allyl-CH) characteristic of an $sp^2$-like carbon and a signal at 37.6 ppm (allyl-$CH_2$) indicative of an $sp^3$-like terminal carbon. The distortion observed for **1.1** is common for other transition-metal allyl complexes which display similar spectroscopic features.[39-42] The endo conformation adopted by the dimethylallyl ligand, as depicted in Figure 1.1, is supported by evidence from selective NOE NMR spectroscopic data.[43]

For related 16e bis(alkyl) species, the presence of the 3e NO ligand results in strong backbonding interactions between the $\pi^*$ orbitals of the NO and the $d_{xz}$ and $d_{yz}$ orbitals of the metal center.[44,45] This interaction results in the stabilization of the metal d-orbitals involved relative to the non-bonding $d_{xy}$ LUMO, thereby rendering the metal center Lewis acidic and prone to coordination by suitable Lewis bases. As an

intramolecular example, the dimethylallyl portion of **1.1** stabilizes the LUMO via the π-donor interaction, to afford an electronically saturated compound. The neopentyl-dimethylallyl complex can thus be described as an 18e complex as a result of the tri-hapticity of the allyl fragment.

## 1.4 The Scope of this Research Project and Format of this Thesis

Chapter 2 describes the synthesis and characterization of products obtained from the thermal reactions of **1.1** in various hydrocarbon solvents, and the thermodynamic product distributions acquired are discussed. The solid-state molecular structures of four of the compounds have been determined, and the metrical parameters are discussed with reference to solution structures established by NMR spectroscopic techniques.

Chapter 3 discusses the mechanism of C-H activation initiated by the precursor neopentyl-dimethylallyl complex. Techniques utilized in the elucidation of the reactive intermediate are described, as are kinetic details. The solid-state molecular structures of two complexes arising from these studies are presented, as are the solution structures determined by means similar to those in Chapter 2.

Chapter 4 describes the multiple C-H bond-activating ability initiated by **1.1** of alkane C-H linkages. This final chapter also discusses possibilities for future work in this area, some of which has already been initiated.

This Thesis is formatted with Chapters 2 and 3 possessing five major Sections. If X is the Chapter number, then the Sections appear as X.1 Introduction, X.2 Results and Discussion, X.3 Epilogue, X.4 Experimental Procedures, and X.5 References and Notes. Subsections of these categories are numbered using legal outlining procedures, e.g. X.1.1, X.1.2, X.1.2.1, etc. All compounds discussed in each Chapter are catalogued numerically, e.g. in Chapter X, compounds appear as X.1, X.2, etc. Schemes, Tables, Figures and Equations are similarly sequenced. The standard experimental methodologies employed during the course of this research are described in detail in this Chapter, Section 1.5.1.

## 1.5 Experimental Procedures

### 1.5.1 General Methods

The following descriptions of methodologies employed throughout the course of this study apply to the entire thesis. All reactions and subsequent manipulations involving organometallic reagents were performed under anaerobic and anhydrous conditions either under high vacuum or an inert atmosphere of pre-purified argon or dinitrogen. Purification of inert gases was achieved by passing them first through a column containing MnO and then a column of activated 4 Å molecular sieves. Conventional glovebox and vacuum-line Schlenk techniques were utilized throughout. The gloveboxes utilized were Innovative Technologies LabMaster 100 and MS-130 BG dual-station models equipped with freezers maintained at – 30 °C. Many reactions were performed in a thick-walled bomb, here defined as a glass vessel possessing a Kontes greaseless stopcock and a side-arm inlet for vacuum-line attachment. Small-scale reactions and NMR spectroscopic analyses were conducted in J. Young NMR tubes which were also equipped with a Kontes greaseless stopcock.

All solvents were dried with appropriate drying agents under dinitrogen or argon atmospheres and distilled prior to use, or were directly transferred under vacuum from the appropriate drying agent. Hydrocarbon solvents, their deuterated analogues, diethyl ether and trimethylphosphine were dried and distilled from sodium or sodium/benzophenone ketyl. Tetrahydrofuran was distilled from molten potassium, and dichloromethane and chloroform were distilled from calcium hydride.

All IR samples were prepared as KBr pellets (~ 1 mg sample: ~ 100 mg KBr) and recorded on a BOMEM MB-100 FT-IR spectrometer unless otherwise noted. All NMR spectra were recorded at room temperature unless otherwise noted. $^{1}H$ NMR spectra were recorded on Bruker AV-300 (300 MHz), Bruker AV-400 (400 MHz), or Bruker AMX-500 (500 MHz) instruments. $^{2}H$ $\{^{1}H\}$ NMR spectra were recorded on a Bruker AMX-500 (77 MHz) instrument. $^{13}C$ $\{^{1}H\}$ NMR spectra were recorded on Bruker AV-300 (75 MHz), Bruker AV-400 (100 MHz) or Bruker AMX-500 (125 MHz) instruments. All chemical shifts are reported in ppm, and all coupling constants are reported in Hz. NMR spectra were referenced to the residual protio-isotopomer present in a particular solvent. $^{2}H\{^{1}H\}$ NMR spectra ($C_6H_6$) are referenced to residual $C_6H_5D$ (7.15 ppm) while $^{13}C\{^{1}H\}$ NMR spectra are referenced to the natural abundance carbon signal of the solvent employed. $^{31}P\{^{1}H\}$ NMR spectra are referenced to external $H_3PO_4$ (85%) in $C_6D_6$ (0.0 ppm). Where necessary, $^{1}H$-$^{1}H$ COSY, $^{1}H$-$^{1}H$ selNOE, $^{1}H$-$^{13}C$ HMQC and $^{1}H$-$^{13}C$ HMBC experiments were carried out to correlate and assign $^{1}H$ and $^{13}C$ signals. Low-resolution mass spectra (EI, 70 eV) were recorded by the staff of the UBC Chemistry Mass Spectrometry Laboratory on a Kratos MS50 spectrometer utilizing the direct-insertion sample introduction method. Elemental analyses were performed by Mr. P. Borda at the Department of Chemistry at UBC and Ms. Pauline Maloney of Canadian Microanalytical Service Ltd. X-ray crystallographic data collection was performed by Dr. B. O. Patrick of the UBC X-ray Crystallographic Laboratory and Dr. R. Bau of the University of Southern California X-ray Crystallographic Laboratory.

### 1.5.2 NMR Assignments

The following format has been employed to help identify peaks in the NMR spectra: XXX ppm (multiplicity, coupling constant(s), relative number of atoms, ligand-part). Subscripts for specific portions of a ligand are as follows: *syn*, *anti* for syn and anticlinal methylene H atoms; *o*, *m*, *p* and *ipso* for positions on an aryl ring; *aryl* if the position is not known; *s* for $H_{syn}$, *a* for $H_{anti}$ and *c* for $H_c$ in allyl complexes.

### 1.5.3 Reagents

The $(CH_2CMe_3)_2Mg{\cdot}x$(dioxane) alkylating reagent and the $Cp^*W(NO)(CH_2CMe_3)(Cl)$ complex were prepared according to published procedures.[46,47]

A modified version of the general synthetic method for dialkyl magnesium reagents was employed for the preparation of the dimethylallyl magnesium reagent. 3,3-Dimethylallyl bromide (Fluka, 10 mL, 0.085 mol) was syringed into a 200-mL two-neck round bottom flask and diluted with $Et_2O$ (100 mL). In a glovebox, a 500-mL three-neck round bottom flask was charged with magnesium powder (4.2 g, 0.172 mol) and a magnetic stir-bar. The 500-mL flask was charged with $Et_2O$ (250 mL), and on a vacuum-line, was fitted with a reflux condenser. Activation of the magnesium powder was accomplished via addition of sufficient dibromoethane (~ 1-2 mL) using a syringe. The suspension was allowed to reflux until all the added dibromoethane had reacted. The

suspension was then cooled in an ice bath to 0 °C, whereupon the ethereal bromide solution was added dropwise via a cannula over a 3-hour period. During this time, the contents of the flask were stirred rapidly, and the solution remained clear. Upon completion of the dropwise addition, the mixture was slowly warmed to room temperature. The transformation of the Grignard reagent into the bis(allyl)magnesium reagent was conducted in the usual manner for bis(alkyl) reagents.[46] ($\eta^3$-1,1-$Me_2C_3H_3)_2Mg{\cdot}x$(dioxane) was isolated as a snow-white powder and titration with 0.1 M HCl afforded a titre of 127 g/mol (2.7 g, 50%).

### 1.5.4 Synthesis of Cp*W(NO)($CH_2CMe_3$)($\eta^3$-1,1-$Me_2C_3H_3$) (1.1)[48]

In a glovebox, a 400-mL Schlenk tube was charged with a magnetic stir bar and Cp*W(NO)($CH_2CMe_3$)Cl (483 mg, 1.15 mmol). A 100-mL Schlenk tube was then charged with a magnetic stir bar and the dimethylallyl magnesium reagent (147 mg, 1.16 mmol). On a vacuum-line, $Et_2O$ (200 mL) from a bomb was cannulated into the Schlenk tube containing the magnesium reagent with vigorous stirring to ensure dissolution. The resulting colourless solution was cooled to – 196 °C using a liquid $N_2$ bath under a strong flow of Ar in an open system to prevent the introduction of air. $Et_2O$ (50 mL) was added in a similar fashion to the Schlenk tube containing the solid Cp*W(NO)($CH_2CMe_3$)Cl to give a purple solution which was then cooled to – 60 °C with a Dry Ice/acetone bath. The resulting mixture was then cannulated dropwise into the 400-mL Schlenk tube (maintained at – 196 °C) at a slow enough rate that allowed the added solution to freeze

upon contact with the solidified ethereal solution. Sufficient $Et_2O$ was added to the 100-mL Schlenk tube and subsequently cannulated into the reaction flask to ensure complete transfer of $Cp^*W(NO)(CH_2CMe_3)Cl$ . The liquid $N_2$ bath was replaced with a liquid $N_2$/acetone bath at – 60 °C to slowly melt the ethereal contents. After being stirred for 5 minutes, the purple solution changed to a straw-yellow colour which then becomes a turbid orange solution after a further 10 minutes. The solution was stirred at – 60 °C for a total of 45 minutes, whereupon the contents were warmed to room temperature to ensure completion of reaction. The volume was reduced under vacuum to ~ 100 mL, and the turbid orange solution was filtered through an alumina (I) column (2 x 3 cm), which was rinsed with fresh $Et_2O$ (2 x 10 mL), to give a clear bright orange filtrate. The volatiles were then removed from the filtrate *in vacuo* to obtain an orange crystalline powder which was allowed to dry under high vacuum for 1 hour. Analysis of this solid by $^1H$ NMR spectroscopy revealed that complex **1.1** was the sole organometallic product. The analytically pure product was obtained as orange microcrystals (296 mg, 57 %) via crystallization from a THF/hexanes mixture (5 mL: 20 mL) at – 25 °C.

**1.1**: IR ($cm^{-1}$) 1546 (s, $\nu_{NO}$). MS (LREI, *m/z*, probe temperature 150 °C) 489 [$P^+$, $^{184}W$]. $^1H$ NMR (300 MHz, $C_6D_6$) δ 0.67 (s, 3H, allyl Me), 1.02 (obs, 1H, Npt $CH_2$), 1.02 (s, 3H, allyl Me), 1.42 (s, 9H, Npt $CMe_3$), 1.42 (obs, 1H, allyl $CH_2$), 1.53 (s, 15H, $C_5Me_5$), 2.69 (m, 1H, allyl $CH_2$), 4.45 (m, 1H, allyl CH); $^1H$ NMR (400 MHz, $CD_2Cl_2$) δ 0.88 (d, $^2J_{HH}$ = 14.2, 1H, Npt $CH_2$), 0.99 (s, 3H, allyl Me), 1.02 (d, $^2J_{HH}$ = 14.2, 1H, Npt $CH_2$), 1.06 (s, 9H, Npt $CMe_3$), 1.24 (s, 3H, allyl Me), 1.61 (m, 1H, allyl $CH_2$), 1.82 (s, 15H, $C_5Me_5$), 2.55 (m, 1H, allyl $CH_2$), 4.40 (m, 1H, allyl CH). $^{13}C\{^1H\}$ NMR (75 MHz,

$CD_2Cl_2$) δ 10.2 ($C_5Me_5$), 19.5, 30.7 (allyl Me), 34.3 (Npt $CMe_3$), 37.6 (allyl $CH_2$), 39.9 (Npt $CMe_3$), 40.7 (Npt $CH_2$), 101.7 (allyl CH), 107.5 ($C_5Me_5$), 147.8 (allyl C). Sel NOE (400 MHz, $C_6D_6$) δ irrad. at 4.45, NOE at 1.02, irrad. at 0.67, NOE at 1.02, 1.42, 1.52 and 2.55. Anal. Calcd. for $C_{20}H_{35}NOW$: C, 49.09; H, 7.21; N, 2.86. Found: C, 49.16; H, 7.03; N, 2.87.

**1.6 References and Notes**

(1) Elschenbroich, C.; Salzer, A. *Organometallics*; 2nd ed.; VCH Publishers Inc.: New York, 1992.

(2) Seyferth, D. *Organometallics* **2001**, *20*, 1488.

(3) Crabtree, R. H. *The Organometallic Chemistry of the Transition Metals*; 3rd ed.; Wiley and Sons: Toronto, 2001.

(4) Crabtree, R. H. *J. Chem. Soc., Dalton Trans.* **2001**, 2437.

(5) Crabtree, R. H. *Chem. Rev.* **1995**, *95*, 987.

(6) Crabtree, R. H. *Chem. Rev.* **1985**, *85*, 245.

(7) Shilov, A. E.; Shul'pin, G. B. *Activation and Catalytic Reactions of Saturated Hydrocarbons in the Presence of Metal Complexes*; Kluwer Academic Publishers: Dordrecht, 2000; Vol. 21.

(8) Labinger, J. A.; Bercaw, J. E. *Nature* **2002**, *417*, 507.

(9) Janowicz, A. H.; Bergman, R. G. *J. Am. Chem. Soc.* **1982**, *104*, 352.

(10) Thompson, M. E.; Baxter, S. M.; Bulls, A. R.; Burger, B. J.; Nolan, M. C.; Santarsiero, B. D.; Schaefer, W. P.; Bercaw, J. E. *J. Am. Chem. Soc.* **1987**, *109*, 203.

(11) Watson, P. L. *J. Am. Chem. Soc.* **1983**, *105*, 6491.

(12) Rothwell, I. P. *Acc. Chem. Res.* **1988**, *21*, 153.

(13) Sadow, A. D.; Tilley, T. D. *J. Am. Chem. Soc.* **2002**, *124*, 6814.

(14) Arndsten, B. A.; Bergman, R. G.; Mobley, T. A.; Peterson, T. H. *Acc. Chem. Res.* **1995**, *28*, 154.

(15) Hill, C. L., Ed. *Activation and Functionalization of Alkanes*; John Wiley and Sons: New York, 1989.

(16) Vidal, V.; Theolier, A.; Thivolle-Cavat, J.; Basset, J. M.; Corker, J. *J. Am. Chem. Soc.* **1996**, *118*, 4595.

(17) Niccolai, G. P.; Basset, J. M. *Appl. Catal. A.* **1996**, *146*, 145.

(18) Sherry, A. E.; Wayland, B. B. *J. Am. Chem. Soc.* **1990**, *112*, 1259.

(19) Wayland, B. B.; Ba, S.; Sherry, A. E. *J. Am. Chem. Soc.* **1991**, *113*, 5305.

(20) Schrock, R. R. *Acc. Chem. Res.* **1979**, *12*, 98.

(21) van Doorn, J. A.; van der Heijden, H.; Orpen, A. G. *Organometallics* **1994**, *13*, 4271.

(22) McDade, C.; Green, J. C.; Bercaw, J. E. *Organometallics* **1982**, *1*, 1629.

(23) Bulls, A. R.; Schaefer, W. P.; Serfas, M.; Bercaw, J. E. *Organometallics* **1987**, *6*, 1219.

(24) Coles, M. P.; Gibson, V. C.; Clegg, W.; Elsegood, M. R. J.; Porelli, P. A. *J. Chem. Soc., Chem. Commun.* **1996**, 1963.

(25) van der Heijden, H.; Hessen, B. *J. Chem. Soc., Chem. Commun.* **1995**, 145.

(26) Cheon, J.; Rogers, D. M.; Girolami, G. S. *J. Am. Chem. Soc.* **1997**, *119*, 6804.

(27) Tran, E.; Legzdins, P. *J. Am. Chem. Soc.* **1997**, *119*, 5071.

(28) Bennett, J. L.; Wolczanski, P. T. *J. Am. Chem. Soc.* **1997**, *119*, 10696.

(29) Schafer II, D. F.; Wolczanski, P. T. *J. Am. Chem. Soc.* **1998**, *120*, 4881.

(30) Cummins, C. C.; Baxter, S. M.; Wolczanski, P. T. *J. Am. Chem. Soc.* **1988**, *110*, 8731.

(31) Walsh, P. J.; Hollander, F. J.; Bergman, R. G. *J. Am. Chem. Soc.* **1988**, *110*, 8729.

(32) Debad, J. D.; Legzdins, P.; Lumb, S. A.; Batchelor, R. J.; Einstein, F. W. B. *J. Am. Chem. Soc.* **1995**, *117*, 3288.

(33) Debad, J. D.; Legzdins, P.; Lumb, S. A.; Rettig, S. J.; Batchelor, R. J.; Einstein, F. W. B. *Organometallics* **1999**, *18*, 3414.

(34) Adams, C. S.; Legzdins, P.; Tran, E. *J. Am. Chem. Soc.* **2001**, *123*, 612.

(35) Adams, C. S.; Legzdins, P.; Tran, E. *Organometallics* **2002**, *21*, 1474.

(36) Wada, K.; Pamplin, C. B.; Legzdins, P. *J. Am. Chem. Soc.* **2002**, *124*, published on web 24 July 2002.

(37) Tran, E. Development of Tungsten Alkylidene Complexes for Activation of Hydrocarbons: Synthesis, Selectivities, and Mechanisms. Ph.D. Thesis, University of British Columbia, Vancouver, BC, December 2001.

(38) Faller, J. W.; DiVerdi, M. J.; John, J. A. *Tetrahedron Lett.* **1991**, *32*, 1271.

(39) Ipaktschi, J.; Mirzaei, F.; Demuth-Eberle, G. J.; Beck, J.; Serafin, M. *Organometallics* **1997**, *16*, 3965.

(40) Frohnapfel, D. S.; White, P. S.; Templeton, J. L. *Organometallics* **1997**, *16*, 3737.

(41) Villanueva, L. A.; Ward, Y. D.; Lachicotte, R.; Liebeskind, L. S. *Organometallics* **1996**, *15*, 4190.

(42) Adams, R. D.; Chodosh, D. F.; Faller, J. W.; Rosan, A. M. *J. Am. Chem. Soc.* **1979**, *101*, 2570.

(43) Direct evidence for *endo*- vs *exo*-allyl conformations using selective NOE NMR spectroscopy is sometimes not available, and logical inferences must be made to ascertain the solution structure. For example, irradiation of the signal due to the central allyl H atom leading to an NOE enhancement of the Cp* methyl H atoms signal is direct

evidence for an exo configuration. However, its absence, and hence the implication of an endo configuration, must be confirmed by irradiation of the trans Me group signal that should exhibit an NOE enhancement of the Cp* ring signal.

(44) Legzdins, P.; Rettig, S. J.; Sanchez, L. J.; Bursten, B. E.; Gatter, M. J. *J. Am. Chem. Soc.* **1985**, *107*, 1411.

(45) Bursten, B. E.; Cayton, R. H. *Organometallics* **1987**, *6*, 2004.

(46) Dryden, N. H.; Legzdins, P.; Trotter, J.; Yee, V. C. *Organometallics* **1991**, *10*, 2857.

(47) Debad, J. D.; Legzdins, P.; Batchelor, R. J.; Einstein, F. W. B. *Organometallics* **1993**, *12*, 2094.

(48) Adams, C.S. C-H Activation of Hydrocarbons by Tungsten Alkylidene and Related Complexes. Ph.D. Thesis, University of British Columbia, Vancouver, BC, October 2001.

# Chapter 2

## *Thermal Reactions of Cp*W(NO)($CH_2CMe_3$)($\eta^3$-1,1-$Me_2C_3H_3$) with Hydrocarbons: Scope of Single C-H Bond Activations*

---



---

## 2.1 Introduction

As described in Chapter One, the preparation of $Cp^*W(NO)(CH_2CMe_3)(\eta^3\text{-}1,1\text{-}Me_2C_3H_3)$ (**1.1**) was an effort to identify the intermediate involved in the coupling reaction that occurs when the well-studied bis(neopentyl) species, $Cp^*W(NO)(CH_2CMe_3)_2$,[1-3] is thermolysed in 2-methyl-2-butene.

The unexpected result observed from the thermal reaction of **1.1** in benzene, namely the formation of an aryl containing organometallic product, encouraged the pursuit of further studies. Presumably, C-H bond activation via some as yet unidentified pathway led to the incorporation of a phenyl group. Reactions were thus performed to assess the breadth of the reactivity of **1.1** towards different hydrocarbon solvents.

This Chapter expands upon the observations mentioned above and provides detailed information pertaining to the scope of the single C-H bond activations initiated by **1.1** under suitable thermolytic conditions. When more than one type of C-H bond is present in a substrate (e.g. $sp^2$ C-H vs $sp^3$ C-H), the formation of more than one organometallic product is observed. The product ratios reflect the thermodynamic distribution of activations initiated by **1.1** for different classes of C-H bonds.

## 2.2 Results and Discussion

### 2.2.1 A Serendipitous Discovery

The formation of Cp*W(NO)($C_6D_5$)($\eta^3$-1,1-$Me_2$-allyl-$d_1$) (**2.1**-$d_6$) as a result of apparent C-D bond activation upon thermolysis of **1.1** in benzene-$d_6$ was an unexpected result. Instead of resonances attributable to the formation of the putative *cis*-diene intermediate, signals resulting from a dimethylallyl-containing organometallic species are detectable in the $^1$H NMR spectrum. $^{13}C\{^1H\}$ NMR data ($C_6D_6$) include signals near the solvent peak ($\delta$ 128.0) assignable to the aryl carbon atoms. These data constitute the first indication of an aryl ligand as no resonances are observed for the deuterated-phenyl ligand in the $^1$H NMR data initially acquired. Further analysis, including the acquisition of $^2$D NMR spectroscopic data ($C_6H_6$), which reveal resonances in the aryl region, and mass spectral data consistent with the supposed formulation, permits the identification of the final product as **2.1**-$d_6$.

This discovery marks the identification of a fourth Legzdins precursor[4-6] that is capable of effecting C-D bond activation of benzene-$d_6$. The thermal reactivity of **1.1** in a variety of different hydrocarbon solvents was then examined in order to elucidate the scope of the C-H bond activations initiated by the neopentyl-dimethylallyl complex.

### 2.2.2 Preliminary Studies on C-H Activation Potential Initiated by 1.1[7]

#### 2.2.2.1 Thermolysis of 1.1 in Benzene

The first obvious substrate to test the C-H activating ability, given the result seen from its deuterated analog, is protio-benzene (eq. 2.1). As expected, the yellow crystalline product from the thermolysis of **1.1** in benzene exhibits NMR spectral features identical to that of the deuterated species, plus resonances in the aryl region in its $^{1}H$ NMR spectrum ($C_6D_6$) which correspond to those seen in the $^{2}D\{^{1}H\}$ NMR spectrum ($C_6H_6$) for complex **2.1**-$d_6$. A single-crystal X-ray crystallographic analysis[8] has been performed to confirm the identity of the final organometallic product, Cp*W(NO)($C_6H_5$)($\eta^3$-1,1-$Me_2C_3H_3$) (**2.1**), and its ORTEP diagram is shown in Figure 2.1 which shows complex **2.1** to possess an 18e, three-legged piano-stool structure.

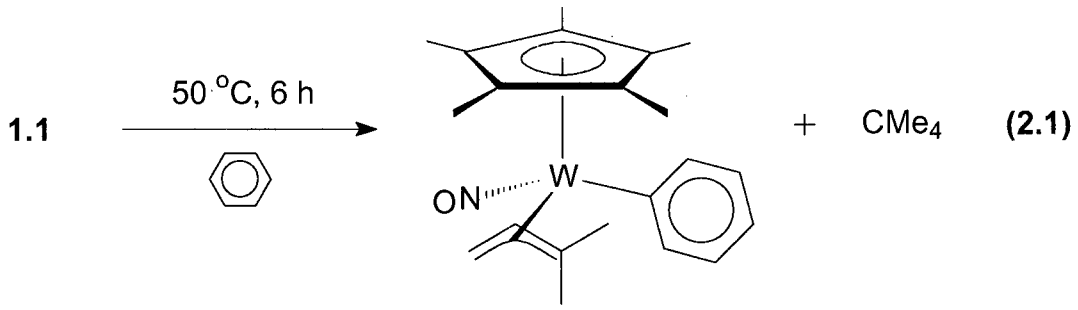


**2.1**

The solid-state molecular structure of **2.1** exhibits features characteristic of σ-π distortion of the dimethylallyl moiety. This feature is manifested as a longer C(7)-C(8) and shorter C(8)-C(9) bond (1.439(6) and 1.365(5) Å respectively), suggestive of more respective

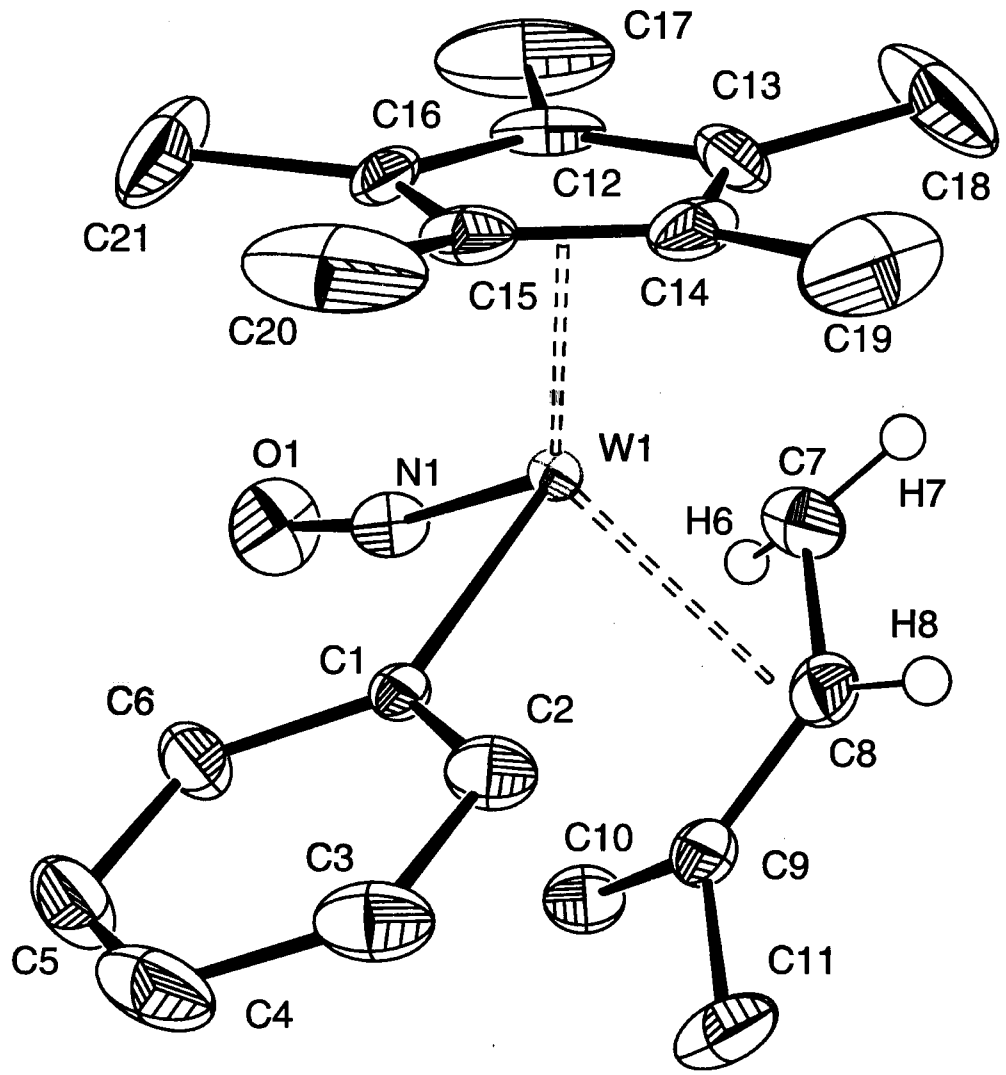


**Figure 2.1** Solid-state molecular structure of Cp*W(NO)($C_6H_5$)($\eta^3$-1,1-$Me_2C_3H_3$) (**2.1**) with 50 % probability thermal ellipsoids shown. Selected interatomic distances (Å) and angles (deg): W(1)-N(1) = 1.762(3), W(1)-C(7) = 2.218(4), W(1)-C(8) = 2.363(4), W(1)-C(9) = 2.768(4), W(1)-C(1) = 2.186(3), N(1)-O(1) = 1.224(4), C(7)-C(8) = 1.439(6), C(8)-C(9) = 1.365(5), W(1)-N(1)-O(1) = 169.5(3), W(1)-C(1)-C(6) = 121.4(2), C(7)-C(8)-C(9) = 124.8(4), W(1)-C(7)-C(8) = 77.3(2), C(8)-C(9)-C(10) = 124.3(4), C(10)-C(9)-C(11) = 113.5(3)

single- and double-bond character.[9] Solution NMR data also support this diagnosis as evinced by its $^{13}C\{^{1}H\}$ NMR spectrum ($C_6D_6$) which exhibits a resonance at 95.3 ppm (allyl-CH) characteristic of an $sp^2$-like carbon and a signal at 37.6 ppm (allyl-$CH_2$) indicative of an $sp^3$-like terminal carbon. Other transition-metal allyl complexes display similar spectroscopic and solid-state metrical features that are consistent with distortions of this type.[10-13] Conversely, a $\eta^1$-dimethylallyl complex exhibits spectroscopic features indicative of the loss of the trihapticity of the allyl fragment (see Section 3.2.4).

Also evident from the ORTEP diagram of complex **2.1** is the expected orientation of the dimethylallyl ligand, with the most substituted carbon atom of the three-carbon allyl backbone situated trans to the NO ligand. This orientation can be explained by the electronic asymmetry at the tungsten center resulting from different acceptor characteristics of the NO and aryl ligand.[14] Furthermore, the substituted allyl ligand is also rotated away from the idealized exo orientation to maximize the $\pi$-interaction between the non-bonding orbital of the allyl ligand and the metal center.[15]

The exo conformation adopted by the dimethylallyl ligand in the solid state is consistent with its apparent solution structure, based on selective NOE NMR spectroscopic data.[16] This is in contrast to the endo configuration observed in solution for complex **1.1**. Theoretical calculations performed on similar asymmetric-allyl transition-metal complexes reveal that there is a minimal energy difference between the idealized endo and exo conformers,[15] thus suggesting that the two different orientations observed for complexes **1.1** and **2.1** are sterically influenced.

As noted previously,[17] the phenyl hydrogen and carbon atoms all exhibit unique resonances in both spectra ($^{1}H$ and $^{13}C\{^{1}H\}$ in $C_6D_6$), similar to that observed for aryl

ligands in similar complexes,[18] and is rationalized as a result of slow rotation about the W-C bond of the phenyl ligand on the NMR timescale. EXSY NMR data confirms the rotation about the W-C bond, as exchange is observed between the two resonances for the *meta*-hydrogens and the two resonances for the *ortho*-hydrogens (see Figure 2.2).

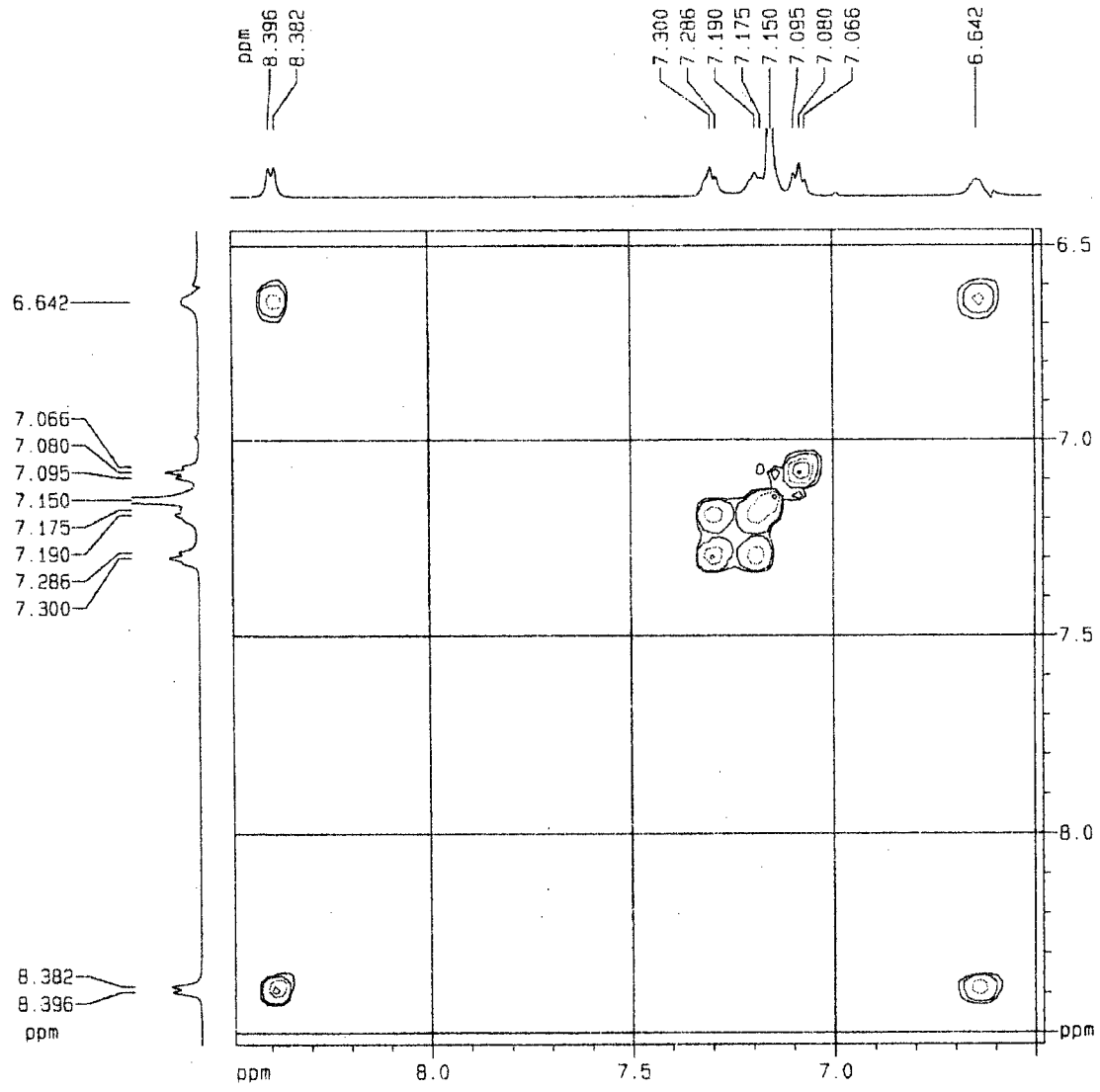


**Figure 2.2** 2D EXSY NMR ($C_6D_6$) plot showing exchange between unique resonances of *o*- and *m*-hydrogens on the phenyl ligand of complex **2.1**

### 2.2.2.2 Thermolysis of 1.1 in Tetramethylsilane

Another prototypical hydrocarbon solvent commonly used in the Legzdins research group for C-H activation experiments is tetramethylsilane, due to the exclusive presence of primary $sp^3$ C-H bonds. Thermolysis of the 18e complex **1.1** in TMS at 50 °C for 6 hours results in the quantitative formation (as determined by $^1H$ NMR spectroscopy) of the 18e alkyl-allyl complex, $Cp^*W(NO)(CH_2SiMe_3)(\eta^3\text{-}1,1\text{-}Me_2C_3H_3)$ (**2.2**) (eq. 2.2).

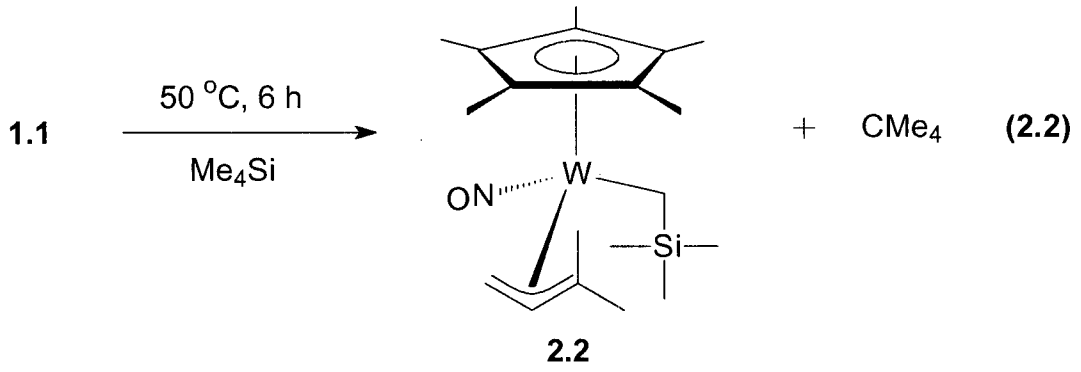


Complex **2.2** is thermally stable in TMS, and the known[19] bis(alkyl) complex, $Cp^*W(NO)(CH_2SiMe_3)_2$, is not formed on prolonged reaction times. A single-crystal X-ray crystallographic analysis has been performed[20] on **2.2,** and the resulting ORTEP diagram is shown in Figure 2.3. The most striking feature of the solid-state molecular structure of **2.2** is the endo configuration adopted by the dimethylallyl ligand. Again, this is consistent with its solution structure as determined by selective NOE NMR spectroscopic data[16] and is possibly due to the steric congestion the molecule experiences between the methyls on the allyl ligand and the rapidly rotating methyls of the trimethylsilylmethyl group.

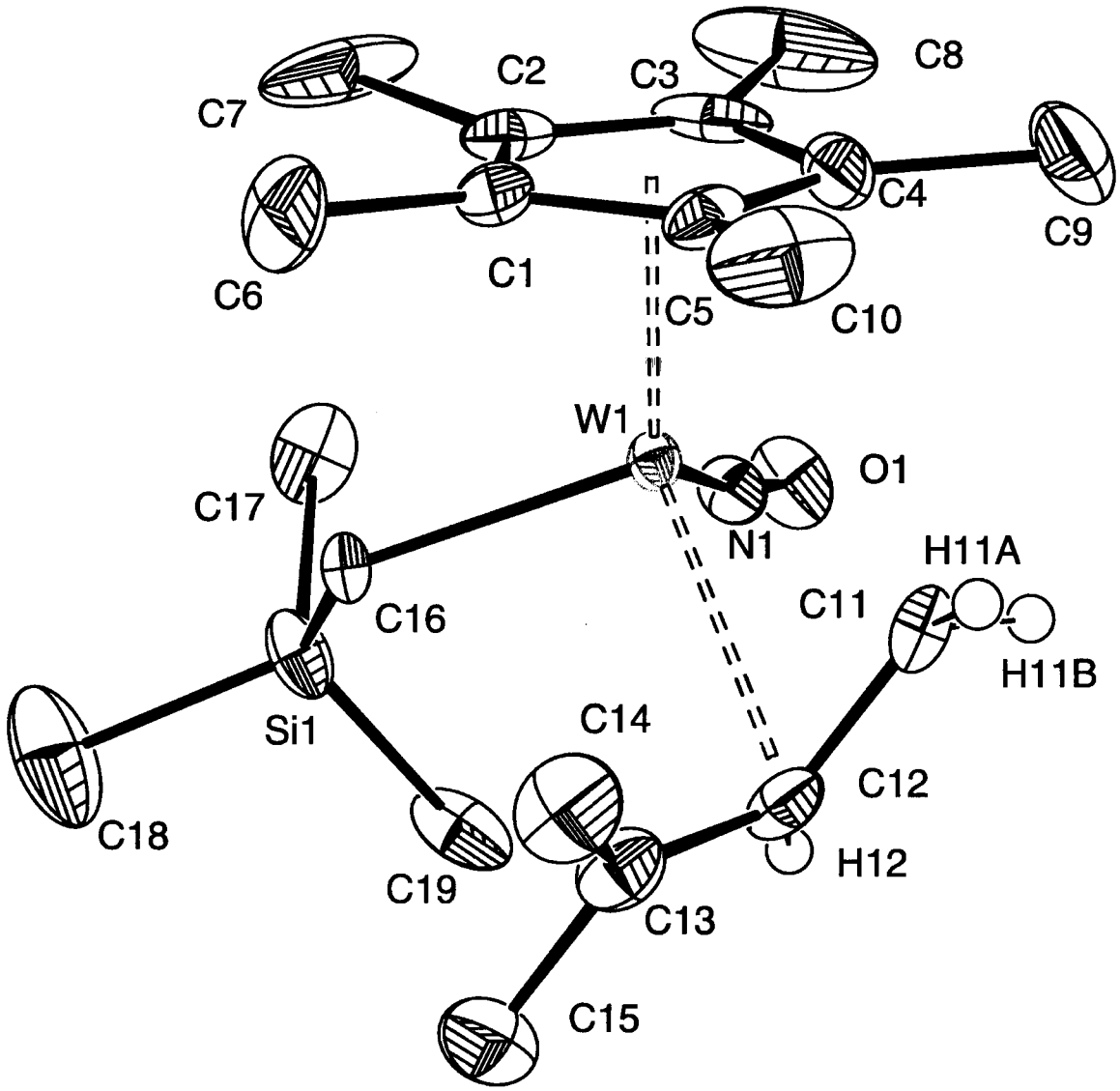


**Figure 2.3** Solid-state molecular structure of Cp*W(NO)($CH_2SiMe_3$)($\eta^3$-1,1-$Me_2C_3H_3$) **(2.2)** with 50 % probability thermal ellipsoids shown. Selected interatomic distances (Å) and angles (deg): W(1)-N(1) = 1.760(5), W(1)-C(11) = 2.182(6), W(1)-C(12) = 2.433(6), W(1)-C(13) = 2.874(6), W(1)-C(16) = 2.217(6), C(11)-C(12) = 1.46(1), C(12)-C(13) = 1.348(9), N(1)-O(1) = 1.237(7), W(1)-N(1)-O(1) = 170.7(5), C(11)-C(12)-C(13) = 124.9(7), W(1)-C(11)-C(12) = 81.2(4), C(12)-C(13)-C(14) = 125.6(7), C(14)-C(13)-C(15) = 113.5(7)

Not surprisingly, the NMR spectroscopic features of **2.2** parallel those of **1.1**, excluding the resonances observed for the alkyl group where obvious differences arise from the substitution of a silicon atom for a carbon atom. Likewise, the IR stretching frequencies observed for the nitrosyl group differ by only 6 wavenumbers (1555 and 1549 $cm^{-1}$ for **1.1** and **2.2**, respectively). The nitrosyl ligands of related compounds display metrical and spectroscopic parameters comparable to those of complex **2.2**.[21]

### 2.2.2.3 Thermolysis of 1.1 in Mesitylene

The thermal reaction of **1.1** in mesitylene results in the exclusive formation of Cp*W(NO)($CH_2C_6H_3$-3,5-$Me_2$)($\eta^2$-1,1-$Me_2C_3H_3$) (**2.3**) (eq. 2.3). A single-crystal X-ray crystallographic analysis has been performed,[22] and the ORTEP diagram is shown in Figure 2.4.

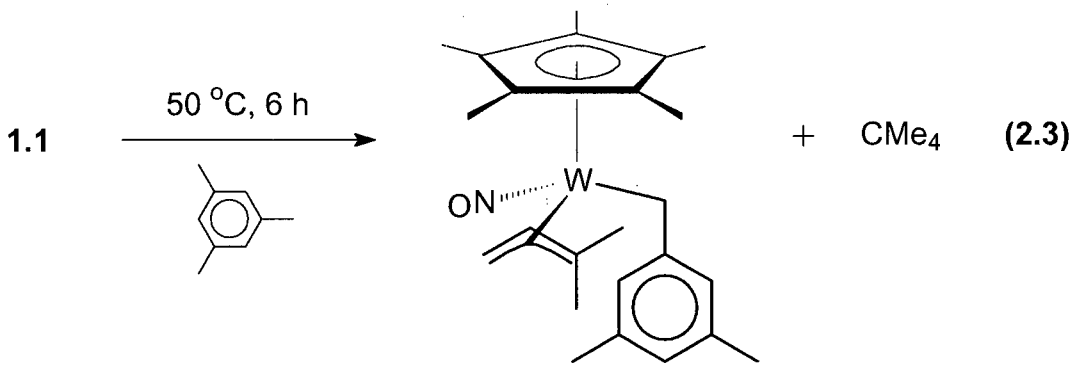


**2.3**

The $^1H$ NMR spectrum ($C_6D_6$) of **2.3** exhibits features indicative of fast rotation about the W(1)-C(11) bond on the NMR timescale, namely the sharp singlet observed for both methyl groups (δ 2.38) and the resonance attributable to both *ortho*-hydrogens on

the aryl ring (δ 7.38). Presumably, the steric congestion present in the phenyl-allyl complex **2.1** is alleviated by the extra C(11)-C(12) bond of the benzyl moiety, similar to that seen for related complexes.[2,23] Again, as in the previously discussed complex **2.2**, the solid-state molecular structure contains an *exo*-allyl conformation which is consistent with the solution structure as determined by selective NOE NMR spectroscopic evidence.[16]

In many respects, complex **2.3** is very similar to the previously studied benzyl-mesityl complex, $Cp^*W(NO)(CH_2C_6H_5)(CH_2C_6H_3\text{-}3,5\text{-}Me_2)$.[2] This similarity is due to the $\eta^2$-bonding mode that the mesityl group adopts, which can be viewed as an extreme form of an $\eta^3$-allyl moiety based on several criteria[23-26] suggested for such complexes (Scheme 2.1). For example, the tungsten-allyl carbon bond lengths (W(1)-C(20) = 2.187(5) and W(1)-C(21) = 2.391(5) Å) displayed by **2.3**, parallel those of the benzyl-mesityl complex (W-C(1) = 2.181(4) and W-C(2) = 2.391(4) Å respectively). As such, the comparison of spectroscopic and structural characteristics exhibited by both complexes is pertinent.

**Scheme 2.1**

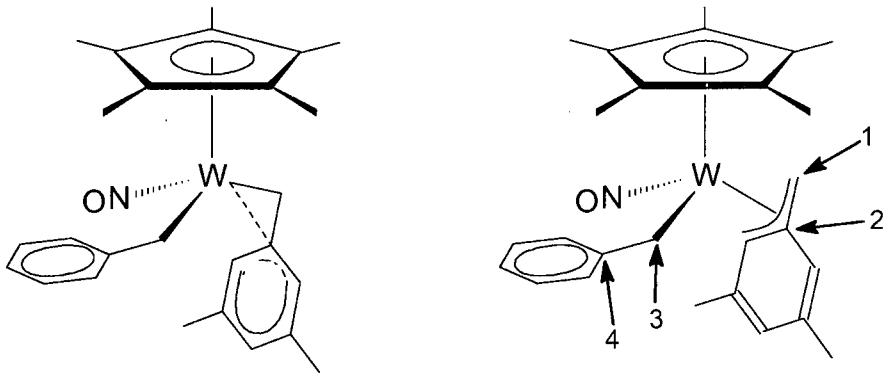


$\eta^2$-benzyl $\eta^3$-benzyl

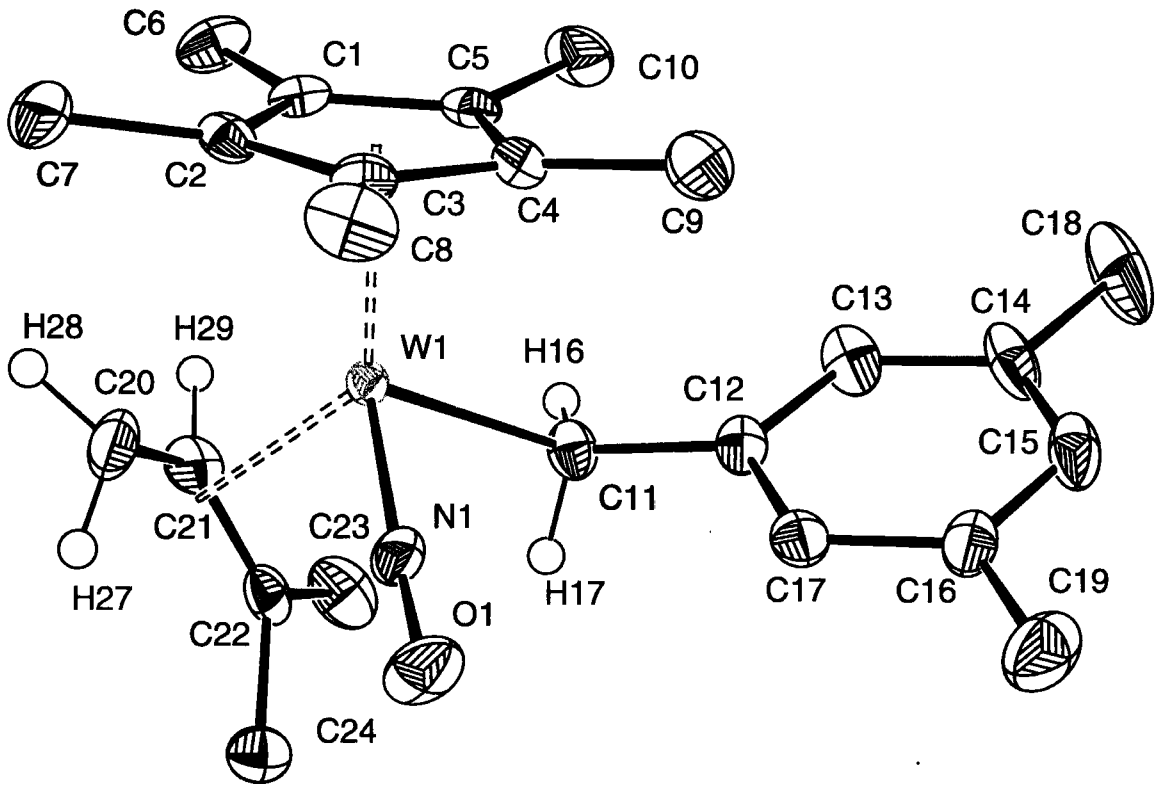


**Figure 2.4** Solid-state molecular structure of Cp*W(NO)($CH_2C_6H_3$-3,5-$Me_2$)($\eta^3$-1,1-$Me_2C_3H_3$) (**2.3**) with 50 % probability thermal ellipsoids shown. Selected interatomic distances (Å) and angles (deg): W(1)-N(1) = 1.753(4), W(1)-C(20) = 2.187(5), W(1)-C(21) = 2.391(5), W(1)-C(22) = 2.961(5), W(1)-C(11) = 2.239(4), N(1)-O(1) = 1.240(5), C(20)-C(21) = 1.454(8), C(21)-C(22) = 1.365(6), C(11)-C(12) = 1.493(6), W(1)-N(1)-O(1) = 171.1(4), W(1)-C(20)-C(21) = 79.3(3), W(1)-C(11)-C(12) = 120.5(3), C(20)-C(21)-C(22) = 125.5(5), C(21)-C(22)-C(24) = 123.5(4), C(23)-C(22)-C(24) = 115.2(4)

The W(1)-C(11)-C(12) bond angle of 120.5(3) $^{o}$ of **2.3** is similar to that observed for the benzyl-mesityl complex (W-C(3)-C(4) = 120.1(3) $^{o}$). The deviation from ideal $sp^3$ hybridization (109.5 $^{o}$) can be attributed to the relief it brings from steric congestion with the bulky pentamethylcyclopentadienyl ligand.

Given that complex **1.1** has been shown to effect bond activation of aryl $sp^2$ C-H linkages (as evinced by the analogous reaction in benzene), the fact that there is exclusive formation of the benzylic C-H activation product when **1.1** is heated in mesitylene is not all that surprising.[2] For aryl C-H activation, the transition-state of an intermediate $\pi$-arene complex is presumably higher in energy than that of the $\sigma$-$sp^3$ C-H complex formed during benzylic C-H activation, as a result of adverse steric interactions imposed by the aryl methyl substituents (vide infra).

### 2.2.3 Thermolyses in Mono- and Di-Substituted Arenes

The thermal reactions of **1.1** in methyl-substituted arenes generate a reactive intermediate that may react with stronger arene C-H bonds (110 kcal/mol) or weaker benzylic C-H bonds (96-102 kcal/mol).[27] It is of importance to understand the selectivities exhibited by transition metal complexes for preferential activation of one type of C-H bond over another.[28] The industrial and catalytic implications are such that it is necessary to ascertain the kinetic selectivities of these potentially important compounds.[29] In this study, however, the issue of thermodynamic distribution of products is addressed.

### 2.2.3.1 Thermolysis of 1.1 in Xylenes

The thermal reaction of **1.1** in *p*-xylene results in the formation of two organometallic products in > 95% overall yield as determined by crude $^1$H NMR spectroscopy ($C_6D_6$) of the final reaction mixture (eq. 2.4).

The product generated upon activation of a benzylic $sp^3$ C-H bond of *p*-xylene, namely Cp*W(NO)($CH_2C_6H_4$-4-Me)($\eta^3$-1,1-$Me_2C_3H_3$) (**2.4**), and that from the activation of an aryl $sp^2$ C-H bond, namely Cp*W(NO)($C_6H_3$-2,5-$Me_2$)($\eta^3$-1,1-$Me_2C_3H_3$) (**2.5**), are formed in an approximate 1:3 respective ratio, which is preserved even after three times the normal reaction time. Statistically, you would expect a 3:2 ratio of benzylic vs aryl activated products due to the availability of the $sp^3$ and $sp^2$ C-H bonds on a molecule of *p*-xylene. Thus, the proportions displayed mark the thermodynamic distribution of the products generated at 50 °C, indicative of a tendency to activate aryl C-H bonds in preference to the benzylic ones.

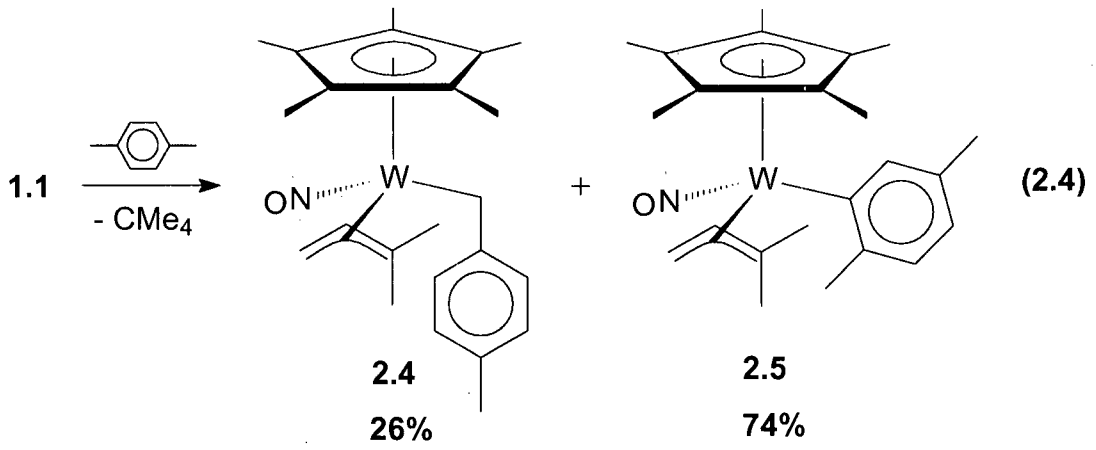

The preferential generation of the aryl-activated species over that of benzylic is a trend commonly seen in many C-H activating transition-metal complexes. The most prevalent rationalization for this selectivity, which is in stark contrast to that observed for mechanisms involving radical species,[30] are the thermodynamics of the bond-breaking and bond-forming involved. Although the bond-dissociation energy for $sp^2$ C-H bond scission is greater than that of $sp^3$ C-H bonds, the resulting metal-carbon interaction is stronger for M-C($sp^2$) than M-C($sp^3$).[28,29,31-33] Another common rationale is the ease of formation of π-arene complexes as opposed to σ-methylarene complexes which lead to the respective aryl and benzylic activated species.[2,28,34]

Both organometallic compounds formed during the reaction are completely separable to permit full characterization of each. Of interest is the $^1$H NMR resonance observed for the *ortho*-hydrogen of the major product, **2.5**, in $C_6D_6$ (δ 6.12) which is a common spectral feature found for ortho H atoms of other hydrocarbyl complexes containing methyl-substituted aryl ligands.[2,18]

A single-crystal X-ray crystallographic analysis has been performed[35] on complex **2.5**, and its ORTEP diagram is displayed in Figure 2.5. As expected, the solid-state structure of **2.5** is similar to that of **2.1**, although most interestingly, the W(1)-C(16)-C(17) bond angle (126.3(4)°) deviates from the anticipated value of 120°. This appears to be a general feature found in the solid-state molecular structures of other transition-metal nitrosyl complexes containing *o*-methylated aryl ligands[2,24] and can be rationalized by relief of steric hindrance between the *o*-methyl group and the W(1)-C(16) linkage. These other compounds are also observed to be thermally unstable and undergo decomposition by β-H elimination, which is a manifestation of the distorted W(1)-C(16)-C(17) bond

angle, placing the β-H of the aryl ligand near the metal-centered LUMO.[2] However, it appears that the presence of the dimethylallyl moiety may stabilize **2.5** as the electronically saturated 18e compound, much like the $\eta^2$-vinyl species in related complexes.[36]

The thermolyses of **1.1** in *m*- and *o*-xylene yield similar findings. The thermal reaction with *m*-xylene yields three products, namely Cp*W(NO)($CH_2C_6H_4$-3-Me)($\eta^3$-1,1-$Me_2C_3H_3$) (**2.6**), Cp*W(NO)($C_6H_3$-2,4-$Me_2$)($\eta^3$-1,1-$Me_2C_3H_3$) (**2.7**) and Cp*W(NO)($C_6H_3$-3,5-$Me_2$)($\eta^3$-1,1-$Me_2C_3H_3$) (**2.8**) (eq. 2.5).

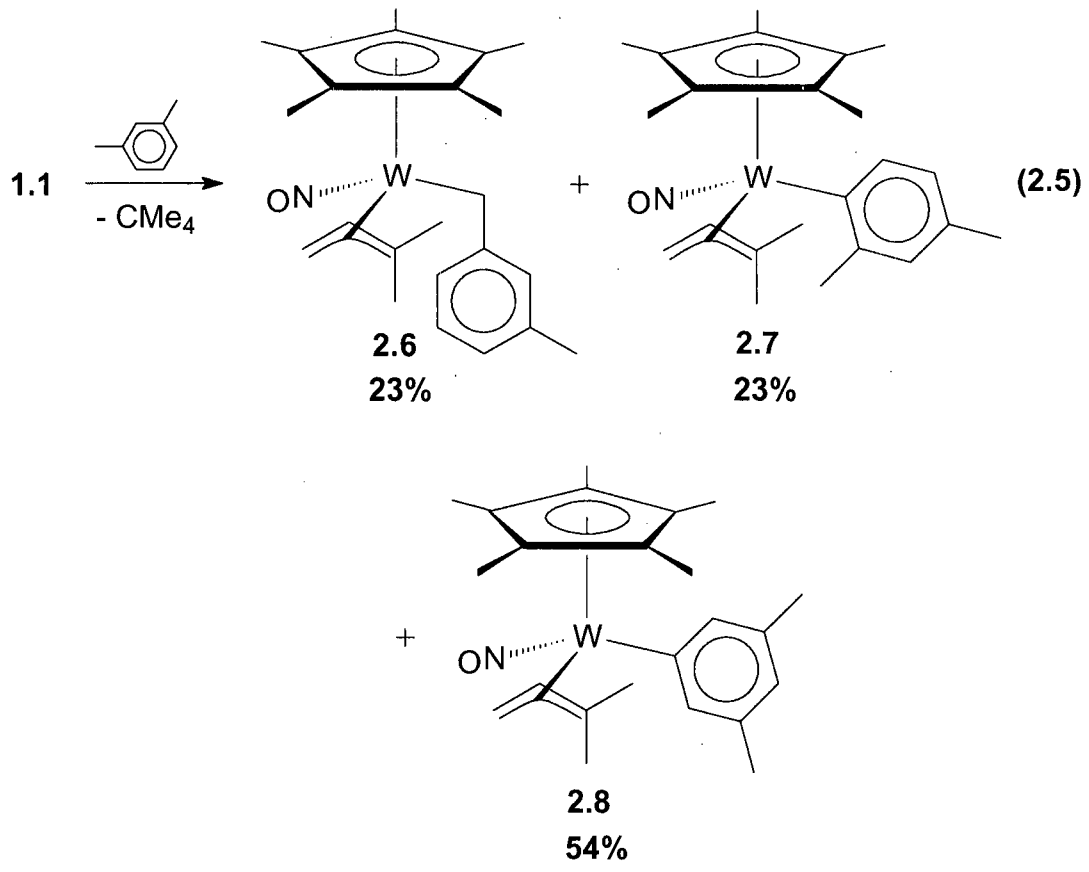

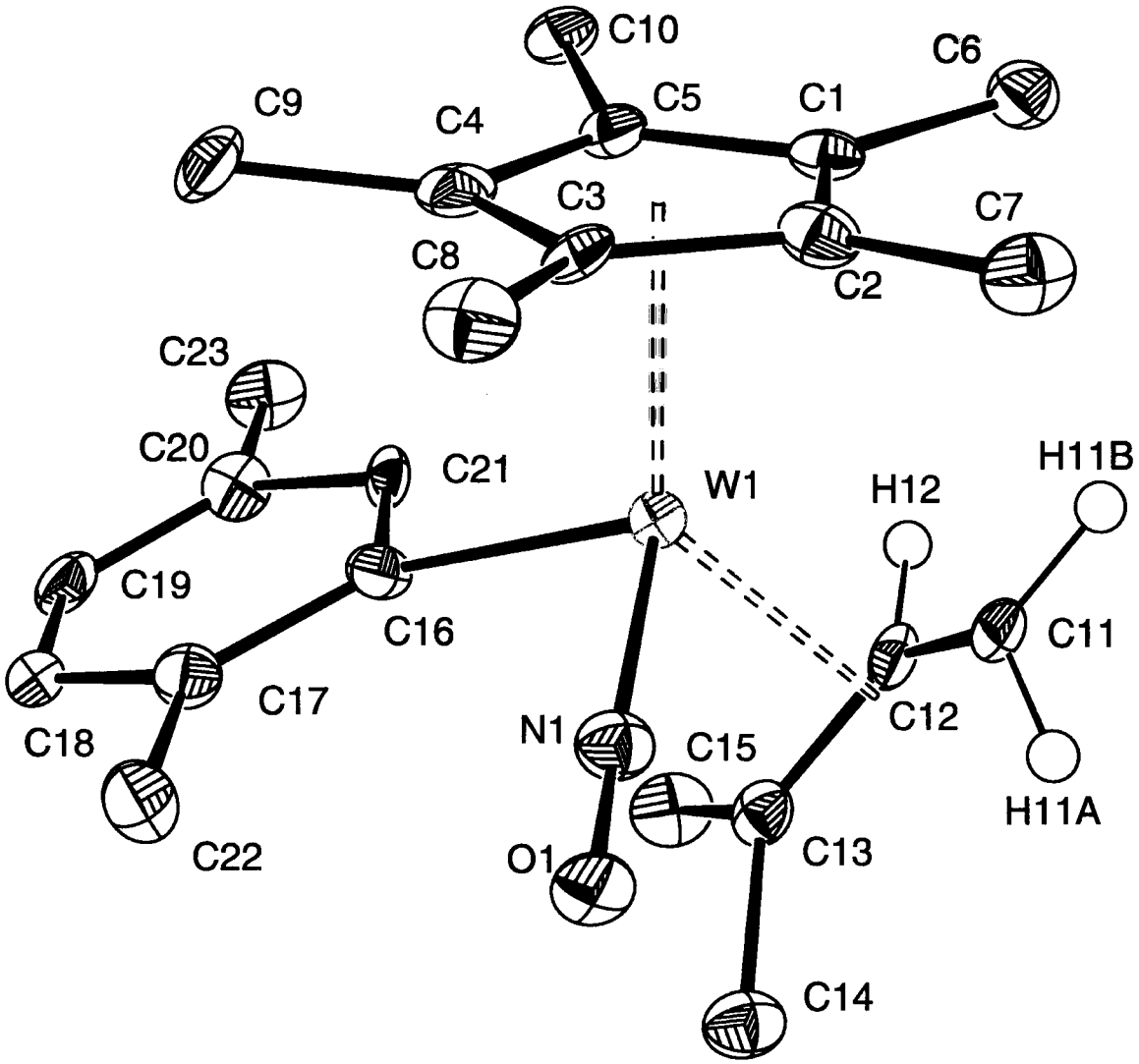


**Figure 2.5** Solid-state molecular structure of Cp*W(NO)($C_6H_3$-2,5-$Me_2$)($\eta^3$-1,1-$Me_2C_3H_3$) (**2.5**) with 50 % probability thermal ellipsoids shown. Selected interatomic distances (Å) and angles (deg): W(1)-N(1) = 1.762(5), W(1)-C(11) = 2.235(6), W(1)-C(12) = 2.363(6), W(1)-C(13) = 2.776(6), W(1)-C(16) = 2.205(6), C(11)-C(12) = 1.438(9), C(12)-C(13) = 1.371(9), N(1)-O(1) = 1.232(7), W(1)-N(1)-O(1) = 168.6(5), W(1)-C(16)-C(17) = 126.3(4), C(11)-C(12)-C(13) = 124.5(6), W(1)-C(11)-C(12) = 76.7(4), C(12)-C(13)-C(14) = 124.6(6), C(14)-C(13)-C(15) = 113.8(6)

Not surprisingly, the product ratio obtained is comparable to that for the benzylic and aryl activated species of complexes **2.4** and **2.5**. Notably, within the two aryl C-H activated species, **2.8** is over two times more prevalent than **2.7** even though statistically, there should be twice the amount of **2.7** over **2.8**. This distribution can be attributed to steric factors that favour the possible formation of π-arene complexes as far removed as possible from the methyl substituents to yield a final product with the methyls meta to the W-C(aryl) linkage, and again is an indication of the thermodynamically favoured product ratio.

The thermal reaction of **1.1** with *o*-xylene generates three organometallic products, namely Cp*W(NO)($CH_2C_6H_4$-2-Me)($\eta^3$-1,1-$Me_2C_3H_3$) (**2.9**), Cp*W(NO)($C_6H_3$-2,3-$Me_2$)($\eta^3$-1,1-$Me_2C_3H_3$) (**2.10**) and Cp*W(NO)($C_6H_3$-3,4-$Me_2$)($\eta^3$-1,1-$Me_2C_3H_3$) (**2.11**) (eq. 2.6).

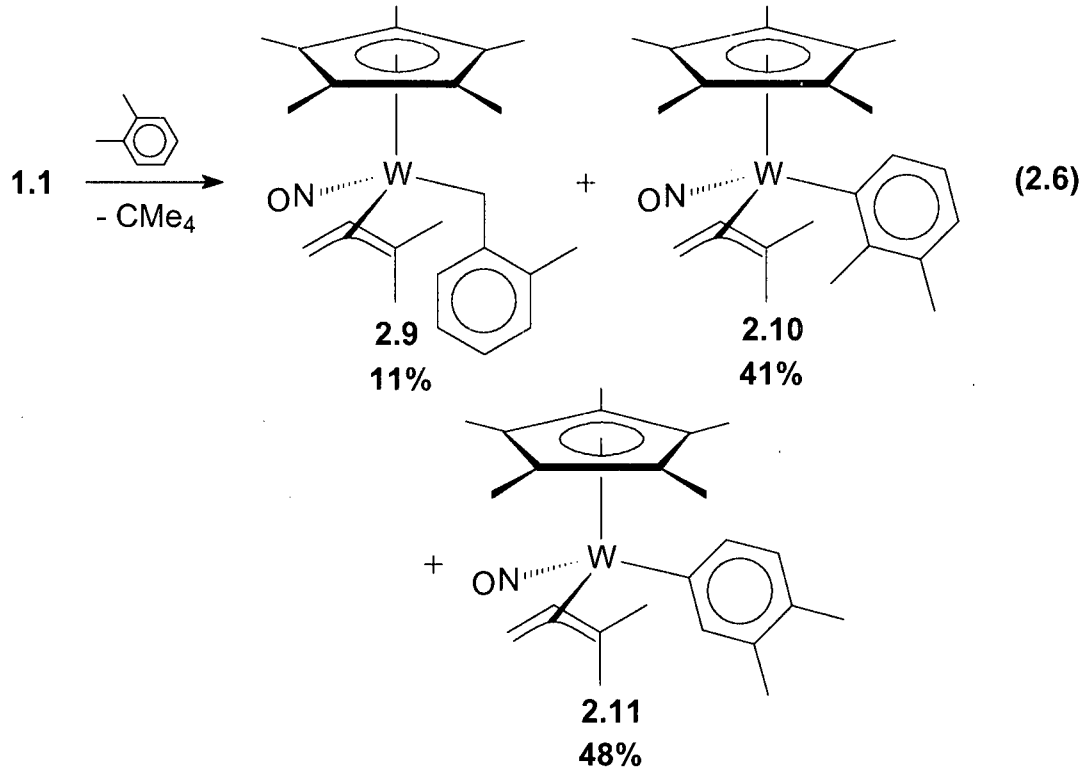


(2.6)

The most striking difference between the product ratio observed is the markedly decreased proportion of the benzylic C-H activated species. Interestingly, the observed trend of decreasing proportions of benzylic activation in different xylene solvents (para > meta > ortho) is analogous to that seen for other related complexes.[2] This feature is perhaps a manifestation of steric hindrance imposed by the adjacent methyl group, subsequently increasing the preference for the formation of the aryl-activated complexes.

### 2.2.3.2 Thermolysis of 1.1 in Toluene

The thermolysis of **1.1** in toluene leads to the generation of all four products of C-H activation, specifically Cp*W(NO)($CH_2C_6H_5$)($\eta^3$-1,1-$Me_2C_3H_3$) (**2.12**), Cp*W(NO)($C_6H_4$-2-Me)($\eta^3$-1,1-$Me_2C_3H_3$) (**2.13**), Cp*W(NO)($C_6H_4$-3-Me)($\eta^3$-1,1-$Me_2C_3H_3$) (**2.14**) and Cp*W(NO)($C_6H_4$-4-Me)($\eta^3$-1,1-$Me_2C_3H_3$) (**2.15**) (eq. 2.7). Complexes **2.12** - **2.15** were characterized as a mixture, and thus many of the resonances expected for each individual compound were not discernable due to overlapping signals, despite extensive use of a multitude of advanced NMR spectroscopic techniques.

Again, the product ratio observed for complexes **2.12** – **2.15** reflects the thermodynamic distributions for benzylic and aryl C-H bond activations initiated by **1.1** under thermal conditions. This notion is supported by the similar proportion of aryl:benzyl species compared to the ratios observed for products from activation of C-H bonds of *m*- and *p*- xylene, and that now statistically there are more sites for formation of the W-C(aryl) linkages with toluene.

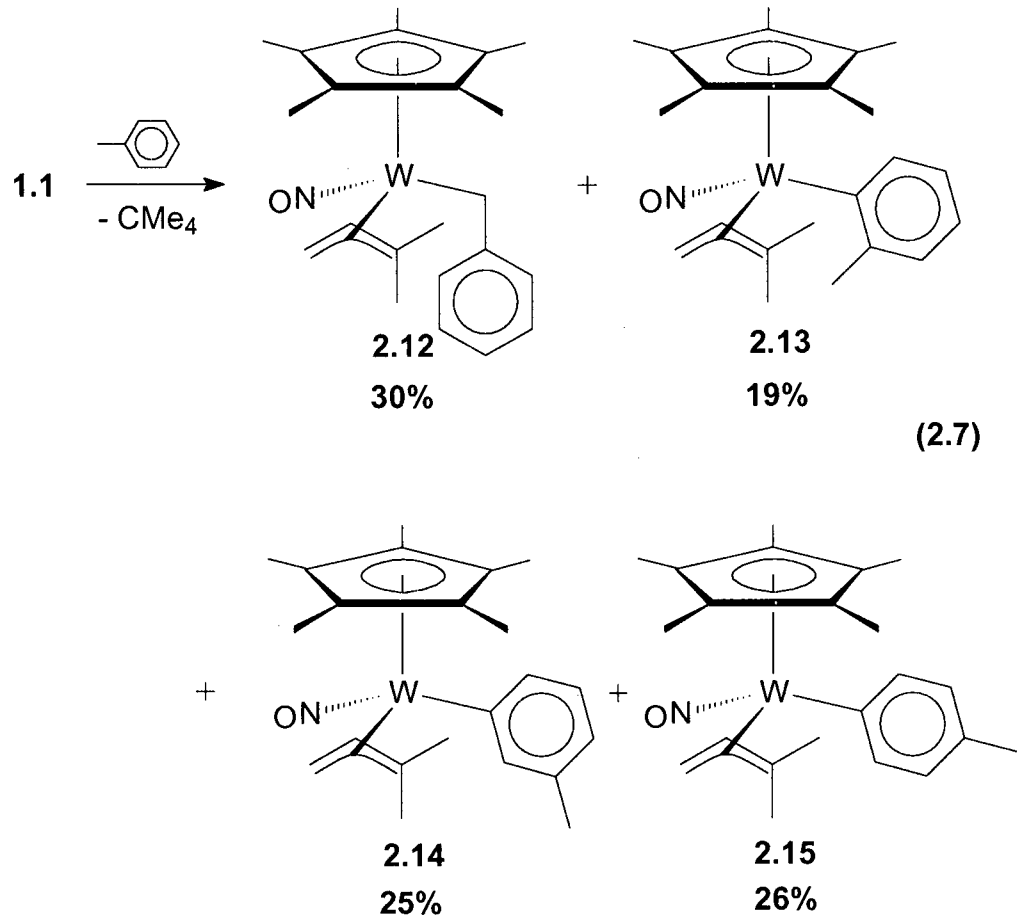


Similar to the spectroscopic features exhibited by the mesityl-dimethylallyl complex (**2.3**), the $^1$H NMR spectrum ($C_6D_6$) of **2.12** displays elements indicative of fast rotation about the W-C bond on the NMR timescale, namely the sharp resonances observed for all of the aryl C-H moieties and the equivalent signals attributable to the *m*- and *o*-aryl C-H linkages (δ 7.32 and 7.71, respectively).

### 2.2.3.3 Attempts to Independently Synthesize Complexes 2.4 – 2.15

Since more than one organometallic species was anticipated from the reactions of **1.1** in methyl-substituted arenes, Cp*W(NO)($\eta^3$-1,1-$Me_2C_3H_3$)(Cl) (**2.16**), has been synthesized with the goal of independently preparing the predicted products, as judged by crude $^1$H NMR spectroscopic data of the final reaction mixtures. Relevant hydrocarbyl metatheses of **2.16** with suitable Grignard reagents have been attempted but, led to the formation of intractable products (eq. 2.8). Other techniques are utilized to isolate the products formed for characterization purposes and these are described in Section 2.4.

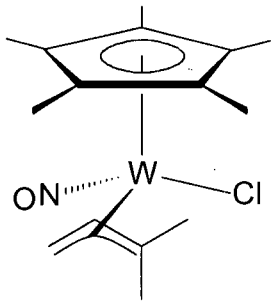


**2.16**

$R_2Mg{\cdot}x$(dioxane)

intractable products **(2.8)**

## 2.3 Epilogue

The studies discussed in this Chapter have elucidated the scope of single C-H bond activations via thermal reactions of **1.1** in the chosen hydrocarbon solvents. In addition, the thermodynamic preference for aryl activations over benzylic are evident in the product distributions observed for the thermolyses with *p*- and *m*-xylene and toluene. Similar reactions conducted with *o*-xylene and mesitylene yield product ratios that are suggestive of steric hindrance of benzylic and aryl C-H activation, respectively. Aside from the exclusive formation of **2.3** from reaction of **1.1** in mesitylene, all other thermolyses performed yield products resulting from the activations of all C-H bonds found in the substrate.

That there appears to be no evidence for the formation of the bis(trimethylsilylmethyl), benzyl-aryl or the bis(mesityl) species upon reaction of **1.1** in tetramethylsilane, toluene, and mesitylene respectively, indicates that the dimethylallyl ligand is not prone to elimination from the metal's coordination sphere to form the reactive alkylidene and benzylidene species which are known to have C-H activating abilities.[1,2]

## 2.4 Experimental Procedures

### 2.4.1 Preparative Thermolyses of 1.1 in Hydrocarbon Solvents: General Comments

Unless otherwise noted, the following general procedure was used to prepare new compounds via thermolysis of **1.1**: a 30 mL bomb was charged with the reported amount of **1.1**, a magnetic stir bar, and sufficient solvent to yield an approximately 10 % (w/w) orange solution. The solvent was either directly pipetted into the reaction vessel from a storage bomb inside a glovebox, or vacuum transferred onto the orange microcrystals on a vacuum line. The sealed bomb was then heated at 50 °C for a period of 6 hours in a VWR Scientific Products Circulating Bath 1160A. During this time, the appearance of the reaction mixture either remained unchanged (deep-orange) or it lightened to an orange-yellow colour. Alternatively, it darkened to a brown colour, whereupon further steps were necessary to extract and isolate the analytically pure organometallic products. The reaction bomb was removed from the bath, and the reaction was quenched by placing the bomb under a flow of cold water, or dipping into a cold bath. The volatiles were removed in vacuo, and the resulting residue was dried under high vacuum for a suitable period of time. It was then dissolved in $C_6D_6$, and the crude $^1H$ NMR spectral data were obtained to determine the number of principal organometallic products present, and the ratios in which they were formed. Average product ratios were determined via multiple integrations of like signals in the $^1H$ NMR spectrum of the final reaction mixture. The NMR solvent was then removed, and the residue was redissolved in the reported solvent or solvent mixtures for recrystallization of the products. The solutions were then

concentrated to the point of incipient crystallization and cooled for a suitable amount of time at – 30 °C, to obtain the organometallic products as crystals. The reported yields are not optimized.

### 2.4.2 Thermolysis of 1.1 in Benzene-$d_6$

Complexes **2.1**-$d_{6a\text{-}c}$ were prepared by the thermolysis of **1.1** (10 mg, 0.02 mmol) in benzene-$d_6$. Yellow crystals of complexes **2.1**-$d_{6a\text{-}c}$ were obtained via crystallization of the residue from 4:1 $Et_2O$/hexanes.

**2.1**-$d_{6a\text{-}c}$: MS (LREI, *m/z*, probe temperature 120 °C) 501 [$P^+$, $^{184}W$]. $^1H$ NMR (400 MHz, $C_6D_6$) δ 0.82 (s, 3H, allyl Me), 1.51 (s, 15H, $C_5Me_5$), 1.62 (br s, 3H allyl Me), 1.73 (br m, 1H, allyl $CH_2$), 2.48 (br m, 1H, allyl $CH_2$), 3.52 (br m, 1H, allyl CH). $^2H\{^1H\}$ NMR (61 MHz, $C_6H_6$) δ 0.78 (allyl Me-$d_1$), 1.61 (allyl Me-$d_1$), 3.52 (allyl CD), 6.60-8.4 (Ph D)

### 2.4.3 Preparation of Cp*W(NO)($C_6H_5$)($\eta^3$-1,1-$Me_2C_3H_3$) (2.1)

Complex **2.1**, first prepared by Craig Adams,[17] was formed during the thermolysis of **1.1** (48 mg, 0.10 mmol) in benzene. Complex **2.1** was isolated as yellow microcrystals by recrystallization of the residue from 4:1 $Et_2O$/hexanes (34 mg, 70 %).

**2.1**: IR ($cm^{-1}$) 1562 (s, $\nu_{NO}$). MS (LREI, *m/z*, probe temperature 150 °C) 495 [$P^+$, $^{184}W$]. $^1H$ NMR (300 MHz, $C_6D_6$) δ 0.82 (s, 3H, allyl Me), 1.51 (s, 15H, $C_5Me_5$), 1.62 (br s, 3H, allyl Me), 1.74 (br m, 1H, allyl $CH_2$), 2.49 (br m, 1H, allyl $CH_2$), 3.54 (br m, 1H, allyl CH), 6.64 (br d, 1H, Ph $H_{ortho}$), 7.08 (t, $^3J_{HH}$ = 7.1, 1H, Ph $H_{para}$), 7.30 (m, 2H, Ph $H_{meta}$), 8.39 (d, $^3J_{HH}$ = 6.7, 1H, Ph $H_{ortho}$); $^1H$ NMR (400 MHz, $CDCl_3$) δ 0.87 (s, 3H, allyl Me), 1.51 (br s, 3H, allyl Me), 1.76 (s, 15H, $C_5Me_5$), 1.90 (br m, 1H, allyl $CH_2$), 2.42 (br m, 1H, allyl $CH_2$), 3.73 (br m, 1H, allyl CH), 6.68 (br d, 1H, Ph $H_{ortho}$), 6.93 (t, $^3J_{HH}$ = 7.1, 1H, Ph $H_{para}$), 7.12 (q, $^3J_{HH}$ = 7.0, 2H, Ph $H_{meta}$), 7.86 (d, $^3J_{HH}$ = 6.4, 1H, Ph $H_{ortho}$). $^{13}C\{^1H\}$ NMR (75 MHz, $CDCl_3$) δ 10.4 ($C_5\mathit{Me}_5$), 21.8, 29.4 (allyl Me), 37.6 (allyl $CH_2$), 95.3 (allyl CH), 107.6 ($\mathit{C}_5Me_5$), 123.4 (Ph $C_{para}$), 126.8, 127.9 (Ph $C_{meta}$), 139.6, 141.9 (Ph $C_{ortho}$), 148.5 (allyl C), 168.8 (Ph $C_{ipso}$). Sel NOE (400 MHz, $C_6D_6$) δ irrad. at 3.54, NOE at 0.82, 1.51 and 1.74, irrad. at 0.82, NOE at 1.51, 1.63, 3.54, 6.64, 8.39. Anal. Calcd. for $C_{21}H_{29}NOW$: C, 50.92; H, 5.90; N, 2.83. Found: C, 50.61; H, 5.95; N, 2.92.

### 2.4.4 Preparation of Cp*W(NO)($CH_2SiMe_3$)($\eta^3$-1,1-$Me_2C_3H_3$) (2.2)

Complex **2.2** was prepared via thermolysis of **1.1** (75 mg, 0.15 mmol) in tetramethylsilane. The reaction mixture was then cooled overnight in a freezer (- 30 °C) to obtain orange needles of **2.2** (47 mg, 61 %)

**2.2**: IR ($cm^{-1}$) 1549 (s, $\nu_{NO}$). MS (LREI, *m/z*, probe temperature 80 °C) 505 [$P^+$, $^{184}W$]. $^1H$ NMR (400 MHz, $C_6D_6$) δ –0.78 (d, $^2J_{HH}$ = 14.09, 1H, $SiCH_2$), –0.59 (d, $^2J_{HH}$ = 14.09, 1H, $SiCH_2$), 0.45 (s, 9H, $SiMe_3$), 0.61 (s, 3H, allyl Me ), 1.12 (s, 3H, allyl Me), 1.18 (m, 1H, allyl $CH_2$), 1.51 (s, 15H, $C_5Me_5$), 2.55 (m, 1H, allyl $CH_2$), 4.43 (m, 1H, allyl CH). $^{13}C\{^1H\}$ NMR (125 MHz, $C_6D_6$) δ 2.01 ($SiCH_2$), 4.34 ($SiMe_3$), 10.2 ($C_5\mathit{Me}_5$), 19.6, 28.9 (allyl Me), 39.3 (allyl $CH_2$), 101.9 (allyl CH), 106.9 ($\mathit{C}_5Me_5$). Sel NOE (400 MHz, $C_6D_6$) δ irrad. at 0.61, NOE at –0.78, 0.45, 1.12, 1.18, 1.51 and 2.55. Anal. Calcd. for $C_{19}H_{35}NOSiW$: C, 45.15; H, 6.98; N, 2.77. Found: C, 45.37; H, 6.92; N, 2.90.

### 2.4.5 Preparation of Cp*W(NO)($CH_2C_6H_3$-3,5-$Me_2$)($\eta^3$-1,1-$Me_2C_3H_3$) (2.3)

Complex **2.3** was prepared by the thermolysis of **1.1** (79 mg, 0.16 mmol) in mesitylene. The volume was reduced to 2 mL, and hexanes (10 mL) were added via a syringe. Cooling of the mixture resulted in the crystallization of **2.3** as orange microcrystals (57 mg, 66 %).

**2.3**: IR ($cm^{-1}$) 1533 (s, $\nu_{NO}$). MS (LREI, *m/z*, probe temperature 120 °C) 537 [$P^+$, $^{184}W$]. $^1H$ NMR (400 MHz, $C_6D_6$) δ 1.08 (s, 3H, allyl Me), 1.17 (s, 3H, allyl Me), 1.46 (s, 15H, $C_5Me_5$), 1.52 (obs, 1H, allyl $CH_2$), 1.79 (d, $^2J_{HH}$ = 9.46, 1H, Mes $CH_2$), 2.38 (s, 6H, Mes $Me_2$), 2.45 (m, 1H, allyl $CH_2$), 2.80 (d, $^2J_{HH}$ = 9.46, 1H, Mes $CH_2$), 3.58 (s, 1H, allyl CH), 6.72 (s, 1H, Mes $H_{\mathit{para}}$), 7.38 (s, 2H, Mes $H_{\mathit{ortho}}$). $^{13}C\{^1H\}$ NMR (125 MHz, $C_6D_6$) δ 9.88 ($C_5\mathit{Me}_5$), 20.63 (allyl Me), 22.03 (Mes $Me_2$), 27.65 (allyl Me), 28.23 (allyl $CH_2$),

39.69 (Mes $CH_2$), 98.86 (allyl CH), 106.49 ($C_5Me_5$), 125.24 (Mes *p*-CH), 128.70 (Mes *o*-CH ), 152.4 (allyl C), 136.5, 169.2 ($C_{aryl}$). Sel NOE (400 MHz, $C_6D_6$) δ irrad. at 3.58, NOE at 1.08, 1.52, 2.45, irrad. at 1.08, NOE at 1.17, 1.46, 1.79, 2.80, 3.58 and 7.38. Anal. Calcd. for $C_{24}H_{35}NOW$: C, 53.64; H, 6.56; N, 2.61. Found: C, 53.80; H, 6.61; N, 2.75.

### 2.4.6 Reaction Products of Thermolyses of 1.1 in Toluene and *o*, *m*, *p*-Xylenes

Thermolysis of **1.1** in toluene and xylene solvents yielded final reaction mixtures with multiple organometallic products due to activation of different C-H bonds present in the hydrocarbons. For the various reaction mixtures, the residues remaining after the reaction solvent had been removed were triturated with pentane (3 x 10 mL) to alleviate the oily appearance. Solid product was isolated via crystallization from hexanes. It was then possible to separate the benzylic C-H activated product from the aryl C-H activated species via two possible methods:

a. Preparative thin-layer chromatography on an alumina (I) plate (20 x 20 x 0.15 cm)

b. Column chromatography through an alumina (I) column (0.5 x 3 cm)

The former separation technique was utilized once for the products from reaction of **1.1** in *p*-xylene and this is discussed in Section 2.4.7. The latter technique was employed for the remainder of the product separations. The products isolated via crystallization were dissolved in a 1:5 $Et_2O$/hexanes solvent mix and eluted through the column described

above which was pre-wetted with the eluting solvent. A yellow eluate resulted which upon concentration and cooling to – 30 °C overnight yielded solely the aryl C-H activated products. Eluting the column with 1:4 $Et_2O$/hexanes gave a solution consisting of small amounts of both aryl and benzylic C-H activated species. Stripping the alumina column with $Et_2O$ yielded an orange solution which upon addition of hexanes, and then subsequent concentration and cooling to – 30 °C overnight yielded solely the benzylic C-H activated product.

### 2.4.7 Preparation of Cp*W(NO)($CH_2C_6H_4$-4-Me)($\eta^3$-1,1-$Me_2C_3H_3$) (2.4) and Cp*W(NO)($C_6H_3$-2,5-$Me_2$)($\eta^3$-1,1-$Me_2C_3H_3$) (2.5)

Complexes **2.4** – **2.5** were formed via the thermolysis of **1.1** (292 mg, 0.60 mmol) in *p*-xylene. The resulting residue following removal of solvent was an orange/yellow oil. The solid products obtained after work-up as outlined in Section 2.4.6 were dissolved in a minimal amount of THF and applied to a preparative-TLC plate using a syringe (26 gauge), leaving a 10 mm thick orange/yellow band. The plate was left to sit for 30 minutes to allow evaporation of the THF solvent. The plate was then loaded into a development chamber charged with $Et_2O$ (200 mL) and sealed to minimise solvent loss and ensure maximum vapour saturation. After 70 minutes of development, the plate was removed from the chamber and allowed to dry. No clear separation was evident, but a definite region was visible where the band was lighter in colour. The alumina above this region was scraped off and stripped of any organometallic product with THF and subsequently filtered thru a Celite plug to obtain a yellow solution that upon

recrystallization from 1:4 $Et_2O$/hexanes yielded yellow needles of complex **2.5** (53 mg, 17 %). The alumina below the lighter region was treated in a similar fashion to obtain orange needles of complex **2.4** (24 mg, 8 %).

### 2.4.8 Preparation of Cp*W(NO)($CH_2C_6H_4$-3-Me)($\eta^3$-1,1-$Me_2C_3H_3$) (2.6), Cp*W(NO)($C_6H_3$-2,4-$Me_2$)($\eta^3$-1,1-$Me_2C_3H_3$) (2.7) and Cp*W(NO)($C_6H_3$-3,5-$Me_2$)($\eta^3$-1,1-$Me_2C_3H_3$) (2.8)

Complexes **2.6** – **2.8** were prepared via the thermolysis of **1.1** (100 mg, 0.20 mmol) in m-xylene. The resulting residue following removal of solvent was an orange/yellow oil. Subsequent work-up and separation of products as outlined in Section 2.4.6 afforded complex **2.6** as orange blocks (15 mg, 14 %) and a mixture of complexes **2.7** and **2.8** as orange/yellow microcrystals (40 mg, 37 %).

### 2.4.9 Preparation of Cp*W(NO)($CH_2C_6H_4$-2-Me)($\eta^3$-1,1-$Me_2C_3H_3$) (2.9), Cp*W(NO)($C_6H_3$-2,3-$Me_2$)($\eta^3$-1,1-$Me_2C_3H_3$) (2.10) and Cp*W(NO)($C_6H_3$-3,4-$Me_2$)($\eta^3$-1,1-$Me_2C_3H_3$) (2.11)

Complexes **2.9** – **2.11** were formed by the thermolysis of **1.1** (205 mg, 0.42 mmol) in *o*-xylene. The resulting residue following removal of solvent was an orange/yellow oil. Subsequent work-up and separation of products as outlined in Section 2.4.6 afforded complex **2.9** as orange microcrystals (21 mg, 10 %) and a mixture of complexes **2.10** and **2.11** as orange/yellow microcrystals (56 mg, 26 %).

### 2.4.10 Preparation of $Cp^*W(NO)(CH_2C_6H_5)(\eta^3\text{-}1,1\text{-}Me_2C_3H_3)$ (2.12), $Cp^*W(NO)(C_6H_4\text{-}2\text{-}Me)(\eta^3\text{-}1,1\text{-}Me_2C_3H_3)$ (2.13), $Cp^*W(NO)(C_6H_4\text{-}3\text{-}Me)(\eta^3\text{-}1,1\text{-}Me_2C_3H_3)$ (2.14) and $Cp^*W(NO)(C_6H_4\text{-}4\text{-}Me)(\eta^3\text{-}1,1\text{-}Me_2C_3H_3)$ (2.15)

Complexes **2.12 – 2.15** were prepared via the thermolysis of **1.1** (200 mg, 0.41 mmol) in toluene. After the 6 hour reaction period, the resulting solution was a dark orange/brown colour which yielded a brown oil upon solvent removal under vacuum. Subsequent work-up and separation of products as outlined in Section 2.4.7 afforded complex **2.12** and a mixture of complexes **2.13** – **2.15** as orange/yellow blocks (156 mg, 75 %). Complex **2.12** was independently synthesized via metathesis for characterization purposes (see Section 2.4.11).

### 2.4.11 Independent Preparation of 2.12 via Metathesis

Complex **2.12** was prepared by a method similar to the procedure published for $Cp^*W(NO)(CH_2C_6H_5)(CH_2CMe_3)$.[1] In the glovebox, a 100-mL Schlenk tube was charged with a magnetic stir bar and $(1,1\text{-}Me_2C_3H_3)_2Mg{\cdot}x$(dioxane) (103 mg, 0.53 mmol). A 200-mL Schlenk tube was then charged with a stir bar and $Cp^*W(NO)(CH_2C_6H_5)(Cl)$ (250 mg, 0.53 mmol). On a vacuum line, THF (80 mL) was vacuum transferred into the Schlenk tube containing the organometallic halide and into the Schlenk tube with the magnesium reagent (10 mL). The two resulting solutions were then mixed at – 78 °C over a period of 5 minutes via a cannula, whereupon the initial deep-red colour of the solution changed to orange/yellow after being stirred at – 78 °C for 10 minutes. The resulting

solution was then warmed to 0 °C and allowed to react for 1 hour. The solvent was then removed at 0 °C over a period of 30 minutes. The product was extracted from the residue with $CH_2Cl_2$ (3 x 10 mL) and filtered through an alumina (I) plug (2 x 3 cm) supported on a frit to yield a yolk-orange solution. The $CH_2Cl_2$ was removed under vacuum, and the residue was dissolved in a 2:1 $Et_2O$/hexanes mix, which afforded complex **2.12** as yellow and orange blocks after subsequent concentration to its incipient crystallization point and cooling to – 30 °C for 2 hours (138 mg, 52 %).

**Table 2.1** Numbering Scheme, Yield and Analytical Data for Complexes **2.4** – **2.15**

| Complex | Cmpd No. | Colour (yield, %[a]) | Anal. Calcd. % (Found %) C | H | N |
|---|---|---|---|---|---|
| **Cp*W(NO)($CH_2C_6H_4$-4-Me)($\eta^3$-1,1-$Me_2C_3H_3$)** | **2.4** | orange (8) | 52.78 (52.66) | 6.36 (6.26) | 2.68 (2.75) |
| **Cp*W(NO)($C_6H_3$-2,5-$Me_2$)($\eta^3$-1,1-$Me_2C_3H_3$)** | **2.5** | yellow (17) | 52.78 (52.67) | 6.36 (6.26) | 2.68 (2.66) |
| **Cp*W(NO)($CH_2C_6H_4$-3-Me)($\eta^3$-1,1-$Me_2C_3H_3$)** | **2.6** | orange (14) | 52.78 (52.76) | 6.36 (6.20) | 2.68 (2.71) |
| **Cp*W(NO)($C_6H_3$-2,4-$Me_2$)($\eta^3$-1,1-$Me_2C_3H_3$)** | **2.7** | yellow (37)[b] | 52.78 (52.54)[b] | 6.36 (6.43)[b] | 2.68 (2.83)[b] |
| **Cp*W(NO)($C_6H_3$-3,5-$Me_2$)($\eta^3$-1,1-$Me_2C_3H_3$)** | **2.8** | *b* | *b* | *b* | *b* |
| **Cp*W(NO)($CH_2C_6H_4$-2-Me)($\eta^3$-1,1-$Me_2C_3H_3$)** | **2.9** | orange (10) | 52.78 (53.02) | 6.36 (6.36) | 2.68 (2.92) |
| **Cp*W(NO)($C_6H_3$-2,3-$Me_2$)($\eta^3$-1,1-$Me_2C_3H_3$)** | **2.10** | yellow (26)[c] | 52.78 (52.93)[c] | 6.36 (6.37)[c] | 2.68 (2.61)[c] |
| **Cp*W(NO)($C_6H_3$-3,4-$Me_2$)($\eta^3$-1,1-$Me_2C_3H_3$)** | **2.11** | *c* | *c* | *c* | *c* |
| **Cp*W(NO)($CH_2C_6H_5$)($\eta^3$-1,1-$Me_2C_3H_3$)** | **2.12** | orange (52) | 51.88 (51.95) | 6.13 (6.25) | 2.75 (2.86) |
| **Cp*W(NO)($C_6H_4$-2-Me)($\eta^3$-1,1-$Me_2C_3H_3$)** | **2.13** | yellow (75)[d] | 51.88 (51.84)[d] | 6.13 (6.49)[d] | 2.75 (2.85)[d] |
| **Cp*W(NO)($C_6H_4$-3-Me)($\eta^3$-1,1-$Me_2C_3H_3$)** | **2.14** | *d* | *d* | *d* | *d* |
| **Cp*W(NO)($C_6H_4$-4-Me)($\eta^3$-1,1-$Me_2C_3H_3$)** | **2.15** | *d* | *d* | *d* | *d* |

*a*: isolated yield, *b*: characterized as a mixture of **2.7** – **2.8**, *c*: characterized as a mixture of **2.10** – **2.11**, *d*: characterized as a mixture of **2.13** – **2.15**

**Table 2.2** MS and IR Characterization Data for Complexes **2.4 – 2.15**

| Compound No. | MS (LREI, *m/z*) | Probe temperature (°C) | IR ($\nu_{NO}$, KBr, $cm^{-1}$) |
|---|---|---|---|
| **2.4** | 523 | 120 | 1553 |
| **2.5** | 523 | 120 | 1567 |
| **2.6** | 523 | 120 | 1560 |
| **2.7 - 2.8**[a] | 523 | 120 | 1552 |
| **2.9** | 523 | 150 | 1552 |
| **2.10 – 2.11**[a] | 523 | 150 | 1552 |
| **2.12** | 509 | 120 | 1552[b] |
| **2.13 - 2.15**[a] | 509 | 120 | 1561 |

*a*: characterized as a mixture, *b*: Nujol mull recorded on ATI Mattson-Genesis FTIR

**Table 2.3** NMR Characterization Data for Complexes **2.4** – **2.15**

| Compound no. | $^1$H NMR ($C_6D_6$) δ | $^{13}$C {1H} NMR ($C_6D_6$) δ |
|---|---|---|
| **2.4**[a] | 1.07 (s, 3H, allyl Me) | 9.7 ($C_5Me_5$) |
| | 1.15 (s, 3H, allyl Me) | 20.5 (allyl Me) |
| | 1.46 (s, 15H, $C_5Me_5$) | 21.0 (Pxyl Me) |
| | 1.46 (obs, 1H, allyl $CH_2$) | 27.4 (allyl Me) |
| | 1.80 (m, 1H, $^2J_{HH}$ = 11.6, Bzl $CH_2$) | 35.2 (Bzl $CH_2$) |
| | 2.26 (s, 3H, Pxyl Me) | 39.6 (allyl $CH_2$) |
| | 2.43 (m, 1H, allyl $CH_2$) | 98.3 (allyl CH) |
| | 2.77 (m, 1H, $^2J_{HH}$ = 11.6, Bzl $CH_2$) | 106.3 ($C_5Me_5$) |
| | 3.56 (m, 1H allyl CH) | 124.8 (Pxyl *p*-CH) |
| | 7.13 (obs , 2H, Pxyl *m*-CH) | 128.0 (obs Pxyl *o*-CH) |
| | 7.62 (d, 2H, $^3J_{HH}$ = 7.6, Pxyl *o*-CH) | 130.4 (Pxyl *m*-CH) |
| | | 149.8 (allyl C) |
| **2.5**[b] | 0.80 (s, 3H, allyl Me) | 10.2 ($C_5Me_5$) |
| | 1.54 (2, 15H, $C_5Me_5$) | 21.0 (Xyl Me) |
| | 1.74 (s, 3H, allyl Me) | 22.6 (allyl Me) |
| | 1.79 (m, 1H, allyl $CH_2$) | 27.6 (Xyl Me) |
| | 2.18 (s, 3H, Xyl Me) | 28.6 (allyl Me) |
| | 2.50 (m, 1H, allyl $CH_2$) | 39.6 (allyl $CH_2$) |
| | 2.80 (s, 3H, Xyl Me) | 96.1 (allyl CH) |
| | 3.70 (m, 1H, allyl CH) | 107.3 ($C_5Me_5$) |
| | 6.12 (s, 1H, Xyl *o*-CH) | 124.8 (Xyl CH) |
| | 6.77 (d, 1H, $^3J_{HH}$ = 7.4, Xyl CH) | 130.4 (Xyl CH) |
| | 7.25 (d, 1H, $^3J_{HH}$ = 7.4, Xyl CH) | 140.4 (Xyl *o*-CH) |
| | | 148.0 (allyl C) |
| | | 170.3 (Xyl $C_{ipso}$) |

**Table 2.3** NMR Characterization Data for Complexes **2.4** – **2.15**

| Compound no. | $^{1}$H NMR ($C_6D_6$) δ | $^{13}$C {1H} NMR ($C_6D_6$) δ |
|---|---|---|
| **2.6**[a] | 1.06 (s, 3H, allyl Me) | 9.7 ($C_5\mathit{Me}_5$) |
| | 1.11 (s, 3H, allyl Me) | 22.0 (Mxyl Me) |
| | 1.45 (s, 15H, $C_5Me_5$) | 27.5 (allyl Me) |
| | 1.53 (m, 1H, allyl $CH_2$) | 27.8 (Mxyl $CH_2$) |
| | 1.79 (d, 1H, $^{2}J_{HH}$ = 11.4, Mxyl $CH_2$) | 39.6 (allyl $CH_2$) |
| | 2.38 (s, 3H, Mxyl Me) | 98.2 (allyl CH) |
| | 2.46 (m, 1H, allyl $CH_2$) | 106.3 ($\mathit{C}_5Me_5$) |
| | 2.81 (d, 1H, $^{2}J_{HH}$ = 11.4, Mxyl $CH_2$) | 124.0 (Mxyl CH) |
| | 3.54 (m, 1H, allyl CH) | 128.0 (obs Mxyl CH) |
| | 6.89 (d, 1H, $^{3}J_{HH}$ = 7.3, Mxyl CH) | 128.0 (obs Mxyl CH) |
| | 7.27 (t, 1H, $^{3}J_{HH}$ = 7.5, Mxyl CH) | 131.4 (Mxyl CH) |
| | 7.54 (d, 1H, $^{3}J_{HH}$ = 7.8, Mxyl CH) | 136.5 (Mxyl C) |
| | 7.58 (s, 1H, Mxyl *o*-CH) | 153.0 (allyl C) |
| **2.7**[a,c] | 0.81 (s, 3H, allyl Me) | 10.3 ($C_5\mathit{Me}_5$) |
| | 1.54 (s, 15H, $C_5Me_5$) | 21.2 (Xyl Me) |
| | 1.74 (s, 3H, allyl Me) | 23.0 (allyl Me) |
| | 1.78 (m, 1H, allyl $CH_2$) | 28.4 (Xyl Me) |
| | 2.28 (s, 3H, Xyl Me) | 28.7 (allyl Me) |
| | 2.49 (m, 1H, allyl $CH_2$) | 39.7 (Xyl Me) |
| | 2.82 (s, 3H, Xyl Me) | 96.0 (allyl CH) |
| | 3.71 (m, 1H, allyl CH) | 107.0 ($\mathit{C}_5Me_5$) |
| | 6.22 (d, 1H, $^{2}J_{HH}$ = 7.4, Xyl CH) | 124.7 (Xyl CH) |
| | 6.82 (d, 1H, $^{2}J_{HH}$ = 7.4, Xyl CH) | 131.7 (Xyl CH) |
| | 7.15 (obs, 1H, Xyl CH) | 139.3 (Xyl CH) |

**Table 2.3** NMR Characterization Data for Complexes **2.4 – 2.15**

| Compound no. | $^1$H NMR ($C_6D_6$) δ | $^{13}$C {1H} NMR ($C_6D_6$) δ |
|---|---|---|
| **2.8**[a,c] | 0.86 (s, 3H, allyl Me) | 10.3 ($C_5Me_5$) |
| | 1.55 (s, 15H, $C_5Me_5$) | 21.4 (Xyl Me) |
| | 1.65 (bs, 3H, allyl Me) | 21.6 (Xyl Me) |
| | 1.77 (m, 1H, allyl $CH_2$) | 21.9 (allyl Me) |
| | 2.28 (s, 3H, Xyl Me) | 29.3 (allyl Me) |
| | 2.34 (s, 3H, Xyl Me) | 37.4 (allyl $CH_2$) |
| | 2.50 (m, 1H, allyl $CH_2$) | 95.6 (allyl CH) |
| | 3.56 (bm, 1H, allyl CH) | 107.3 ($C_5Me_5$) |
| | 6.30 (bs, 1H, Xyl CH) | 125.6 (Xyl CH) |
| | 6.71 (s, 1H, Xyl CH) | 138.3 (Xyl CH) |
| | 8.04 (s, 1H, Xyl CH) | 140.0 (Xyl CH) |
| **2.9**[b] | 0.81 (m, 1H, allyl $CH_2$) | 9.7 ($C_5Me_5$) |
| | 1.20 (s, 3H, allyl Me) | 20.3 (allyl Me) |
| | 1.27 (s, 3H, allyl Me) | 21.5 (Oxyl Me) |
| | 1.49 (s, 15H, $C_5Me_5$) | 26.9 (allyl Me) |
| | 2.04 (m, 1H, allyl $CH_2$) | 26.9 (Bzl $CH_2$) |
| | 2.19 (d, 1H, $^2J_{HH}$ = 10.7, Bzl $CH_2$) | 103.2 (allyl CH) |
| | 2.36 (d, 1H, $^2J_{HH}$ = 10.7, Bzl $CH_2$) | 106.5 ($C_5Me_5$) |
| | 2.45 (s, 3H, Oxyl Me) | 125.1 (Oxyl CH) |
| | 3.98 (m, 1H, allyl CH) | 125.8 (Oxyl CH) |
| | 7.05 (m, 1H, Oxyl CH) | 129.0 (Oxyl CH) |
| | 7.10 (obs 1H, Oxyl CH) | 130.1 (Oxyl CH) |
| | 7.10 (obs, 1H, Oxyl CH) | |
| | 7.23 (d, 1H, $^3J_{HH}$ = 7.0, Oxyl CH) | |

**Table 2.3** NMR Characterization Data for Complexes **2.4 – 2.15**

| Compound no. | $^{1}$H NMR ($C_6D_6$) δ | $^{13}$C {1H} NMR ($C_6D_6$) δ |
|---|---|---|
| **2.10**[a,d] | 0.85 (s, 3H, allyl Me) | 10.3 ($C_5Me_5$) |
| | 1.55 (s, 15H, $C_5Me_5$) | 19.6 (Xyl Me) |
| | 1.59 (s, 3H, allyl Me) | 19.8 (Xyl Me) |
| | 1.76 (obs, 1H, allyl $CH_2$) | 24.7 (allyl Me) |
| | 2.21 (br s, 6H, 2 Xyl Me) | 28.4 (allyl Me) |
| | 2.50 (m, 1H, allyl $CH_2$) | 37.4 (allyl $CH_2$) |
| | 3.56 (br m, 1H, allyl CH) | 95.9 (allyl CH) |
| | 6.45 (br s, 2H, 2 Xyl CH) | 106.9 ($C_5Me_5$) |
| | 7.07 (d, 1H, $^{3}J_{HH}$ = 7.4, Xyl CH) | 128.8 (Xyl CH) |
| | | 137.8 (Xyl CH) |
| | | 141.7 (Xyl CH) |
| **2.11**[a,d] | 0.88 (s, 3H, allyl Me) | 10.3 ($C_5Me_5$) |
| | 1.55 (s, 15H, $C_5Me_5$) | 19.5 (Xyl Me) |
| | 1.65 (br s, 3H, allyl Me) | 19.8 (Xyl Me) |
| | 1.76 (obs, 1H, allyl $CH_2$) | 21.8 (allyl Me) |
| | 2.18 (s, 3H, Xyl Me) | 29.4 (allyl Me) |
| | 2.27 (s, 3H, Xyl Me) | 37.3 (allyl $CH_2$) |
| | 2.50 (m, 1H, allyl $CH_2$) | 95.8 (allyl CH) |
| | 3.56 (br s, 1H, allyl CH) | 106.9 ($C_5Me_5$) |
| | 7.13 (obs, 1H, Xyl CH) | 130.2 (Xyl CH) |
| | 8.17 (obs, 1H, Xyl CH) | 140.2 (Xyl CH) |
| | 8.19 (s, 1H, Xyl CH) | 143.7 (Xyl CH) |

**Table 2.3** NMR Characterization Data for Complexes **2.4** – **2.15**

| Compound no. | $^1$H NMR ($C_6D_6$) δ | $^{13}$C {1H} NMR ($C_6D_6$) δ |
|---|---|---|
| **2.12**[b] | 1.04 (s, 3H, allyl Me) | 9.7 ($C_5Me_5$) |
| | 1.14 (s, 3H, allyl Me) | 20.5 (allyl Me) |
| | 1.43 (s, 15H, $C_5Me_5$) | 27.5 (allyl Me) |
| | 1.55 (br s, 1H, allyl $CH_2$) | 27.8 (bzl $CH_2$) |
| | 1.78 (d, 1H, $^2J_{HH}$ = 11.5, Bzl $CH_2$) | 39.8 (allyl $CH_2$) |
| | 2.46 (m, 1H, allyl $CH_2$) | 97.9 (allyl CH) |
| | 2.81 (d, 1H, $^2J_{HH}$ = 11.5, Bzl $CH_2$) | 106.4 ($C_5Me_5$) |
| | 3.52 (m, 1H, allyl CH) | 123.1 (aryl *p*-CH) |
| | 7.03 (t, 1H, $^3J_{HH}$ = 7.4, aryl *p*-CH) | 127.7 (aryl *m*-CH) |
| | 7.32 (t, 2H, $^3J_{HH}$ = 7.4, aryl *m*-CH) | 130.4 (aryl *o*-CH) |
| | 7.71 (d, 2H, $^3J_{HH}$ = 7.4, aryl *o*-CH) | 153.4 (allyl C) |
| **2.13**[a,e] | 2.26 (s, 3H, Tol Me) | 10.2 ($C_5Me_5$) |
| | 3.55 (br m, 1H, allyl CH) | 21.7 (Tol Me) |
| | 6.47 (br s, 1H, Tol CH) | 95.8 (allyl CH) |
| | 6.88 (d, 1H, $^3J_{HH}$ = 7.1, Tol CH) | 106.9 ($C_5Me_5$) |
| | 7.25 (t, 1H, $^3J_{HH}$ = 7.1, Tol CH) | 124.8 (Tol CH) |
| | 8.21 (d, 1H, $^3J_{HH}$ = 7.1, Tol CH) | 128.0 (obs, Tol CH) |
| | | 139.5 (Tol CH) |
| | | 141.2 (Tol CH) |

**Table 2.3** NMR Characterization Data for Complexes **2.4 – 2.15**

| Compound no. | $^1$H NMR ($C_6D_6$) δ | $^{13}$C {1H} NMR ($C_6D_6$) δ |
|---|---|---|
| **2.14**[a,e] | 2.35 (s, 3H, Tol Me) | 10.2 ($C_5Me_5$) |
| | 3.55 (br m, 1H, allyl CH) | 21.9 (Tol Me) |
| | 6.47 (br s, 1H, Tol CH) | 95.8 (allyl CH) |
| | 6.94 (d, 1H, $^3J_{HH}$ = 6.6, Tol CH) | 106.9 ($C_5Me_5$) |
| | 7.16 (obs, 1H, Tol CH) | 123.5 (Tol CH) |
| | 8.24 (s, 1H, Tol CH) | 126.9 (Tol CH) |
| | | 137.2 (Tol CH) |
| | | 143.1 (Tol CH) |
| **2.15**[a,e] | 2.28 (s, 3H, Tol Me) | 10.2 ($C_5Me_5$) |
| | 3.55 (br m, 1H, allyl CH) | 21.5 (Tol Me) |
| | 6.58 (br s, 1H, Tol CH) | 95.8 (allyl CH) |
| | 7.08 (d, 1H, $^3J_{HH}$ = 6.6, Tol CH) | 106.9 ($C_5Me_5$) |
| | 7.16 (obs, 1H, Tol CH) | 128.0 (obs Tol CH) |
| | 8.31 (d, 1H, $^3J_{HH}$ = 7.1, Tol CH) | 129.6 (Tol CH) |
| | | 140.1 (Tol CH) |
| | | 142.4 (Tol CH) |

*a*: $^1$H NMR (400 MHz); $^{13}$C {$^1$H} NMR (100 MHz)
*b*: $^1$H NMR (500 MHz); $^{13}$C {$^1$H} NMR (125 MHz)
*c*: characterized as a mixture of **2.7 – 2.8**
*d*: characterized as a mixture of **2.10 – 2.11**
*e*: characterized as a mixture of **2.13 – 2.15**

### 2.4.12 Synthesis of Cp*W(NO)($\eta^3$-1,1-$Me_2C_3H_3$)(Cl) (2.16)

In a glovebox, a 100-mL Schlenk tube with a magnetic stir bar was charged with Cp*W(NO)$Cl_2$ (203 mg, 48 mmol) while another Schlenk was charged with ($\eta^3$-1,1-$Me_2C_3H_3)_2$Mg•*x*dioxane (66 mg, 52 mmol). On a vacuum line, sufficient THF was added to both Schlenk tubes to dissolve the contents and give a turquoise coloured solution of Cp*W(NO)$Cl_2$ and a clear, colourless solution of the magnesium reagent. The former solution was chilled to – 78 °C with a liquid $N_2$/acetone bath, and the latter solution was solidified via cooling to – 196 °C with a liquid $N_2$ bath. The two components were added together via cannulation at a rate which allowed the solution to freeze upon contact with the solid. The reaction vessel was then warmed and maintained at – 78 °C for 2 hours while the melted THF solution was stirred, and changed in appearance from a clear turquoise to a turbid orange solution. The volatiles were removed in vacuo, and the resulting orange/brown solid was dissolved in 1:4 $Et_2O$/hexanes and eluted through an alumina (I) column (0.5 x 1 cm) with $Et_2O$. Subsequent concentration and cooling of the filtrate afforded orange microcrystals of complex **2.16** (20 mg, 9 %).

**2.16**: IR ($cm^{-1}$) 1578 (s, $\nu_{NO}$). MS (LREI, *m/z*, probe temperature 120 °C) 453 [$P^+$, $^{184}W$], 423 [$P^+$ - NO]. $^1H$ NMR (500 MHz, $C_6D_6$) δ 1.55 (s, 3H, allyl Me), 1.57 (s, 15H, $C_5Me_5$), 1.68 (bs, 1H, allyl $CH_2$), 1.95 (bs, 3H, allyl Me), 2.48 (bs, 1H, allyl $CH_2$), 3.57 (bs, 1H, allyl CH). $^{13}C\{^1H\}$ NMR (125 MHz, $C_6D_6$) δ 9.97 ($C_5\mathit{Me}_5$), 21.37 (allyl Me), 29.97 (allyl Me), 39.31 (allyl $CH_2$), 96.24 (allyl CH), 108.46 ($\mathit{C}_5Me_5$). Anal. Calcd. for $C_{15}H_{24}ClNOW$: C, 39.71; H, 5.33; N, 3.09. Found: C, 40.03; H, 5.43; N, 3.03

## 2.5 References and Notes

(1) Adams, C. S.; Legzdins, P.; Tran, E. *J. Am. Chem. Soc.* **2001**, *123*, 612.

(2) Adams, C. S.; Legzdins, P.; Tran, E. *Organometallics* **2002**, *21*, 1474.

(3) Adams, C. S.; Legzdins, P.; McNeil, W. S. *Organometallics* **2001**, *20*, 4931.

(4) Tran, E.; Legzdins, P. *J. Am. Chem. Soc.* **1997**, *119*, 5071.

(5) Debad, J. D.; Legzdins, P.; Lumb, S. A.; Batchelor, R. J.; Einstein, F. W. B. *J. Am. Chem. Soc.* **1995**, *117*, 3288.

(6) Legzdins, P.; Martin, J. T.; Einstein, F. W. B.; Jones, R. H. *J. Am. Chem. Soc.* **1987**, *6*, 1826.

(7) Ng, S. H. K.; Adams, C. S.; Legzdins, P. *J. Am. Chem. Soc.* **2002**, *124*, published on web 23 July 2002.

(8) Crystal data for **2.1**: monoclinic, space group $P2_1/c$, $a$ = 12.8869(3) Å, $b$ = 9.0219(3) Å, $c$ = 16.7835(7) Å, $\beta$ = 92.439(2) °, $V$ = 1949.6(1) Å$^3$, $Z$ = 4, $R_1$ = 0.038, $wR_2$ = 0.066, and GOF($F^2$) = 1.07 for 4484 reflections and 229 variables.

(9) Bent, H. A. *Chem. Rev.* **1961**, *61*, 275.

(10) Ipaktschi, J.; Mirzaei, F.; Demuth-Eberle, G. J.; Beck, J.; Serafin, M. *Organometallics* **1997**, *16*, 3965.

(11) Frohnapfel, D. S.; White, P. S.; Templeton, J. L. *Organometallics* **1997**, *16*, 3737.

(12) Villanueva, L. A.; Ward, Y. D.; Lachicotte, R.; Liebeskind, L. S. *Organometallics* **1996**, *15*, 4190.

(13) Adams, R. D.; Chodosh, D. F.; Faller, J. W.; Rosan, A. M. *J. Am. Chem. Soc.* **1979**, *101*, 2570.

(14) Faller, J. W.; DiVerdi, M. J.; John, J. A. *Tetrahedron Lett.* **1991**, *32*, 1271.

(15) Schilling, B. E. R.; Hoffman, R.; Faller, J. W. *J. Am. Chem. Soc.* **1979**, *101*, 592.

(16) Direct evidence for *endo*- vs *exo*-allyl conformations using selective NOE NMR spectroscopy is sometimes not available, and logical inferences must be made to ascertain the solution structure. For example, irradiation of the signal due to the central allyl H atom leading to an NOE enhancement of the Cp* methyl H atoms signal is direct evidence for an exo configuration. However, its absence, and hence the implication of an endo configuration, must be confirmed by irradiation of the trans Me group signal that should exhibit an NOE enhancement of the Cp* ring signal.

(17) Adams, C.S. C-H Activation of Hydrocarbons by Tungsten Alkylidene and Related Complexes. Ph.D. Thesis, University of British Columbia, Vancouver, BC, October 2001.

(18) Debad, J. D.; Legzdins, P.; Batchelor, R. J.; Einstein, F. W. B. *Organometallics* **1993**, *12*, 2094.

(19) Bau, R.; Mason, S. A.; Patrick, B. O.; Adams, C. S.; Sharp, W. B.; Legzdins, P. *Organometallics* **2001**, *20*, 4492.

(20) Crystal data for **2.2**: monoclinic, space group *C*2/c, $a$ = 15.3944(6) Å, $b$ = 8.4977(3) Å, $c$ = 32.326(1) Å, $\beta$ = 90.753(3) °, $V$ = 4228.4(3) Å$^3$, $Z$ = 8, $R_1$ = 0.053, $wR_2$ = 0.0107, and GOF($F^2$) = 1.60 for 4410 reflections and 221 variables.

(21) Legzdins, P.; Rettig, S. J.; Sanchez, L. *Organometallics* **1988**, *7*, 2394.

(22) Crystal data for **2.3**: monoclinic, space group Pbca, $a$ = 14.2207(7) Å, $b$ = 15.9939(7) Å, $c$ = 19.5926(9) Å, $V$ = 4456.2(3) Å$^3$, $Z$ = 8, $R_1$ = 0.063, $wR_2$ = 0.082, and GOF($F^2$) = 0.80 for 5645 reflections and 264 variables.

(23) Legzdins, P.; Jones, R. H.; Phillips, E. C.; Yee, V. C.; Trotter, J.; Einstein, F. W. B. *Organometallics* **1991**, *10*, 986.

(24) Dryden, N. H.; Legzdins, P.; Trotter, J.; Yee, V. C. *Organometallics* **1991**, *10*, 2857.

(25) Cotton, F. A.; LaPrade, M. D. *J. Am. Chem. Soc.* **1968**, *90*, 5418.

(26) Carmona, E.; Marin, J. M.; Paneque, M.; Poveda, M. L. *Organometallics* **1987**, *6*, 1757.

(27) Castelhano, A. L.; Griller, D. *J. Am. Chem. Soc.* **1982**, *104*, 3655.

(28) Jones, W. D.; Feher, F. J. *Acc. Chem. Res.* **1989**, *22*, 91.

(29) Jones, W. D.; Hessell, E. T. *J. Am. Chem. Soc.* **1993**, *115*, 554.

(30) Pryor, W. A.; Tang, F. Y.; Tang, R. H.; Church, D. F. *J. Am. Chem. Soc.* **1982**, *104*, 2885 and references cited therein.

(31) Johansson, L.; Ryan, O. B.; Romming, C.; Tilset, M. *J. Am. Chem. Soc.* **2001**, *123*, 6579.

(32) Bryndza, H. E.; Fong, L. K.; Paciello, R. A.; Tam, W.; Bercaw, J. E. *J. Am. Chem. Soc.* **1987**, *109*, 1444.

(33) Jones, W. D.; Feher, F. J. *J. Am. Chem. Soc.* **1984**, *106*, 1650.

(34) Debad, J. D.; Legzdins, P.; Lumb, S. A.; Rettig, S. J.; Batchelor, R. J.; Einstein, F. W. B. *Organometallics* **1999**, *18*, 3414.

(35) Crystal data for **2.5**: monoclinic, space group R-3, $a = 21.258(5)$ Å, $b = 21.258(5)$ Å, $c = 21.258(5)$ Å, $\beta = 118.048(4)$ °, $V = 3447.2(14)$ Å$^3$, $Z = 6$, $R_1 = 0.0495$, $wR_2 = 0.1134$, and GOF($F^2$) = 1.083 for 5208 reflections and 258 variables.

(36) Legzdins, P.; Smith, K. M.; Rettig, S. J. *Can. J. Chem.* **2001**, *79*, 502.

# Chapter 3

## *Mechanistic Investigations into the Thermal Chemistry of $Cp^*W(NO)(CH_2CMe_3)(\eta^3\text{-}1,1\text{-}Me_2C_3H_3)$*

---



---

## 3.1 Introduction

The primary purpose of the earlier work carried out during the course of this research project was to identify the C-H activation products resulting from thermal reactions of **1.1** in several representative hydrocarbon solvents, namely protio-benzene, tetramethylsilane, mesitylene, xylenes, and toluene.

Preliminary research performed by C. S. Adams[1] had already ascertained that **1.1** is easily synthesized using methods similar to that employed for the well-studied $Cp^*W(NO)(CH_2CMe_3)(CH_2C_6H_5)$, and that it reacts with benzene under thermal conditions. The serendipitous discovery of the C-H bond-activating chemistry initiated by **1.1** towards benzene provided a convenient starting point for our mechanistic investigations. Thus, $^1H$ NMR kinetic studies in deuterio-benzene were utilized to establish suitable thermolytic temperatures and reaction times that were used throughout the course of this study.

Further mechanistic insight was obtained by several different methods that were employed to ascertain the identity of the reactive intermediate involved in the C-H bond activating chemistry of **1.1** under thermal conditions.

This Chapter provides full details of the investigations briefly mentioned above, studies to identify fully the organometallic products formed during the mechanistic studies, and the route taken to confirm the formation of the reactive intermediate from gentle heating of **1.1**.

## 3.2 Results and Discussion

### 3.2.1 Kinetic Studies

The observed clean conversion of **1.1** to **2.1** during the reaction with benzene prompted a study of the reaction kinetics. The reaction of **1.1** with benzene-$d_6$ at 50 °C for 250 minutes (~ 4 ½ half-lives) has provided kinetic data that enables the standardization of suitable thermolytic conditions that were employed in these studies. **1.1** decomposes by a first-order process with a rate constant of 2.2(1) x $10^{-4}$ $s^{-1}$ ($R^2$ = 0.999) that eliminates neopentane to generate several new organometallic complexes, namely Cp*W(NO)($C_6D_5$)($\eta^3$-1,1-$Me_2CCDCH_2$) (**2.1**-$d_{6a}$), Cp*W(NO)($C_6D_5$)($\eta^3$-1,1-$Me(CH_2D)C_3H_3$) (**2.1**-$d_{6b}$) and Cp*W(NO)($C_6D_5$)($\eta^3$-1,1-$(CH_2D)MeC_3H_3$) (**2.1**-$d_{6c}$) which are deuterated variants of the already characterized phenyl-dimethylallyl complex **2.1** (eq. 3.1, Figure 3.1).

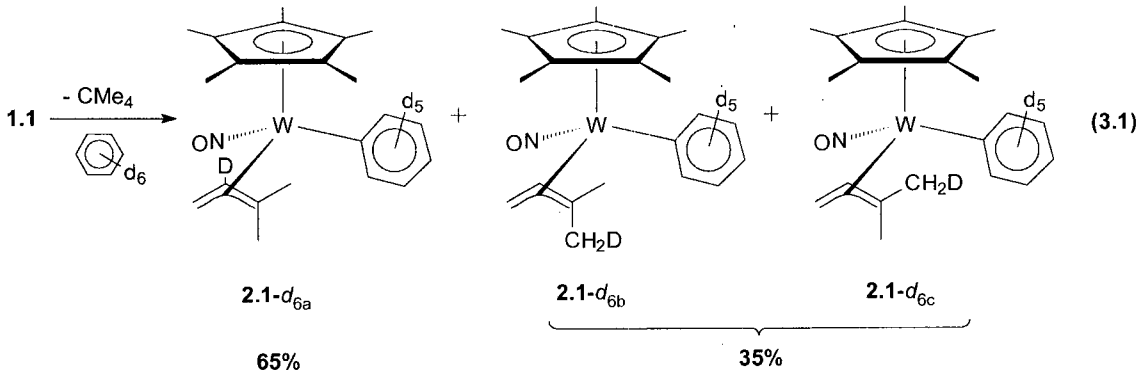


(3.1)

The rate constant calculated for the reaction in $C_6D_6$ under the conditions utilized is consistent with data collected in similar systems that exhibit rate-limiting dissociation of hydrocarbon via hydrogen abstraction from an ancillary ligand.[2] The half-life of 53 minutes at 50 °C prompted the use of a 6 hour reaction period to ensure > 99 % generation of the reactive intermediate responsible for the C-H bond activating chemistry of **1.1** under thermal conditions.

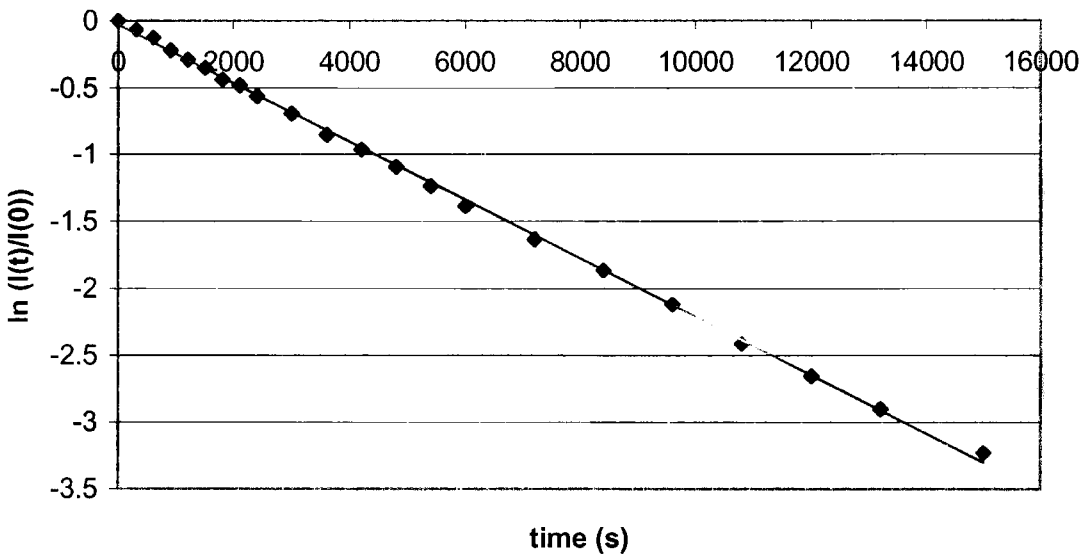


**Figure 3.1** Kinetic data plot showing that the C-D bond activating ability of **1.1** is a first order process concurrent with the elimination of neopentane (see Appendix B for data)

### 3.2.2 Deuterium Labelling Studies

Complexes **2.1**-$d_{6a\text{-}c}$ have been identified using $^2$H NMR and $^1$H NMR spectroscopic data which also afford the product ratios given in eq. 3.1.[3] Deuterium incorporation into the dimethylallyl ligand of the final product as shown initially suggests three potential reactive intermediates (an allene, a *cis*-diene, and a *trans*-diene complex) generated via hydrogen abstraction from the dimethylallyl ligand to form a transition-state entity that eventually eliminates neopentane. The activation of a C-D bond could then proceed via the microscopic reverse to yield the final phenyl-allyl complex. Scheme 3.1 depicts a potential pathway by which the C-D bond activation could occur through the proposed reactive dimethylallene intermediate. Similar pathways can be drawn for C-D bond activation via the suggested *cis*-diene and *trans*-diene reactive intermediates. It should be noted that the $^2$H NMR spectrum ($C_6H_6$) shows no incorporation of deuterium into the Cp* ring, thereby eliminating the possibility of a C-H activation pathway via oxidative addition of a tucked in Cp*-methyl C-H bond.[4]

Preliminary analysis of the product ratios for complexes **2.1**-$d_{6a\text{-}c}$ indicates the incorporation of 1.12 atoms of deuterium into the allyl ligand of the final product, which is quite surprising, given that similar studies conducted on other Legzdins C-H activating complexes clearly indicate mono-inclusion of deuterium.[2] This observation suggests that more than simple hydrogen-for-deuterium substitution is occurring during the C-D activation of benzene-$d_6$. For example, it is plausible that a portion of the final products included more than one atom of deuterium substituting hydrogens in the dimethylallyl moiety.

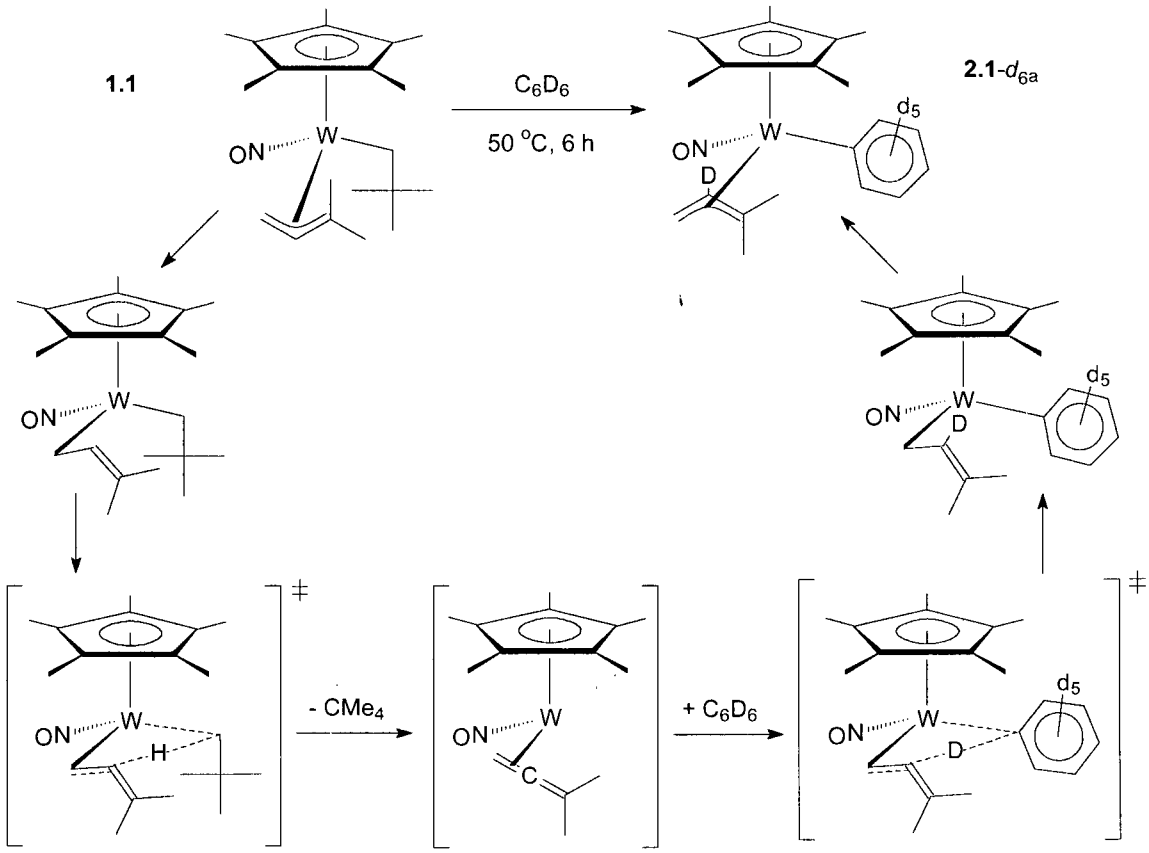


**Scheme 3.1**

As a result, it was initially proposed that the phenyl-allyl complex formed in this reaction could potentially eliminate benzene-$d_5$H in an analogous fashion to that of neopentane and activate another molecule of benzene-$d_6$, via a pathway that generated one of the other proposed reactive intermediates discussed in this section, but at a slow enough rate such that only a small portion could perform the second activation under the thermolytic conditions utilized. This corresponding rate would be understandably slower due to the stronger bond energy exhibited by metal-($sp^2$-carbon) vs metal-($sp^3$-carbon) linkages, as in the case of **1.1**.

The thermolysis of **2.1** in benzene-$d_6$ results in the re-isolation of starting product, as determined by $^1$H and $^2$D NMR spectroscopic data which show no evidence for deuterium incorporation in the spectral window employed, thereby substantiating the irreversibility of the C-D activation in question. Presumably, if the phenyl complex was capable of activating a C-D bond of deuterio-benzene under these conditions, the organometallic product from such a reaction would have deuterium signals in the aryl region and at the chemical shifts corresponding to the allyl $CH_3$ groups and central allyl hydrogen.

Rigorous statistical analysis[3] subsequently performed on the spectroscopic data suggests that the activation of deuterio-benzene results in the incorporation of only one atom of deuterium into the dimethylallyl ligand of **2.1**-$d_{6a\text{-}c}$ ($1.12 \pm 0.14$), thereby indicating that the reaction occurs stoichiometrically and providing further evidence that supports the thermal stability of complexes **2.1**-$d_{6a\text{-}c}$ in benzene-$d_6$.

### 3.2.3 Independent Synthesis of a Possible Reactive Intermediate

In a further effort to identify the reactive intermediate, a process of elimination has been employed. Specifically, one of the possible intermediates has been synthesized and thermolyzed in benzene to test the thermal stability and the C-D bond activation potential. In this study, one of the proposed $\eta^4$-diene intermediates has been synthesized and fully characterized before testing. An X-ray analysis was attempted on the product in an effort to conclusively identify the solid-state stereochemistry of the diene moiety, but

unfortunately the crystals grown were extremely disordered. Selective NOE NMR spectroscopy experiments identify the prepared product as the *trans*-2-methybutadiene complex (**3.1**), as evinced by observed NOE enhancements of the resonances attributed to synclinal hydrogens on both of the $CH_2$ groups when irradiating the Me resonance. This observation is only possible if the diene ligand exists in the trans form (see Figure 3.2)

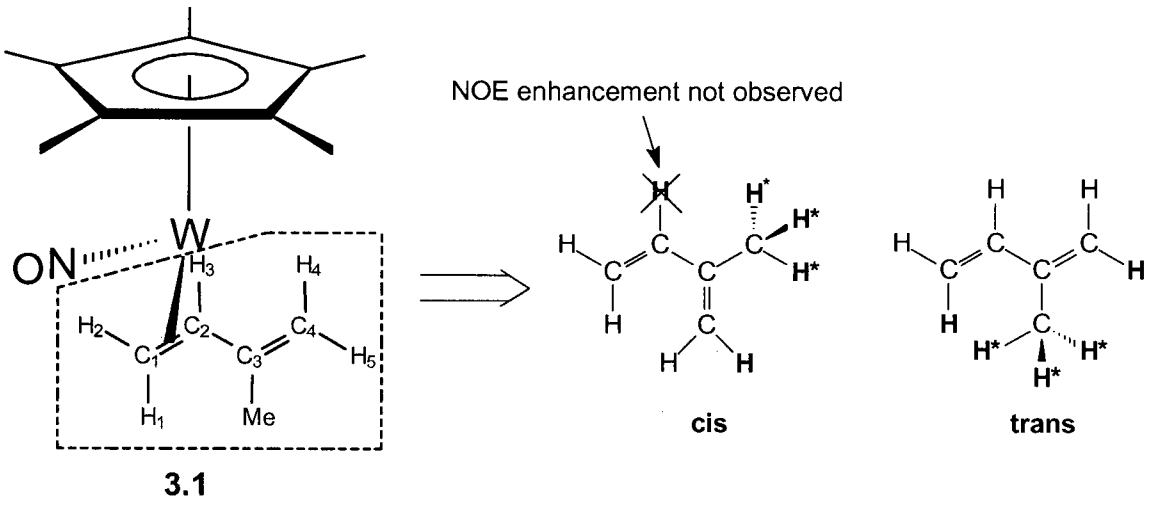


**Figure 3.2** Identifying the synthesized diene as the trans isomer based on characteristic NOE enhancements observed.

Thermolysis of complex **3.1** in benzene-$d_6$ leads to no reaction, and isolation of the originally synthesized complex. This result, in conjunction with the apparent formation of $Cp^*W(NO)(C_6D_5)(\eta^3\text{-}1,1\text{-}(CH_2D)MeC_3H_3)$ **2.1**-$d_{6c}$ from the presumed *trans*-diene reactive intermediate in the initial mechanistic study, suggests the existence of a possible mechanism by which the two methyl substituents on the dimethylallyl

ligand can exchange. This would account for the possible generation of complex **2.1**-$d_{6c}$ from its sister-*cis*-equivalent, **2.1**-$d_{6b}$. On the NMR timescale at room temperature, EXSY NMR spectroscopic data exhibit cross peaks attributable to rapid exchange of the methyl groups of the allyl ligand, thereby suggesting the potential for a mechanism as shown in Scheme 3.2. This proposed pathway hinges on the ability of σ-π distorted $\eta^3$-allyl fragments to break the 2e bond, rotate about the remaining single bonds to exchange the terminal allyl substituents, and revert back to the original endo or exo configuration. [5-8]

**Scheme 3.2**

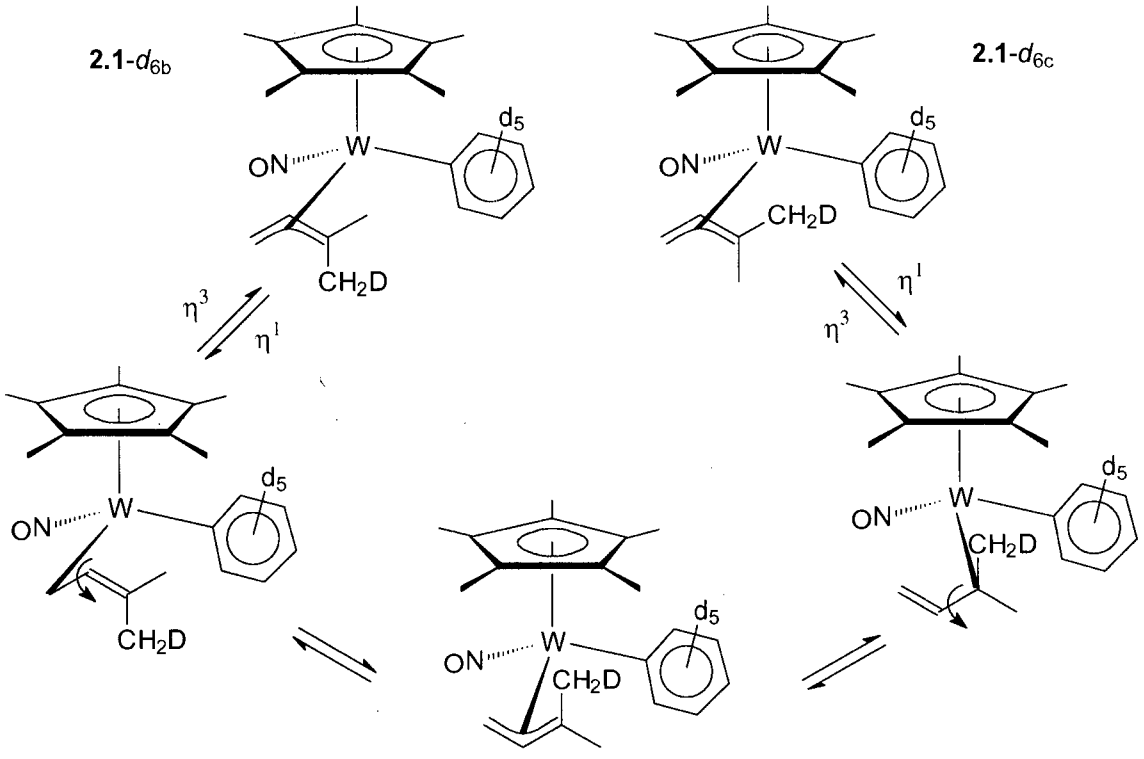


The spectroscopic properties of complex **3.1** exhibit features similar to those of related molybdenum species that have been structurally characterized. The closest

resemblance to compound **3.1** is the previously reported isostructural CpMo(NO)($\eta^4$-*trans*-2-methylbutadiene) complex.[9] Unlike the molybdenum congener, the tungsten diene exists only as one isomer with the methyl substituent anti to the Cp* ring. Presumably, this is the result of steric crowding in the syn conformer between the pentamethylcyclopentadienyl ring and the methyl group that does not exist for the less sterically hindered cyclopentadienyl molybdenum analogue.

| | *$^1$H NMR ($C_6D_6$) δ* | | | | | | *$^{13}C\{^1H\}$ NMR ($C_6D_6$) δ* | | | | |
|---|---|---|---|---|---|---|---|---|---|---|---|
| *Assignment* | $H_1$ | $H_2$ | $H_3$ | $H_4$ | $H_5$ | Me | $C_1$ | $C_2$ | $C_3$ | $C_4$ | Me |
| *Complex **3.1*** | 3.15 | 2.35 | 1.11 | 0.95 | 3.29 | 2.05 | 50.4 | 80.3 | 103.9 | 55.2 | 18.5 |
| *CpMo Analogue* | 2.88 | 3.35 | 2.37 | 1.94 | 3.45 | 1.53 | 50.5 | 79.7 | 115.8 | 55.3 | 18.1 |

**Table 3.1** Comparison of $^{13}C\{^1H\}$ and $^1H$ NMR spectroscopic resonances of complex **3.1** and CpMo(NO)($\eta^4$-*trans*-2-methylbutadiene) (see Figure 3.2 for numbering scheme)

As expected with related complexes such as these, the chemical shifts exhibited by each hydrogen and carbon atom within the *trans*-2-methylbutadiene framework are extremely similar. The geminal coupling observed in complex **3.1** and the Mo analogue for $H_1$ and $H_2$ (2.8 and 4.2 Hz respectively) as well as for $H_4$ and $H_5$ (3.8 and 3.1 Hz respectively) are alike, as is the vicinal coupling between $H_1$ and $H_3$ (13.9 and 14.4 Hz respectively) and the four-bond coupling observed between $H_3$ and $H_4$ (1.0 and 0.8 Hz respectively).

The analytical and spectroscopic evidence obtained for complex **3.1** is consistent with its formulation as an 18e, "three-legged piano-stool" molecular structure, with the diene ligand attached to the metal centre in a twisted transoidal fashion, much like the structurally characterized CpMo($\eta^4$-*trans*-2,5-dimethyl-2,4-hexadiene).[10]

### 3.2.4 Attempt to Couple the Reactive Species with 2,3-dimethyl-2-butene

One method of elucidating the intermediate is to employ a reagent capable of undergoing a coupling reaction upon coordination to the metal centre. Characterization of the product can often result in the suggestion of the bonding nature of the intermediate based on the observed C-C bond formation in the final species.

The reaction of 2,3-dimethyl-2-butene with the acetylene intermediate previously mentioned in Section 1.2.1 for the alkyl-vinyl complex affords a $\eta^3$-allyl cyclic complex as a result of dual C-H bond activation and reductive coupling (Scheme 3.3).[11]

**Scheme 3.3**

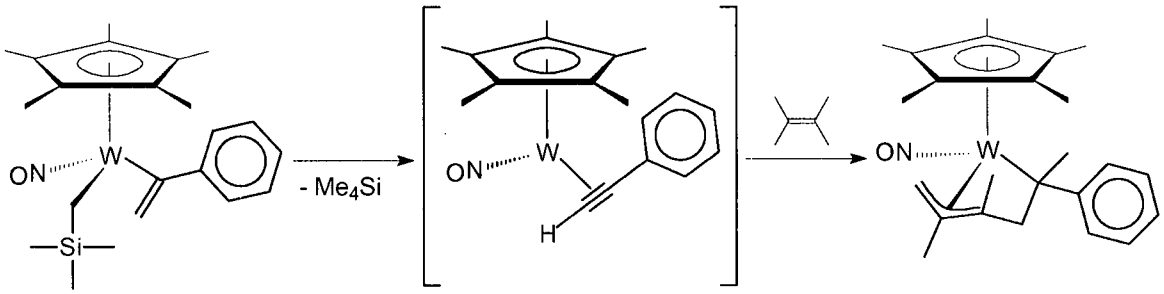

Although the final allyl product does not implicate a reactive acetylene intermediate, the thermal reaction of **1.1** with 2,3-dimethyl-2-butene might form an organometallic complex, as a coupled product, which would implicate one of the proposed intermediates as being the species responsible for the C-H bond activating chemistry of **1.1** under mild conditions (Scheme 3.4).

**Scheme 3.4**

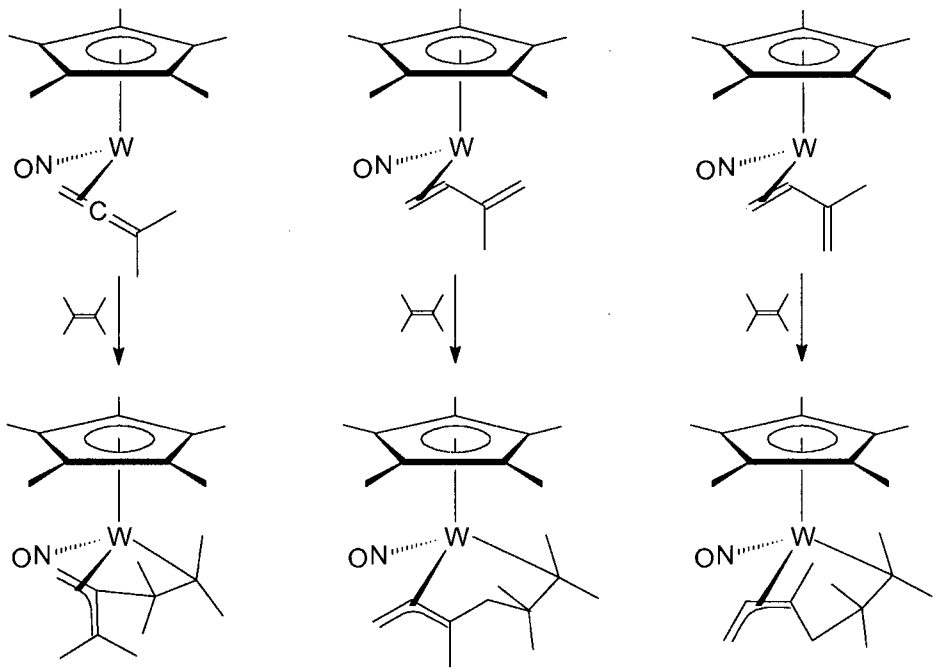


The rationale for the potential formation of the compounds illustrated in Scheme 3.4 is the result of other coupling reactions seen in organometallic chemistry. There have been numerous examples of C-C bond formation observed with the central carbon of the allene backbone to give metallocyclic-vinyl and allyl products.[12-15] The formation of

these complexes upon reaction with the substituted alkene could effectively lead to the identity of the reactive species.

Upon thermolysis of **1.1** in 2,3-dimethyl-2-butene, the initial pale orange solution changes to a bright orange-red hue, and the product isolated from the reaction mixture as red blocks has been characterized by extensive NMR spectroscopic techniques and analytical methods. However, the data from the initial analytical studies do not provide enough evidence to distinguish the final product. A single-crystal X-ray crystallographic analysis has been performed[16] to ascertain the connectivity of the organometallic complex, and its ORTEP diagram is shown in Figure 3.3.

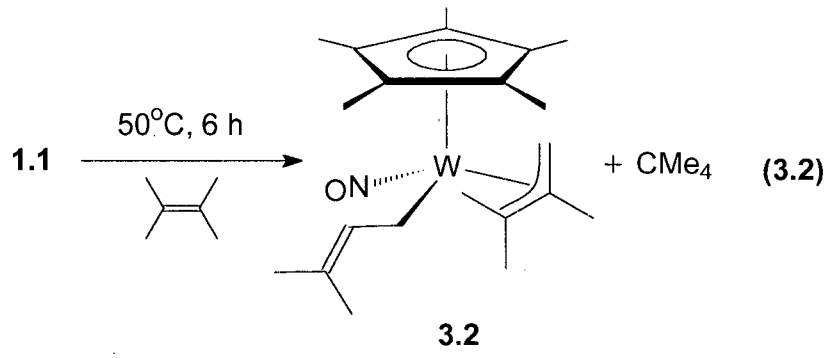


The formation of this alternate allyl complex from the activation of a methyl C-H bond of 2,3-dimethyl-2-butene leaves the dimethylallyl moiety σ-bound in the solid state (eq. 3.2). This feature is evident from the orientation of the dimethylallyl group and the C(11)-C(12) and C(12)-C(13) bond lengths of 1.500(6) and 1.342(7) Å respectively, each typical of C-C single- and double- bond character, respectively. One last indication of the loss of its previous $\eta^3$ coordination is the W(1)-C(11)-C(12) bond angle of 113.3(3)°,

which is much more obtuse towards ideal $sp^3$ character than previously observed angles ranging from 77.3 - 81.2°.

Perhaps the most notable feature of the $^1H$ NMR spectrum of **3.2** in $C_6D_6$ is the significant downfield shift of the signal for the β-hydrogen of the $\eta^1$-allyl fragment (δ 5.82) from its typical values (δ 3.54 – 4.43), indicative of the loss of metal-to-ligand electron density transfer that existed in the $\eta^3$-allyl fragment. The exclusively σ-bound dimethylallyl ligand in the solid state is also manifested by solution NMR spectroscopy as the distinguishable triplet of the central hydrogen resonance. This feature demonstrates the inability of the dimethylallyl fragment to undergo the $\eta^3$ to $\eta^1$ dynamic processes evident in other compounds (see Section 3.2.3).

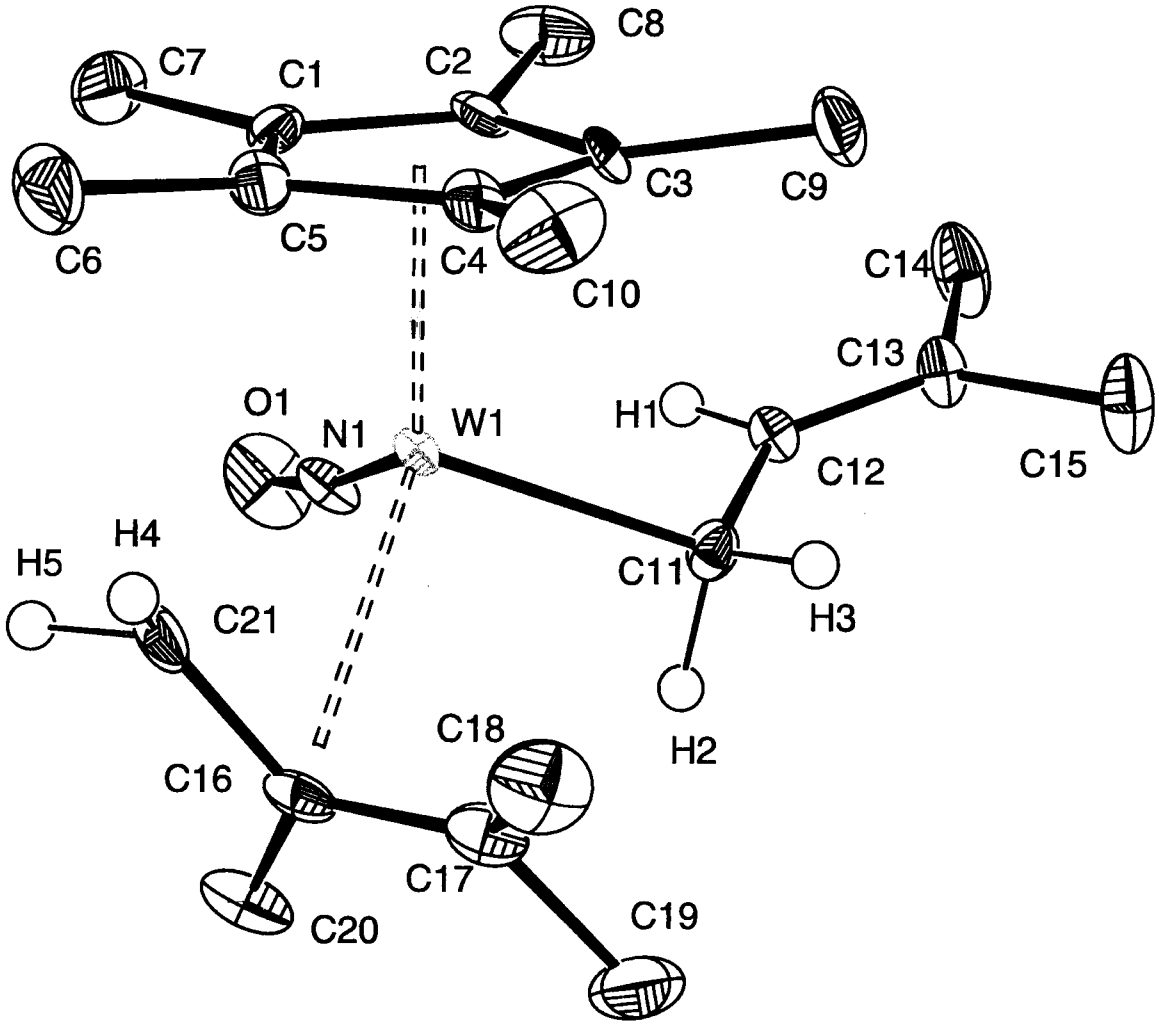


**Figure 3.3** Solid-state molecular structure of Cp*W(NO)($\eta^3$-1,1,2-$Me_3C_3H_2$)($\eta^1$-3,3-$Me_2C_3H_3$) (**3.2**) with 50 % probability thermal ellipsoids shown. Selected interatomic distances (Å) and angles (deg): W(1)-C(11) = 2.236(5), C(11)-C(12) = 1.500(6), C(12)-C(13) = 1.342(7), W(1)-C(21) = 2.219(5), W(1)-C(16) = 2.403(5), W(1)-C(17) = 2.696(5), C(21)-C(16) = 1.438(7), C(16)-C(17) = 1.375(7), N(1)-O(1) = 1.221(5), C(17)-C(16)-C(21) = 119.9 (5), C(11)-C(12)-C(13) = 130.3(5), W(1)-C(11)-C(12) = 113.3(3), W(1)-N(1)-O(1) = 170.9(4), C(14)-C(13)-C(15) = 114.4(4), W(1)-C(21)-C(16) = 79.0(3)

### 3.2.5 Definitive Evidence for the Dimethylallene Reactive Intermediate

Common trapping experiments involve the use of a suitable Lewis base that can stabilize the reactive electronically unsaturated metal centre, effectively taking a "snap-shot" of the connectivity that the reactive species exhibits at the time of coordination. The thermal reaction of **1.1** in neat trimethylphosphine yields the base-stabilized adduct of the dimethylallene complex, namely $Cp^*W(NO)(PMe_3)(\eta^2\text{-}H_2C{=}C{=}CMe_2)$ (**3.3**) (Scheme 3.5). Initially characterized by NMR spectroscopic data, suitable single crystals were eventually grown and analyzed by X-ray diffraction.[17] Figure 3.4 shows the ORTEP diagram of the trimethylphosphine adduct and presents its selected bond lengths and angles. This structure confirms the identity of the reactive intermediate responsible for the C-H bond activating chemistry of **1.1** as the $\eta^2$-dimethylallene complex.

**Scheme 3.5**

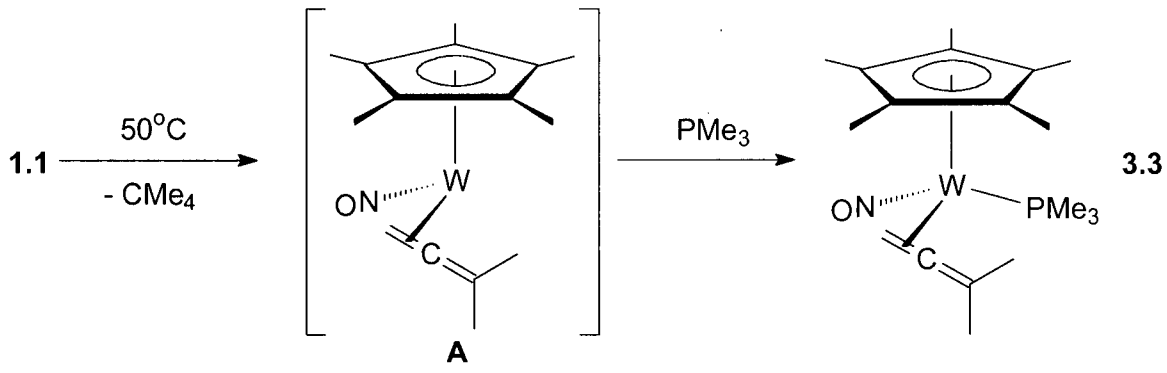

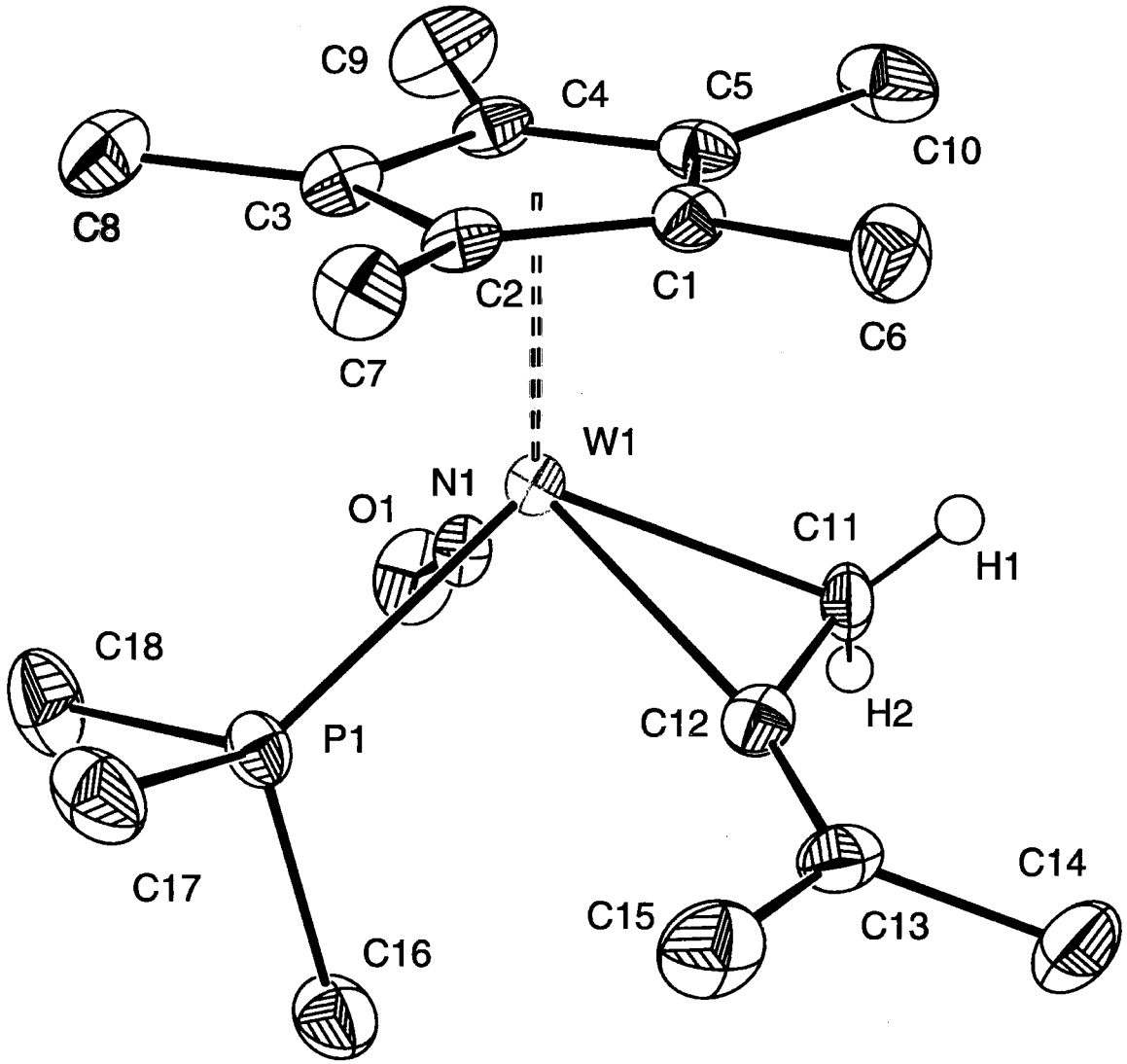


**Figure 3.4** Solid-state molecular structure of Cp*W(NO)($PMe_3$)($\eta^2$-$H_2C$=C=$CMe_2$) (**3.3**) with 50 % probability thermal ellipsoids shown. Selected interatomic distances (Å) and angles (deg): W(1)-N(1) = 1.795(4), W(1)-C(11) = 2.205(4), W(1)-C(12) = 2.148(5), W(1)-P(1) = 2.4660(12), N(1)-O(1) = 1.224(5), C(11)-C(12) = 1.436(7), C(12)-C(13) = 1.324(7), W(1)-N(1)-O(1) = 175.0(4), N(1)-W(1)-C(11) = 91.00(18), C(12)-W(1)-C(11) = 38.49(18), C(11)-C(12)-C(13) = 134.0(5), C(12)-C(13)-C(14) = 121.8(5), C(12)-C(13)-C(15) = 124.3(5)

A major topic of discussion with regards to transition-metal allene complexes is the uncertainty of the exact bonding mode of the cumulated diene ligand; whether they should be described as metallacyclopropane derivatives via two σ-bonds from the carbon backbone to the metal (X), or as π-complexes to the metal centre (Y) (see Figure 3.5).[18,19]


**(X)** **(Y)**

**Figure 3.5** Two extreme types of bonding proposed in monometallic allene complexes

In other monometallic allene complexes, the allene fragment behaves similiarly to an olefin-like ligand.[20] As such, the dual-component bonding interaction originally proposed by Dewar,[21] Chatt and Duncanson[22] remains the paramount approach to describing the interaction of an alkene with a transition metal,[23] and thus likewise the interaction of an allene with a metal. Whether a complex exhibits more attributes of π-adduct or metallacyclopropane character is dependant on the relative extents of metal-to-ligand and ligand-to-metal electron-density transfer.[24]

The most striking feature of the solid-state molecular structure of **3.3** is the non-linear nature of the allene framework, C(11)-C(12)-C(13), which has also been documented for other $\eta^2$-allene complexes.[14,15,18,19,25-30] The established angle of 134.0(5) ° is among the most acute found for acyclic allene complexes[31] and is a manifestation of the considerable back-donation of electron density from the metal to the

alkene π* orbitals, probably as a result of the increased contribution from the trimethylphosphine ligand.[32] In addition, this large back-donation results in the increased difference in the coordinated C=C bond length (1.436(7) Å) versus that of the uncoordinated C=C (1.324(7) Å). The elongation of C(11)-C(12) suggests a decrease in the bond order from formally two towards one. This proposal is further supported by evidence gathered from $^{1}H$ and $^{13}C\{^{1}H\}$ NMR spectroscopic data. The large upfield shifts observed for the methylene carbon (δ 7.7) and hydrogen (δ 0.67, 1.97) signals are consistent with considerable $sp^3$ character of the terminal carbon.[33] This upfield shift is also evident for the central carbon atom signal (δ 165.7), while the remaining assignable resonances are relatively unchanged from free dimethylallene.

In the solid-state molecular structures of other $\eta^2$-allene transition-metal complexes, the distance from the metal to the bound terminal carbon of the allene backbone is normally 0.05 – 0.19 Å greater than the distance from the metal to the central carbon, akin to the metrical parameters exhibited by **3.3** (W(1)-C(11) = 2.205(4) Å, W(1)-C(12) = 2.148(5) Å). This has been rationalized by the ability of the two orthogonal π* -orbitals of the central carbon atom to overlap with a filled d orbital of the metal,[20,34] and the higher electron density resulting from that interaction.[19]

### 3.3 Epilogue

This appears to be the first definitive demonstration of the C-H bond activating ability of a transition-metal allene complex, but not the first example exhibited by an allyl-alkyl organometallic compound. Bergman and McGhee reported the C-H activation of benzene-$d_6$ by an ($\eta^3$-allyl)(alkyl)iridium complex.[35] Based on deuterium labelling studies, an allene intermediate was proposed, but they were unable to conclusively identify the reactive species.

The first-order rate constant determined for the thermolysis of **1.1** in benzene-$d_6$ ($2.2(1) \times 10^{-4}$ $s^{-1}$) is consistent with the rate-determining step being the intramolecular generation of **A** via elimination of neopentane (formed through hydrogen abstraction from the dimethylallyl ligand).

The synthesis and characterization of the $\eta^4$-*trans*-diene complex, **3.1**, reveals spectroscopic data remarkably similar to that of the CpMo congener. Presumably **3.1** adopts the twisted transoidal diene ligand attachment to the metal centre observed for other related complexes. Thermolysis of the diene compound in benzene-$d_6$ for 6 hours at 50 °C revealed its stability under those conditions and ruled it out as a potential reactive intermediate of the C-H activating species formed via hydrogen abstraction and subsequent ejection of neopentane from the metal's coordination sphere.

The formation of a new allyl complex, namely **3.2**, from the thermolysis of **1.1** in 2,3-dimethyl-2-butene, opens a new study on C-H activation by alkyl-allyl complexes. Presumably, due to the absence of the central hydrogen on the $\eta^3$ fragment, the formation

of an allene complex is impossible. However, perhaps this will open a new route to the formation of diene complexes that may possess C-H activating character.

## 3.4 Experimental Procedures

### 3.4.1 Kinetic Studies and the Concurrent Preparation of Cp*W(NO)($C_6D_5$)($\eta^3$-1,1-$Me_2$-allyl-$d_1$) (**2.1**-$d_{6a-c}$)

A J. Young NMR tube was charged with **1.1** (10 mg, 0.020 mmol), benzene-$d_6$ (0.8 mL) and an inert internal standard, hexamethyldisilane (1 mg, 0.007 mmol), and the contents were mixed thoroughly. The thermolysis was monitored by $^1$H NMR spectroscopy at 323.0 K, with the number of scans set to one. The loss of starting material vs time was determined by the integration of the neopentyl $CMe_3$ signal vs the hexamethyldisilane signal, except for the t = 0 value which was extrapolated from the plot of starting material loss vs time. The first-order rate constant for the decomposition of **1.1** was determined by the plot of ln(I(t)/I(0)) vs time. After 4.5 h, the sample was removed from the probe, and the crystalline product **2.1**-$d_{6a-c}$ was analyzed by NMR and MS spectroscopic techniques.

### 3.4.2 Thermolysis of 2.1 in Benzene-$d_6$

A thermolysis of the protio-phenyl complex, **2.1** (10 mg, mmol), was performed in benzene-$d_6$ (1 mL) for 6 h at 50 $^o$C to test its thermal stability. After the reaction time, $^1$H NMR spectroscopic data ($C_6D_6$) suggested that no reaction had occurred as the resonances observed exactly matched those of the starting complex. $^2$D NMR

spectroscopic data ($C_6H_6$) showed no deuterium signals within the spectral window employed.

### 3.4.3 Synthesis of Cp*W(NO)($\eta^4$-*trans*-$H_2C$=CHC(Me)=$CH_2$) (3.1)

Preparation of the $\eta^4$-*trans*-diene tungsten complex was performed using a modified version of the previously published procedure, using isoprene as the trapping agent.[36] Previous research in the Legzdins group showed that the likelihood of forming the *cis*-isomer was unlikely, as similar diene complexes that had been prepared would spontaneously isomerise to the thermodynamically more favoured trans form.[9,10,37] In a thick-walled bomb, Cp*W(NO)($CH_2SiMe_3$)$_2$ (401 mg, 0.77 mmol) was dissolved in pentane (60 mL), and isoprene (3 mL, 30 mmol) was syringed into the reaction vessel. The resulting mixture was frozen using a liquid $N_2$ bath, and $H_2$ gas (14 psig) was then introduced. The contents were allowed to warm up and react overnight while being stirred. After 16 hours, the final mixture was concentrated and cooled to obtain yellow crystals of **3.1** (20 mg, 6 %).

**3.1**: IR (Nujol, $cm^{-1}$) 1560 (w, $\nu_{NO}$). MS (LREI, *m/z*, probe temperature 120 °C) 417 [$P^+$, $^{184}W$]. $^1H$ NMR (400 MHz, $C_6D_6$) δ 0.95 (dd, $^2J_{HH}$ = 3.91, $^4J_{HH}$ = 0.98, 1H, C=$CH_2$), 1.11 (m, 1H, CH), 1.64 (s, 15H, $C_5Me_5$), 2.05 (s, 3H, CMe), 2.35 (m, 1H, CH=C$H_2$), 3.15 (dd, $^2J_{HH}$ = 4.16, $^3J_{HH}$ = 13.94, 1H, CH=C$H_2$), 3.29 (d, $^2J_{HH}$ = 3.67, 1H, C=$CH_2$). $^{13}C\{^1H\}$ NMR (125 MHz, $C_6D_6$) δ 10.2 ($C_5Me_5$), 18.5 (C*Me*), 50.4 (CH=*C*$H_2$),

55.2 (C=$CH_2$), 80.3 (CH), 103.9 ($C$(Me)=$CH_2$), 110.2 ($C_5Me_5$). Sel NOE (400 MHz, $C_6D_6$) δ irrad. at 2.05, NOE at 3.15 and 3.29, irrad. at 1.64, NOE at 0.95, 1.11, 2.35 and 3.29. Anal. Calcd. for $C_{15}H_{23}NOW$: C, 43.18; H, 5.56; N, 3.36. Found: C, 43.26; H, 5.39; N, 3.34.

### 3.4.4 Thermolysis of 3.1 in Benzene-$d_6$

A thermolysis of complex **3.1** was performed in benzene-$d_6$ at 50 °C for 6 h to test its thermal stability. After the reaction time, $^1$H NMR spectroscopic data ($C_6D_6$) suggested that no reaction had occurred as the resonances observed exactly matched those of the starting complex.

### 3.4.5 Preparation of Cp*W(NO)($\eta^3$-1,1,2-$Me_3C_3H_2$)($\eta^1$-3,3-$Me_2C_3H_3$) (3.2)

Complex **3.2** was prepared by the thermolysis of **1.1** (66 mg, 0.13 mmol) in 2,3-dimethyl-2-butene. The resulting residue was a bright orange/red oil which was triturated with hexanes (2 x 10 mL) to obtain red specks among the oil upon removal of the hexanes under high vacuum. The residue was dissolved in $Et_2O$ and eluted through an alumina (I) column (0.5 x 3 cm). The solvent was then removed from the eluate, and orange blocks of **3.2** were isolated by recrystallization of the residue from pentane (26 mg, 38 %)

**3.2**: IR ($cm^{-1}$) 1577 (s, $\nu_{NO}$). MS (LREI, *m/z*, probe temperature 120 °C) 501 [$P^+$, $^{184}W$]. $^1H$ NMR (400 MHz, $C_6D_6$) δ 0.70 (s, 3H, $\eta^3$-allyl Me), 1.07 (d, $^2J_{HH}$ = 4.6, 1H, $\eta^3$-allyl $CH_2$), 1.33 (s, 3H, $\eta^3$-allyl Me), 1.56 (obs, 1H, $\eta^1$-allyl $CH_2$), 1.59 (s, 15H, $C_5Me_5$), 1.96 (s, 3H, $\eta^1$-allyl Me), 1.97 (obs, 1H, $\eta^1$-allyl $CH_2$), 1.98 (s, 3H, $\eta^1$-allyl Me), 2.19 (s, 3H, $\eta^3$-allyl CMe), 2.48 (d, $^2J_{HH}$ = 4.6, 1H, $\eta^3$-allyl $CH_2$), 5.82 (t, $^3J_{HH}$ = 7.3, 1H, $\eta^1$-allyl CH. $^{13}C\{^1H\}$ NMR (100 MHz, $C_6D_6$) δ 9.9 ($C_5Me_5$), 18.6 ($\eta^1$-allyl Me), 18.6 ($\eta^1$-allyl $CH_2$), 22.6 ($\eta^3$-allyl Me), 22.6 ($\eta^3$-allyl Me), 22.8 ($\eta^3$-allyl Me), 26.0 ($\eta^1$-allyl Me), 44.8 ($\eta^3$-allyl $CH_2$), 106.9 ($C_5Me_5$), 133.3 ($\eta^1$-allyl-CH). Sel NOE (400 MHz, $C_6D_6$) δ irrad. at 1.59, NOE at 0.70 and 1.07. Anal. Calcd. for $C_{21}H_{35}NOW$: C, 50.31; H, 7.04; N, 2.79. Found: C, 50.58; H, 7.20; N, 2.89.

### 3.4.6 Preparation of Cp*W(NO)($PMe_3$)($\eta^2$-$H_2C$=C=$CMe_2$) (3.3)

Complex **3.3** was prepared by the thermolysis of **1.1** (67 mg, 0.14 mmol) in neat trimethylphosphine. The resulting residue was triturated with hexanes (2 x 10 ml) and the solvent was removed. The product was allowed dried for 1 hour under high vacuum, whereupon hexane extracts of the residue were transferred to the top of an alumina (I) column (0.5 x 3 cm), and eluted with $Et_2O$ to obtain a yellow solution. The solvent was once again removed from the eluate and the final residue was recrystallized from a 3:1 pentane/$Et_2O$ solvent mix to obtain complex **3.3** as yellow blocks (16 mg, 24 %).

**3.3**: IR ($cm^{-1}$) 1541 (s, $\nu_{NO}$). MS (LREI, *m/z*, probe temperature 120 °C) 493 [$P^+$, $^{184}W$]. $^1H$ NMR (400 MHz, $C_6D_6$) δ 0.67 (d, $^2J_{HH}$ = 7.31, 1H, allene $CH_2$), 1.27 (d, $^2J_{HP}$ = 8.8, 9H, $PMe_3$), 1.67 (s, 15H, $C_5Me_5$), 1.78 (s, 3H, allene Me), 1.97 (br s, 1H, allene $CH_2$), 2.44 (s, 3H, allene Me). $^{13}C\{^1H\}$ NMR (100 MHz, $C_6D_6$) δ 7.7 (allene *C*$H_2$), 10.4 ($C_5$*Me*$_5$), 17.3 (d, $^2J_{CP}$ = 31, $PMe_3$), 25.9 (allene Me), 31.9 (allene Me), 104.6 (*C*$_5$Me$_5$), 165.7 (=*C*=$CH_2$). $^{31}P\{^1H\}$ NMR (121 MHz, $C_6D_6$) δ -21.4 (s, $^1J_{PW}$ = 345, $PMe_3$). Sel NOE (400 MHz, $C_6D_6$) δ irrad. at 0.67, NOE at 1.67, 1.97 and 2.44, irrad. at 1.78, NOE at 1.27 and 2.44. Anal. Calcd. for $C_{18}H_{32}NOPW$: C, 43.83; H,6.54; N, 2.84. Found: C, 43.65; H, 6.53; N, 2.97.

**3.5 References and Notes**

(1) Adams, C.S. C-H Activation of Hydrocarbons by Tungsten Alkylidene and Related Complexes. Ph.D. Thesis, University of British Columbia, Vancouver, BC, October 2001.

(2) Adams, C. S.; Legzdins, P.; Tran, E. *J. Am. Chem. Soc.* **2001**, *123*, 612.

(3) The method utilized in the statistical analysis of integral data for the quantitative incorporation of deuterium was provided by Natalie Thompson of the UBC Department of Mathematics. Her consultation report as well as a the raw integral data collected is included in Appendix B.

(4) Schock, L. E.; Brock, C. P.; Marks, T. J. *Organometallics* **1987**, *6*, 232.

(5) Becconsall, J. K.; Job, B. E.; O'Brien, S. *J. Chem. Soc. A* **1967**, 423.

(6) Benn, R.; Rufinska, A.; Schroth, G. *J. Organomet. Chem.* **1981**, *217*, 91.

(7) Thompson, M. E.; Baxter, S. M.; Bulls, A. R.; Burger, B. J.; Nolan, M. C.; Santarsiero, B. D.; Schaefer, W. P.; Bercaw, J. E. *J. Am. Chem. Soc.* **1987**, *109*, 203.

(8) Abrams, M. B.; Yoder, J. C.; Loeber, C.; Day, M. W.; Bercaw, J. E. *Organometallics* **1999**, *18*, 1389.

(9) Christensen, N. J.; Hunter, A. D.; Legzdins, P. *Organometallics* **1989**, *8*, 930.

(10) Hunter, A. D.; Legzdins, P.; Nurse, C. R. *J. Am. Chem. Soc.* **1985**, *107*, 1791.

(11) Debad, J. D.; Legzdins, P.; Lumb, S. A.; Rettig, S. J.; Batchelor, R. J.; Einstein, F. W. B. *Organometallics* **1999**, *18*, 3414.

(12) Yin, J.; Jones, W. M. *Tetrahedron* **1995**, *51*, 4395.

(13) Doxsee, K. M.; Juliette, J. J. J.; Zientara, K.; Nieckarz, G. *J. Am. Chem. Soc.* **1994**, *116*, 2147.

(14) Choi, J. C.; Sarai, S.; Koizumi, T.; Osakada, K.; Yamamoto, T. *Organometallics* **1998**, *17*, 2037.

(15) Lee, L.; Wu, I. Y.; Lin, Y. C.; Lee, G. H.; Wang, Y. *Organometallics* **1994**, *13*, 2521.

(16) Crystal data for **3.2**: monoclinic, space group $P2_1/n$, $a = 9.1734(7)$ Å, $b = 16.9621(11)$ Å, $c = 13.2647(10)$ Å, $\beta = 95.201(4)$ °, $V = 2055.5(3)$ Å$^3$, $Z = 4$, $R_1 = 0.0378$, $wR_2 = 0.0748$, and GOF($F^2$) = 0.983 for 4496 reflections and 247 variables.

(17) Crystal data for **3.3**: monoclinic, space group $P2_1/c$, $a = 9.1458(5)$ Å, $b = 13.6500(7)$ Å, $c = 15.9576(9)$ Å, $\beta = 98.724(3)$ °, $V = 1969.10(18)$ Å$^3$, $Z = 4$, $R_1 = 0.0358$, $wR_2 = 0.0667$, and GOF($F^2$) = 0.946 for 4135 reflections and 217 variables.

(18) Okamoto, K.; Kai, Y.; Yasuoka, N.; Kasai, N. *J. Organomet. Chem.* **1974**, *65*, 427.

(19) Racanelli, P.; Pantini, G.; Immirzi, A.; Allegra, G.; Porri, L. *Chem. Commun.* **1969**, 361.

(20) Bowden, F. L.; Giles, R. *Coord. Chem. Rev.* **1976**, *20*, 81.

(21) Dewar, M. J. S. *Bull. Soc. Chim. Fr.* **1951**, *18*, C71.

(22) Chatt, J.; Duncanson, L. A. *J. Chem. Soc.* **1953**, 2939.

(23) Albright, T. A.; Hoffman, R.; Thibeault, J. C.; Thorn, D. L. *J. Am. Chem. Soc.* **1979**, *101*, 3801.

(24) Greaves, E. O.; Lock, C. J. L.; Maitlis, P. M. *Can. J. Chem.* **1968**, *46*, 3879.

(25) Binger, P.; Langhauser, F.; Wedeman, P.; Gabor, B.; Mynott, R.; Kruger, C. *Chem. Ber.* **1994**, *127*, 39.

(26) Clark, H. C.; Dymarski, M. J.; Payne, N. C. *J. Organomet. Chem.* **1979**, *165*, 117.

(27) Lentz, D.; Willemsen, S. *Organometallics* **1999**, *18*, 3962.

(28) Werner, H.; Schneider, D.; Schulz, M. *J. Organomet. Chem.* **1993**, *451*, 175.

(29) Pu, J.; Peng, T.-S.; Arif, A. M.; Gladysz, J. A. *Organometallics* **1992**, *11*, 3232.

(30) Yasuoka, N.; Morita, M.; Kai, Y.; Kasai, N. *J. Organomet. Chem.* **1975**, *90*, 111.

(31) Yin, J.; Abboud, K. A.; Jones, W. M. *J. Am. Chem. Soc.* **1993**, *115*, 3810.

(32) The exceptionally strong π-donor ability of the related Cp*W(NO)($PPh_3$) fragment has been documented, see: Burkey, D. J.; Debad, J. D.; Legzdins, P. *J. Am. Chem. Soc.* **1997**, *119*, 1139.

(33) Gibson, V. C.; Parkin, G.; Bercaw, J. E. *Organometallics* **1991**, *10*, 220.

(34) Hewitt, T. G.; De Boer, J. J. *J. Chem. Soc. A.* **1971**, 817.

(35) McGhee, W. D.; Bergman, R. G. *J. Am. Chem. Soc.* **1988**, *110*, 4246.

(36) Debad, J. D.; Legzdins, P.; Young, M. A. *J. Am. Chem. Soc.* **1993**, *115*, 2051.

(37) Hunter, A. D.; Legzdins, P.; Nurse, C. R.; Einstein, F. W. B.; Willis, A. C.; Bursten, B. E.; Gatter, M. J. *J. Am. Chem. Soc.* **1986**, *108*, 3843.

# Chapter 4

## *Multiple C-H Bond Activations of Hydrocarbons by $Cp^*W(NO)(\eta^2\text{-}H_2C{=}C{=}CMe_2)$: Towards Functionalization of Alkanes*

---



---

## 4.1 Introduction

Chapters 2 and 3 describe the C-H activation reactions of Cp*W(NO)($\eta^2$-$H_2C{=}C{=}CMe_2$) (**A**) with tetramethylsilane, benzene, benzene-$d_6$, and various methyl-substituted arenes to yield their respective hydrocarbyl-dimethylallyl complexes. Some of these reactions permit the elucidation of the thermodynamic distribution of products, based on the different C-H bond environments found on the hydrocarbon in question (e.g. $sp^2$ aryl C-H bond vs $sp^3$ benzylic C-H bond). However, the question of thermodynamic distributions for different types of $sp^3$ hybridized C-H bonds (e.g. primary vs secondary vs tertiary) has yet to be addressed.

As mentioned in Chapter 1, alkanes constitute a large proportion of the worlds' hydrocarbon feedstocks, and thus the ultimate goal is to convert these abundant, relatively inexpensive, and inert substrates into more desirable materials of commercial value. The first step towards the functionalization of these alkane substrates is the C-H activation process that opens the doors for incorporation of new functional groups that are of potential synthetic utility.

In this context, this Chapter seeks to elucidate the organometallic products formed during reactions of **A** with saturated alkane solvents such as methylcyclohexane and cyclohexane, and provide some preliminary discussion pertaining to the thermodynamic distribution of the final products generated. In addition, pertinent discussion is presented regarding potential alkane functionalization processes based on the C-H bond-activating chemistry exhibited by the tungsten-allene complex.

## 4.2 Results and Discussion

### 4.2.1 Thermolysis of 1.1 in Methylcyclohexane

Given the similarity in C-H activating chemistry initiated by the well-studied bis(neopentyl) complex, namely $Cp^*W(NO)(CH_2CMe_3)_2$,[1-3] it is not unreasonable to anticipate the generation of similar organometallic species upon thermolysis of **1.1** in alkyl-substituted cyclic alkanes. Consistently, two principal products are formed in the reaction between the tungsten-allene reactive intermediate (**A**) and methylcyclohexane, namely the two isomeric species, $Cp^*W(NO)(\eta^3\text{-}C_7H_{11})(H)$ (**4.1** and **4.2**) (eq. 4.1).

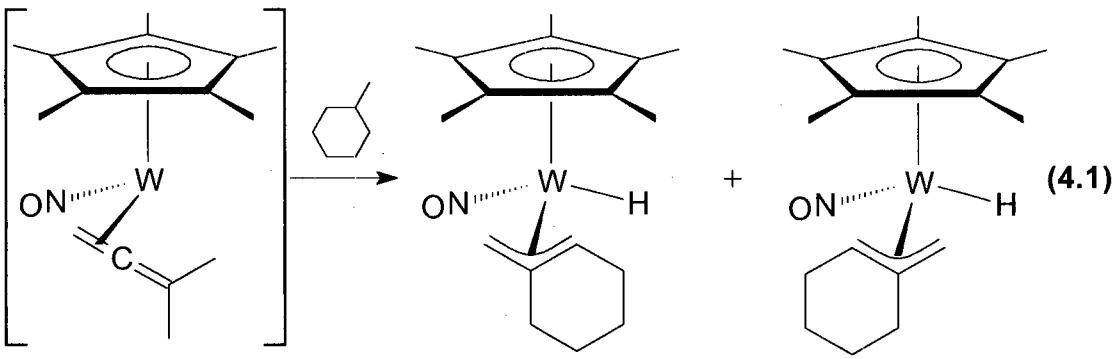


Compounds **4.1** and **4.2** are identical to the principal organometallic species isolated from the reactions of the intermediate neopentylidene and benzylidene species ($Cp^*W(NO)(=CHCMe_3)$ and $Cp^*W(NO)(=CHC_6H_5)$, respectively) described in Section 1.2.2 with methylcyclohexane. The major product in all three cases, **4.1**, is formed in

greater than 90 % yield as indicated by $^{1}H$ NMR spectroscopy and exhibits an exocyclic *endo*-$\eta^3$-allyl linkage with the terminal $CH_2$ group cis to the nitrosyl ligand. Analogous to the dimethylallyl moiety of the majority of complexes characterized and presented in this Thesis, the $^{13}C\{^{1}H\}$ NMR spectrum of complex **4.1** ($C_6D_6$) exhibits a high-field signal assignable to the terminal allyl-carbon cis to the NO group that is indicative of $sp^3$-like character ($\delta$ 41.3), and low-field resonances for the remaining two carbons of the allyl backbone, suggestive of $sp^2$-like character ($\delta$ 80.0 CH, 121.1 C). These spectroscopic features are consistent with the familiar $\sigma$-$\pi$ distortions observed for allyl-nitrosyl complexes due to the $\pi$-accepting nature of the NO ligand in solution and in the solid state.[4-7] The previously determined solid-state molecular structure of **4.1** also reveals evidence for the distortion seen in solution.[2] The minor product, **4.2**, has been identified as an isomer of **4.1**, with the allyl $CH_2$ group found trans to the NO ligand, as shown in eq. 4.1. NOE spectroscopic techniques were unable to decisively distinguish between the possible exo or endo configurations for the exocyclic-allyl species. However, as with **4.1**, the steric bulk of the methylcyclohexenyl group in an exo conformer with the large Cp* ring is highly unfavoured. Thus, it is fair to assume that **4.2** also adopts an endo configuration. There is also evidence for the interconversion of **4.1** and **4.2** based on spin-saturation transfer observed between the resonances attributable to the allyl CH atoms of both complexes in NOE experiments, possibly via rotation about the W-C linkage of an $\eta^1$-allyl intermediate. Therefore, the product ratio observed reflects the thermodynamic distribution of complexes **4.1** and **4.2** generated at 50°C (~ 49:1 respectively). The corresponding alkylidene reactions performed at an elevated temperature (70 °C) yield a ratio of ~ 9:1, which further supports the notion that **4.1** is the thermodynamically

preferred conformation for the two possible isomers. The apparent exclusive formation of exocyclic $\eta^3$-allyl complexes vs the endocyclic species suggests that **A** preferentially activates the thermodynamically stronger primary C-H bonds, much like other metal-based alkane activation systems.[8]

### 4.2.2 Thermolysis of 1.1 in Cyclohexane[9]

Reaction of **A** with cyclohexane leads to the generation of a cyclohexenyl-hydrido complex, namely Cp*W(NO)($\eta^3$-$C_6H_9$)(H) (**4.3**) (eq. 4.2). This transformation constitutes a novel mode of multiple C-H activations of cyclohexane, a relatively inert solvent that has frequently been used to study the C-H activations of other hydrocarbons.[10-12]

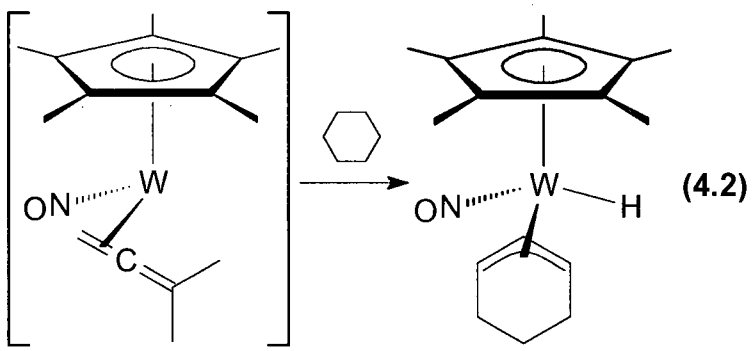


**A** **4.3** **(4.2)**

For comparison, the well-studied bis(alkyl) species such as Cp*W(NO)($CH_2CMe_3$)$_2$ react with cyclohexane in a completely different manner. Their thermolyses in the presence of an excess of trimethylphosphine in cyclohexane at 70 °C

for 40 hours result in the formation of two base-stabilized complexes, namely the alkylidene and the cyclohexene adducts.[1] However, in the absence of a suitable Lewis base, only decomposition occurs to afford intractable products, presumably due to the elevated temperatures employed. The thermal reaction of **1.1** in cyclohexane in the presence of excess trimethylphosphine results in the exclusive generation of the base-stabilized allene adduct. These reactivity differences suggest that new avenues of alkane activation chemistry may well be accessible through alkyl-allyl complexes such as **1.1**.

The solution NMR spectroscopic data show that the nitrosyl ligand also effects σ-π distortion on the cyclohexenyl fragment as seen in other allyl structures. The $^{13}C\{^1H\}$ NMR spectrum of **4.3** ($C_6D_6$) displays a resonance at low field corresponding to the $sp^3$-like terminal allyl-carbon cis to the NO ligand (δ 93.2), and high-field $sp^2$-like resonances for the central and remaining terminal allyl-carbon atoms (δ 61.8, 73.4). Furthermore, no signals attributable to any other isomers are present. Presumably, the formation of the endo species is, as in the case of **4.1** and **4.2**, highly unfavourable due to inevitable steric interactions between the cyclohexenyl fragment and the Cp* ring.

A single-crystal X-ray crystallographic analysis has been performed on **4.3**, confirming the connectivity as shown in eq. 4.2. Unfortunately, the quality of the diffraction data collected precludes any meaningful discussion of the metrical parameters of **4.3** and, in addition, the hydride could not be conclusively located. However, the $^1H$ NMR spectrum of **4.3** ($C_6D_6$) displays a distinctive hydride resonance (δ -0.57, $J_{WH}$ = 132) (Figure 4.1), and the IR spectrum (KBr pellet) exhibits a $\nu_{WH}$ stretching frequency at 1898 $cm^{-1}$,[2] thereby confirming the proposed formulation of **4.3**.

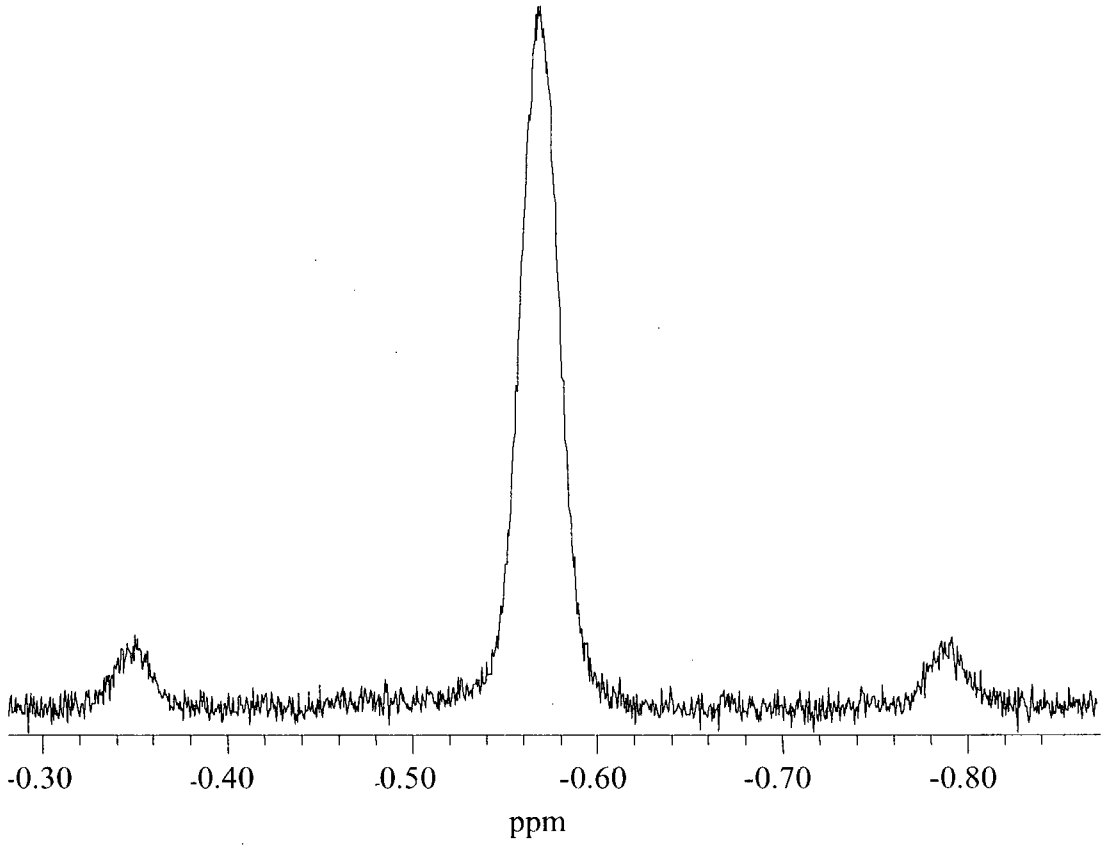


**Figure 4.1** Hydride region of $^{1}H$ NMR spectrum of cyclohexenyl-hydrido complex **4.3** in $C_6D_6$. ($^{183}W$ I = ½ [14.4%], $J_{WH}$ = 131.7 Hz, $\delta$ = -0.57 ppm )

## 4.3 Potential Functionalization of Alkanes: Future Work

The formation of new organometallic species as a consequence of successive C-H bond-activation reactions of alkane substrates is an extremely interesting feature, although it is not unique to these systems. For example, Crabtree and Baudry showed that cyclopentane reacts with Ir and Re systems to form cyclopentadienyl-containing species as a result of multiple hydrogen loss. However, an alkene must be added as a hydrogen acceptor for the reactions to proceed (Scheme 4.1).[13-16] Seemayer reported the multiple C-H bond activation of cyclohexane by early-transition metal cations ($Sc^+$, $Ti^+$ and $V^+$), to give $\eta^6$-benzene species.[17] However, this transformation has little practical implications since it is performed in the gas phase. Intramolecular multiple C-H bond activations have also been observed, but are less useful for purposes of direct alkane-functionalization.[18-21]

**Scheme 4.1**

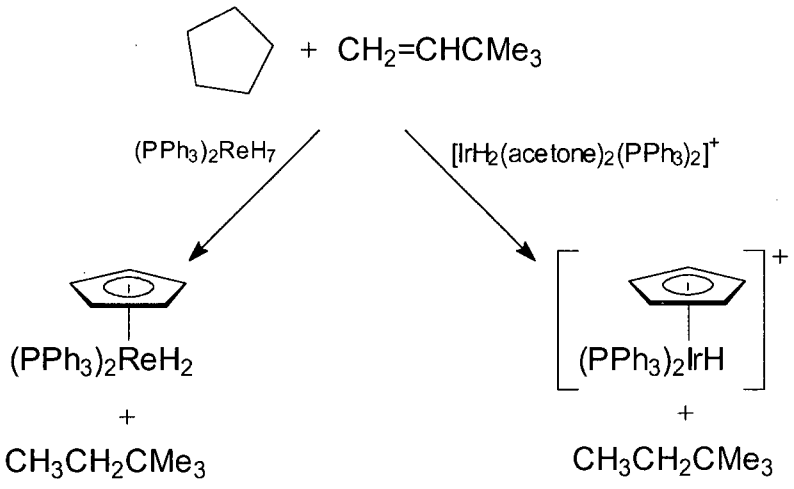

The potential for functionalization of hydrocarbons using the tungsten-allene system is most evident in the cases of the formation of $Cp^*W(NO)(\eta^3\text{-}2,3,3\text{-}Me_3C_3H_2)(\eta^1\text{-}3,3\text{-}Me_2C_3H_3)$ (**3.2**), **4.1,** and **4.3** from thermal reactions of **1.1** in 2,3-dimethyl-2-butene, methylcyclohexane and cyclohexane, respectively. In these instances, new allyl complexes are formed from the hydrocarbon substrate, and are thus potentially suitable reagents for organic syntheses based on the research conducted on CpMo(NO)(allyl) fragments.[5,6,22-28] That the Cp*W and CpMo fragments possess comparable structural and electronic features suggests the metal-allyl species mentioned above (**3.2**, **4.1** – **4.3**) may exhibit similar reactivity to form organic products.[29-32]

The selectivity exhibited by $CpMo(NO)(X)(\eta^3\text{-allyl})$ (X = halide) complexes for the generation of homoallylic alcohols is due to the electronic asymmetry arising from variations in acceptor properties of the nitrosyl and halide ligands (eq. 4.3).[23,33]

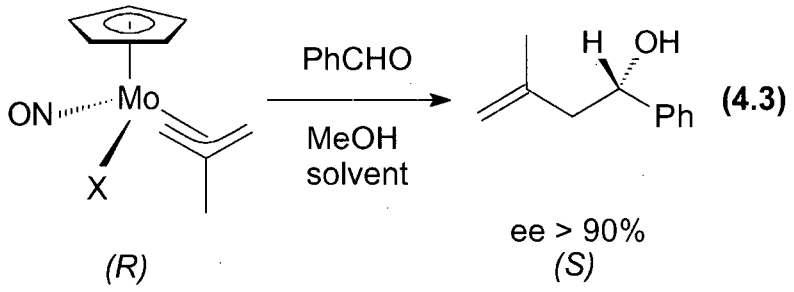


The σ-π distortions common to metal-allyl-nitrosyl complexes permit the allyl ligand to adopt an $\eta^1$ configuration with the bond retained being between the metal center and the terminal allyl-carbon cis to the NO ligand.[23] This effectively opens up a Lewis acidic site at the metal center where an aldehyde could bind and generate a chair-like transition state for the coupling of the two organic fragments to occur (Scheme 4.2).[33]

**Scheme 4.2**

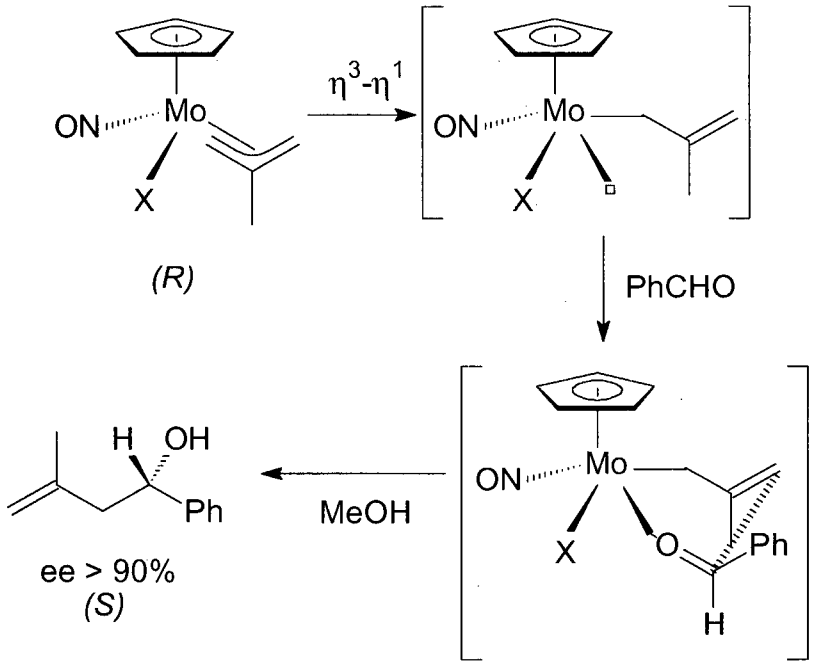


The generation of similar homoallylic alcohols may be plausible by applying this known reaction to the Cp*W(NO)(allyl)(hydrido) systems. It is known that transition-metal hydride complexes can be converted to the corresponding halide species by dissolution in halogenated organic solvents such as dichloromethane,[34] whereupon analogous σ-π distortions can lead to the opening of a coordination site for an aldehyde to bind, and undergo the same reactivity to yield the desired organic product. Scheme 4.3 illustrates a possible reaction pathway to generate homoallylic alcohols starting from the cyclohexenyl-hydrido complex (**4.3**). A similar reaction pathway could be drawn for the analogous reaction with the exocyclic $\eta^3$-allyl methylcyclohexenyl-hydrido complex.

**Scheme 4.3**

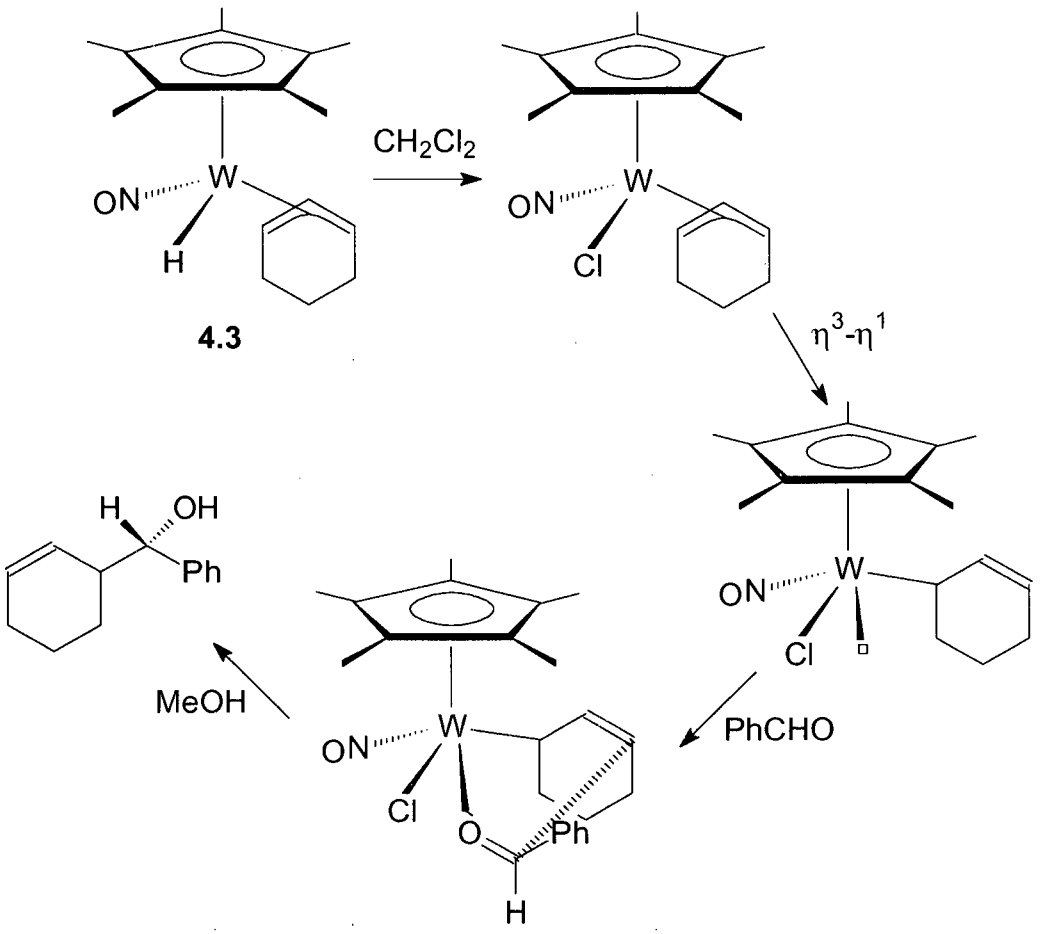


All of the work presented thus far concerns the characterization of the final organometallic species present in the reaction mixtures. However, the issue of organic products generated during the thermolyses requires thorough investigation, and could potentially yield some interesting results. In this regard, studies are required to identify the non-organometallic species synthesized concurrently with the compounds discussed in this Thesis.

Preliminary data collected from the thermolysis of **1.1** in cyclohexane yield an interesting result. As well as the generation of **4.3**, GC-MS data suggest that the coupled

organic product, 1,1-dimethylpropylcyclohexane, is also present in the final reaction mixture. This product is possibly formed as a result of coupling between a coordinated cyclohexenyl group and an alkyl fragment derived from the precursor dimethylallyl ligand (Scheme 4.4).

**Scheme 4.4**

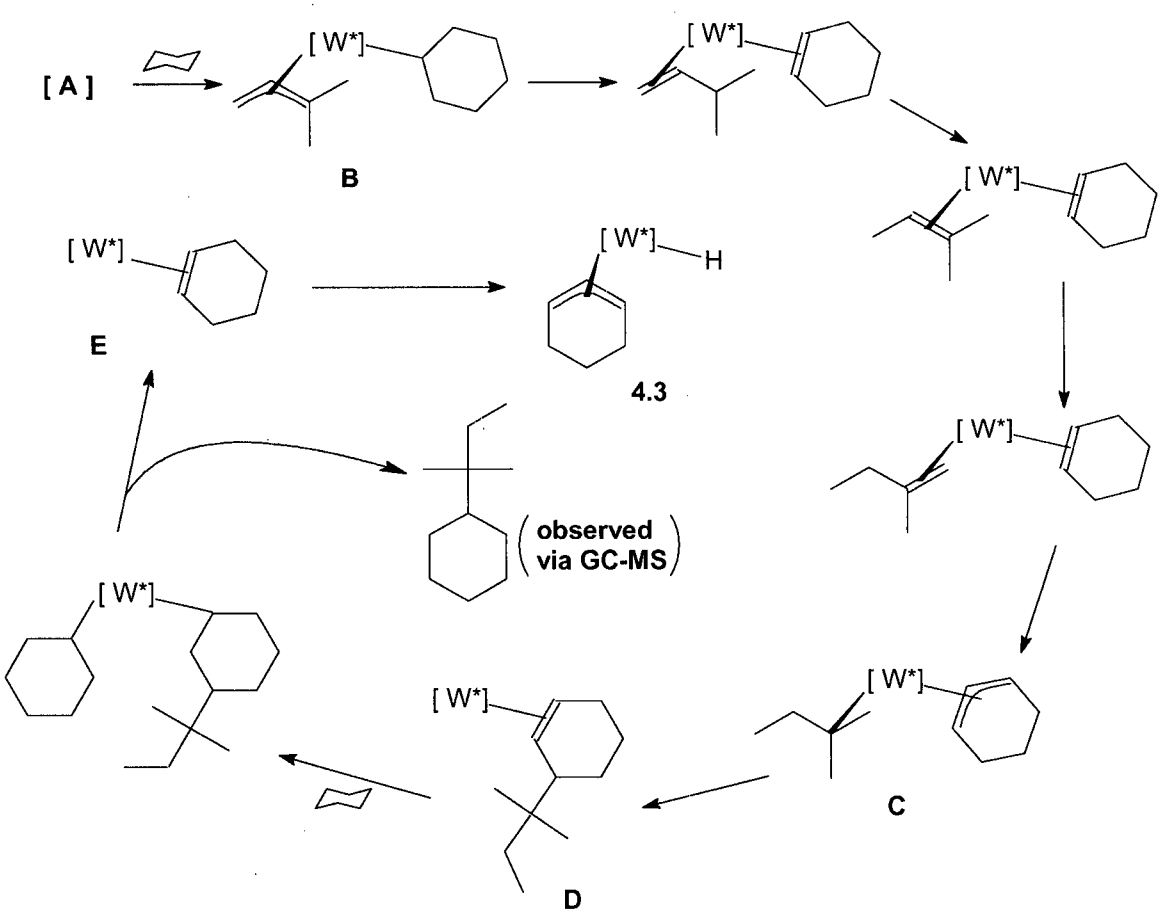


In the reaction pathway proposed in Scheme 4.4, initial single C-H bond activation of cyclohexane affords the allyl-alkyl product (**B**), which can undergo double

β-H elimination to generate an alternative alkyl-allyl (**C**). The allyl moiety could then switch to a $\eta^1$ binding mode, providing an accessible double bond that subsequently couples with the alkyl group much like the tungsten-acetylene system[35] to give an alkene complex (**D**). Complex **D** can then activate a second molecule of cyclohexane and subsequent β-H elimination can lead to the ejection of the purported 1,1-dimethylpropylcyclohexane from the metal's coordination sphere, leaving a cyclohexene adduct (**E**) that β-H eliminates to yield the final cyclohexenyl-hydrido complex, **4.3**.

Preliminary experiments have been initiated in an effort to further elucidate the scope of alkane C-H bond-activation chemistry exhibited by **A**. The $^1$H NMR spectrum of the crude residue from the thermolysis of **1.1** in pentane reveals the generation of multiple organometallic species, as evinced by a plethora of resonances attributable to hydride ligands.

## 4.4 Epilogue

Reaction of **A** with methylcyclohexane gives an indication of the selectivity for different $sp^3$ C-H bonds. The formation of the exocyclic allyl species and the absence of evidence for any endocyclic isomer suggests the preference of **A** to activate primary C-H bonds, a common feature observed for other metal-based alkane C-H activating complexes.

The generation of allyl-hydrido organometallic species as a consequence of multiple C-H bond activations of saturated alkane substrates by **A** is a result of great interest. Given the rigorous studies that have been conducted on the structurally and electronically similar CpMo(NO)(allyl)(X) (X = halide) species, the potential reactivity of the hydrido complexes to ultimately yield homoallylic alcohols of synthetic use in organic chemistry opens new avenues of research regarding the functionalization of alkanes using the precursor neopentyl-dimethylallyl complex.

The apparent generation of the coupled organic product from the thermal reaction of **1.1** with cyclohexane is also bound to spark much interest in the chemical community as another means of functionalizing saturated alkanes by the same precursor species.

As such, there is still much work to be performed on this diverse system that is, to our knowledge, the first reported C-H activating system that has been confirmed to involve a reactive allene intermediate.

## 4.5 Experimental Procedures

### 4.5.1 Preparation of Cp*W(NO)($\eta^3$-$C_7H_{11}$)(H) (4.1 and 4.2) and Cp*W(NO)($\eta^3$-$C_6H_9$)(H) (4.3)

Complexes **4.1** and **4.2** were formed via the thermolysis of **1.1** (80 mg, 0.16 mmol) in methylcyclohexane and complex **4.3** was formed via thermolysis of **1.1** (50 mg, 0.10 mmol) in cyclohexane The reaction mixtures at the end of the 6-hour period were a dark orange/brown colour, and the residues formed upon removal of the solvent were brown oils. The residues were triturated with hexanes (2 x 10 mL) which were dried under high vacuum for approximately 1 hour to obtain mixtures of dark specks interspersed in brown oils, which were then redissolved in a 1:3 $Et_2O$/hexanes solvent mixture and eluted through an alumina (I) column (0.5 x 3 cm) to afford yellow solutions. The solvent was once again removed, and the final residues were recrystallized from 3:1 pentane/$Et_2O$ solvent mixes to obtain complexes **4.1** and **4.2** as yellow microcrystals (3.5 mg, 5 %), and complex **4.3** as yellow blocks (14 mg, 32 %). Complexes **4.1** and **4.2** were identified by comparison of their $^1$H NMR resonances to those previously reported.[2]

**4.3**: IR ($cm^{-1}$) 1568 (s, $\nu_{NO}$), 1898 (m, $\nu_{WH}$). MS (LREI, *m/z*, probe temperature 120 °C) 431 [$P^+$, $^{184}$W]. $^1$H NMR (500 MHz, $C_6D_6$) $\delta$ –0.57 (s, $^1J_{WH}$ = 132, 1H, WH), 1.16 (m, 1H, cyclohexenyl $C_aH_2$), 1.42 (m, 1H, cyclohexenyl $C_aH_2$), 1.69 (s, 15H, $C_5Me_5$), 2.46 (m, 1H, cyclohexenyl $C_bH_2$), 2.58 (m, 1H, cyclohexenyl $C_bH_2$), 2.62 (m, 2H, cyclohexenyl $C_cH_2$), 2.75 (m, 1H, allyl $C_xH$), 3.59 (m, 1H, allyl $C_yH$), 5.30 (m, 1H, allyl $C_zH$). $^{13}C\{^1H\}$ NMR (125 MHz, $C_6D_6$) $\delta$ 10.4 ($C_5\mathit{Me}_5$), 19.9 (cyclohexenyl $C_aH_2$),

26.6 (cyclohexenyl $C_cH_2$), 28.7 (cyclohexenyl $C_bH_2$), 61.8 (allyl $C_yH_2$), 73.4 (allyl $C_zH$), 93.2 (allyl $C_xH_2$), 103.9 ($C_5Me_5$). Anal. Calcd. for $C_{16}H_{25}NOSiW$: C, 44.56; H, 5.84; N, 3.25. Found: C, 44.40; H, 5.76; N, 3.24.

### 4.5.2 Thermolysis of 1.1 in Cyclohexane in the Presence of Excess $PMe_3$

Complex **3.3** was formed via thermolysis of **1.1** (26 mg, 0.05mmol) in cyclohexane and trimethylphosphine (0.2 mL, 1.93 mmol). The volatiles were removed in vacuo, and the resulting residue was worked-up as described in Section 3.4.6.

### 4.5.3 Preliminary Identification of Organic Products generated during Thermolysis of 1.1 in Cyclohexane

The thermal reaction of **1.1** in cyclohexane was conducted as described in Section 4.5.2, except that the volatiles were removed in vacuo and collected in a GC bomb. A blank reaction of neat cyclohexane was also performed, and its volatiles were also collected in a GC bomb in an identical fashion. Both sets of volatiles were analysed via GC-MS, and their spectra were subtracted to obtain a spectrum devoid of peaks attributable to inherent products from the heating of cyclohexane. Preliminary analysis suggests the presence of 1,1-dimethylpropylcyclohexane. Organic volatiles analysis was performed using an Agilent 6890 Series gas chromatograph with an HP-5 MS column coupled to an Agilent 5973 Network mass-selective detector.

**4.6 References and Notes**

(1) Tran, E.; Legzdins, P. *J. Am. Chem. Soc.* **1997**, *119*, 5071.

(2) Adams, C. S.; Legzdins, P.; Tran, E. *J. Am. Chem. Soc.* **2001**, *123*, 612.

(3) Adams, C. S.; Legzdins, P.; Tran, E. *Organometallics* **2002**, *21*, 1474.

(4) Schilling, B. E. R.; Hoffman, R.; Faller, J. W. *J. Am. Chem. Soc.* **1979**, *101*, 592.

(5) Adams, R. D.; Chodosh, D. F.; Faller, J. W.; Rosan, A. M. *J. Am. Chem. Soc.* **1979**, *101*, 2570.

(6) Faller, J. W.; Nguyen, J. T.; Ellis, W.; Mazzieri, M. R. *Organometallics* **1993**, *12*, 1434.

(7) Ipaktschi, J.; Mirzaei, F.; Demuth-Eberle, G. J.; Beck, J.; Serafin, M. *Organometallics* **1997**, *16*, 3965.

(8) Arndsten, B. A.; Bergman, R. G.; Mobley, T. A.; Peterson, T. H. *Acc. Chem. Res.* **1995**, *28*, 154.

(9) Ng, S. H. K.; Adams, C. S.; Legzdins, P. *J. Am. Chem. Soc.* **2002**, *124*, published on web 23 July 2002.

(10) McGhee, W. D.; Bergman, R. G. *J. Am. Chem. Soc.* **1988**, *110*, 4246.

(11) Cummins, C. C.; Baxter, S. M.; Wolczanski, P. T. *J. Am. Chem. Soc.* **1988**, *110*, 8731.

(12) Schaller, C. P.; Cummins, C. C.; Wolczanski, P. T. *J. Am. Chem. Soc.* **1996**, *118*, 591.

(13) Crabtree, R. H.; Mihelcic, J. M.; Quirk, J. M. *J. Am. Chem. Soc.* **1979**, *101*, 7738.

(14) Crabtree, R. H.; Mellea, M. F.; Mihelcic, J. M.; Quirk, J. M. *J. Am. Chem. Soc.* **1982**, *104*, 107.

(15) Crabtree, R. H.; Demou, P. C.; Eden, D.; Mihelcic, J. M.; Parnell, C. A.; Quirk, J. M.; Morris, G. E. *J. Am. Chem. Soc.* **1982**, *104*, 6994.

(16) Baudry, D.; Ephritikine, M.; Felkin, H. *J. Chem. Soc., Chem. Commun.* **1980**, 1243.

(17) Seemeyer, K.; Schroder, D.; Kempf, M.; Lettau, O.; Muller, J.; Schwarz, H. *Organometallics* **1995**, *14*, 4465.

(18) Prinz, M.; Grosche, M.; Herdtweck, E.; Herrmann, W. A. *Organometallics* **2000**, *19*, 1692.

(19) Kickham, J. E.; Guerin, F.; Stewart, J. C.; Stephan, D. W. *Angew. Chem. Int. Ed.* **2000**, *39*, 3263.

(20) Kickham, J. E.; Guerin, F.; Stewart, J. C.; Urbanska, E.; Stephan, D. W. *Organometallics* **2001**, *20*, 1175.

(21) Stephan, D. W. *Can. J. Chem.* **2002**, *80*, 125.

(22) Faller, J. W.; Linebarrier, D. L. *Organometallics* **1990**, *9*, 3182.

(23) Faller, J. W.; DiVerdi, M. J.; John, J. A. *Tetrahedron Lett.* **1991**, *32*, 1271.

(24) Faller, J. W.; Murray, D. L.; White, D. L.; Chao, K. H. *Organometallics* **1983**, *2*, 400.

(25) Faller, J. W.; Chao, K. H. *J. Am. Chem. Soc.* **1983**, *105*, 3893.

(26) Faller, J. W.; Mazzieri, M. R. *J. Organomet. Chem.* **1990**, *383*, 161.

(27) Vanarsdale, W. E.; Winter, R. E. K.; Kochi, J. K. *J. Organomet. Chem.* **1985**, *296*, 31.

(28) Vanarsdale, W. E.; Winter, R. E. K.; Kochi, J. K. *Organometallics* **1986**, *5*, 645.

(29) Legzdins, P.; Veltheer, J. E. *Acc. Chem. Res.* **1993**, *26*, 41.

(30) Poli, R.; Smith, K. M. *Organometallics* **2000**, *19*, 2858.

(31) Bursten, B. E.; Cayton, R. H. *Organometallics* **1987**, *6*, 2004.

(32) Legzdins, P.; Rettig, S. J.; Sanchez, L. J.; Bursten, B. E.; Gatter, M. J. *J. Am. Chem. Soc.* **1985**, *107*, 1411.

(33) Faller, J. W.; Linebarrier, D. L. *J. Am. Chem. Soc.* **1989**, *111*, 1937.

(34) Crabtree, R. H. *The Organometallic Chemistry of the Transition Metals*; 3rd ed.; Wiley and Sons: Toronto, 2001.

(35) Debad, J. D.; Legzdins, P.; Lumb, S. A.; Rettig, S. J.; Batchelor, R. J.; Einstein, F. W. B. *Organometallics* **1999**, *18*, 3414.

# APPENDIX A

## Solid-state Molecular Structure X-ray Crystallographic Data Refinement, and Structural Solution and Refinement Data for Compounds 2.1, 2.2, 2.3, 2.5, 3.2 and 3.3

**Table A1** Data Refinement, and Structural Solution and Refinement Data for Compounds **2.1**, **2.2** and **2.3**

| **Crystal Data** | **2.1** | **2.2** | **2.3** |
|---|---|---|---|
| Empirical formula | $C_{21}H_{29}NOW$ | $C_{19}H_{35}NOWSi$ | $C_{24}H_{35}NOW$ |
| Crystal Habit, color | Prism, yellow | Platelet, orange | Block, orange |
| Crystal size (mm) | 0.30 x 0.20 x 0.20 | $0.30 \times 0.15 \times 0.08$ | $0.40 \times 0.30 \times 0.15$ |
| Crystal system | Monoclinic | Monoclinic | Orthorhombic |
| Space group | $P2_1/C$ | C2/c | Pbca |
| Volume ($Å^3$) | 1949.6(1) | 4228.4(3) | 4456.2(3) |
| a (Å) | 12.8869(3) | 15.3944(6) | 14.2207(7) |
| b (Å) | 9.0219(3) | 8.4977(3) | 15.9939(7) |
| c (Å) | 16.7835(7) | 32.326(1) | 19.5926(9) |
| $\alpha$ (°) | 90 | 90 | 90 |
| $\beta$ (°) | 92.439(2) | 90.753(3) | 90 |
| $\gamma$ (°) | 90 | 90 | 90 |
| Z | 4 | 8 | 8 |
| Density (calculated) ($Mg/m^3$) | 1.687 | 1.500 | 1.602 |
| Absorption coefficient ($cm^{-1}$) | 59.39 | 54.73 | 52.03 |
| $F_{000}$ | 976.00 | 1904.00 | 2144.00 |

**Table A1** Data Refinement, and Structural Solution and Refinement Data for Compounds **2.1**, **2.2** and **2.3** (cont'd)

| **Crystal Data** | **2.1** | **2.2** | **2.3** |
|---|---|---|---|
| Formula weight (g/mol) | 495.32 | 477.34 | 537.40 |
| Radiation | MoKα, 0.71069 Å | MoKα, 0.71069 Å | MoKα, 0.71069 Å |
| $2\theta_{max}$ (°) | 57.5 | 55.9 | 55.7 |
| Measured Reflections: Total | 13123 | 12879 | 41082 |
| Measured Reflections: Unique | 4484 | 4410 | 5645 |
| **Structure Solution and Refinement** | | | |
| Structure Solution Method | Direct | Direct | Direct |
| Refinement | Full-matrix least-squares | Full-matrix least-squares | Full-matrix least-squares |
| No. Observations | 4264 | 4156 | 5120 |
| No. Variables | 229 | 221 | 264 |
| Final R Indices[a] | R1 = 0.038, wR2 = 0.066 | R1 = 0.036, wR2 = 0.071 | R1 = 0.031, wR2 = 0.038 |
| Goodness-of-fit on $F^{2}$[b] | 1.07 | 1.60 | 0.80 |
| Largest diff. peak and hole ($e^{-}$ Å$^{-3}$) | 1.08 and –1.64 | 2.01 and –1.75 | 3.30 and –2.01 |

[a] R1 on $F = \Sigma \mid (|F_o| - |F_c|) \mid / \Sigma |F_o|$; $wR2 = = [ (\Sigma ( F_o^2 - F_c^2 )^2 ) / \Sigma w(F_o^2)^2]^{1/2}$; $w = [ \sigma^2 F_o^2 ]^{-1}$; [b] GOF = $[ \Sigma (w ( |F_o| - |F_c| )^2 ) / \textit{degrees of freedom} ]^{1/2}$.

**Table A2** Data Refinement, and Structural Solution and Refinement Data for Compounds **2.5**, **3.2** and **3.3**

| **Crystal Data** | **2.5** | **3.2** | **3.3** |
|---|---|---|---|
| Empirical formula | $C_{23}H_{33}NOW$ | $C_{21}H_{35}NOW$ | $C_{18}H_{32}NOPW$ |
| Crystal Habit, color | Brick, orange | Prism, yellow | Chip, yellow |
| Crystal size (mm) | 0.11 x 0.09 x 0.04 | 0.45 x 0.35 x 0.20 | 0.25 x 0.20 x 0.10 |
| Crystal system | Rhombohedral | Monoclinic | Monoclinic |
| Space group | R-3 | $P2_1/n$ | $P2_1/c$ |
| Volume ($Å^3$) | 3447.2(14) | 2055.5(3) | 1969.10(18) |
| a (Å) | 21.258(5) | 9.1734(7) | 9.1458(5) |
| b (Å) | 21.258(5) | 16.9621(11) | 13.6500(7) |
| c (Å) | 21.258(5) | 13.2647(10) | 15.9576(9) |
| $\alpha$ (°) | 118.048(4) | 90 | 90 |
| $\beta$ (°) | 118.048(4) | 95.201(4) | 98.724(3) |
| $\gamma$ (°) | 118.048(4) | 90 | 90 |
| Z | 6 | 4 | 4 |
| Density (calculated) ($Mg/m^3$) | 1.513 | 1.62 | 1.664 |
| Absorption coefficient ($cm^{-1}$) | 50.37 | 58.05 | 59.50 |
| $F_{000}$ | 1560 | 1000 | 976 |

**Table A2** Data Refinement, and Structural Solution and Refinement Data for Compounds **2.5**, **3.2** and **3.3** (cont'd)

| **Crystal Data** | **2.5** | **3.2** | **3.3** |
|---|---|---|---|
| Formula weight (g/mol) | 523.35 | 501.35 | 493.27 |
| Radiation | MoKα, 0.71073 Å | MoKα, 0.71069 Å | MoKα, 0.71069 Å |
| $2\theta_{max}$ (°) | 55.06 | 55.74 | 55.74 |
| Measured Reflections: Total | 20952 | 4496 | 18136 |
| Measured Reflections: Unique | 5208 | 4496 | 4135 |
| **Structure Solution and Refinement** | | | |
| Structure Solution Method | Direct | Direct | Direct |
| Refinement | Full-matrix least-squares | Full-matrix least-squares | Full-matrix least squares |
| No. Observations | 5208 | 4496 | 4135 |
| No. Variables | 258 | 247 | 217 |
| Final R Indices[a] | R1 = 0.0413, wR2 = 0.098 | R1 = 0.0311, wR2 = 0.073 | R1 = 0.0281, wR2 = 0.065 |
| Goodness-of-fit on $F^{2}$[b] | 1.083 | 0.985 | 0.947 |
| Largest diff. peak and hole ($e^{-}$ Å$^{-3}$) | 0.222 and –0.866 | 0.169 and –1.460 | 0.154 and –2.497 |

[a] R1 on $F = \Sigma \mid (|F_o| - |F_c|) \mid / \Sigma |F_o|$; $wR2 = = [ (\Sigma ( F_o^2 - F_c^2 )^2 ) / \Sigma w(F_o^2)^2]^{1/2}$; $w = [ \sigma^2 F_o^2 ]^{-1}$; [b] GOF = $[ \Sigma (w ( |F_o| - |F_c| )^2 ) / \textit{degrees of freedom} ]^{1/2}$.

**Table A3** Bond Distances (Å) in the Solid-State Molecular Structure Determined for **2.1**

| | | |
|---|---|---|
| W(1) N(1) 1.762(3) | C(1) C(6) 1.397(4) | C(9) C(11) 1.500(5) |
| W(1) C(1) 2.186(3) | C(2) C(3) 1.383(5) | C(12) C(13) 1.411(6) |
| W(1) C(7) 2.218(4) | C(3) C(4) 1.375(6) | C(12) C(16) 1.408(6) |
| W(1) C(8) 2.363(4) | C(4) C(5) 1.368(7) | C(12) C(17) 1.513(6) |
| W(1) C(12) 2.306(3) | C(5) C(6) 1.401(5) | C(13) C(14) 1.409(7) |
| W(1) C(13) 2.398(3) | C(7) C(8) 1.439(6) | C(13) C(18) 1.510(6) |
| W(1) C(14) 2.430(3) | C(7) H(6) 1.06(4) | C(14) C(15) 1.403(5) |
| W(1) C(15) 2.389(3) | C(7) H(7) 0.91(4) | C(14) C(19) 1.501(5) |
| W(1) C(16) 2.306(3) | C(8) C(9) 1.365(5) | C(15) C(16) 1.405(5) |
| O(1) N(1) 1.224(4) | C(8) H(8) 1.00(5) | C(15) C(20) 1.489(6) |
| C(1) C(2) 1.406(5) | C(9) C(10) 1.495(5) | C(16) C(21) 1.502(5) |

**Table A4** Bond Angles (°) in the Solid-State Molecular Structure Determined for **2.1**

| | | |
|---|---|---|
| N(1) W(1) C(1) 93.3(1) | C(13) W(1) C(14) 33.9(2) | C(13) C(12) C(16) 107.6(3) |
| N(1) W(1) C(7) 92.1(2) | C(13) W(1) C(15) 56.4(1) | C(13) C(12) C(17) 127.1(5) |
| N(1) W(1) C(8) 104.6(1) | C(13) W(1) C(16) 57.8(1) | C(16) C(12) C(17) 125.2(5) |
| N(1) W(1) C(12) 95.4(1) | C(14) W(1) C(15) 33.8(1) | W(1) C(13) C(12) 69.0(2) |
| N(1) W(1) C(13) 127.7(1) | C(14) W(1) C(16) 57.6(1) | W(1) C(13) C(14) 74.3(2) |
| N(1) W(1) C(14) 149.5(1) | C(15) W(1) C(16) 34.8(1) | W(1) C(13) C(18) 128.8(3) |
| N(1) W(1) C(15) 121.7(1) | W(1) N(1) O(1) 169.5(3) | C(12) C(13) C(14) 108.6(3) |
| N(1) W(1) C(16) 92.3(1) | W(1) C(1) C(2) 123.0(2) | C(12) C(13) C(18) 126.7(5) |
| C(1) W(1) C(7) 130.1(1) | W(1) C(1) C(6) 121.4(2) | C(14) C(13) C(18) 124.3(5) |
| C(1) W(1) C(8) 94.7(1) | C(2) C(1) C(6) 115.5(3) | W(1) C(14) C(13) 71.8(2) |
| C(1) W(1) C(12) 133.1(1) | C(1) C(2) C(3) 122.5(3) | W(1) C(14) C(15) 71.5(2) |
| C(1) W(1) C(13) 129.6(1) | C(2) C(3) C(4) 120.3(4) | W(1) C(14) C(19) 128.1(3) |
| C(1) W(1) C(14) 95.8(1) | C(3) C(4) C(5) 119.3(4) | C(13) C(14) C(15) 107.1(3) |
| C(1) W(1) C(15) 78.5(1) | C(4) C(5) C(6) 120.4(4) | C(13) C(14) C(19) 123.8(5) |
| C(1) W(1) C(16) 98.2(1) | C(1) C(6) C(5) 121.9(4) | C(15) C(14) C(19) 128.7(5) |
| C(7) W(1) C(8) 36.4(2) | W(1) C(7) C(8) 77.3(2) | W(1) C(15) C(14) 74.7(2) |
| C(7) W(1) C(12) 95.5(1) | W(1) C(7) H(6) 110(3) | W(1) C(15) C(16) 69.4(2) |
| C(7) W(1) C(13) 81.8(1) | W(1) C(7) H(7) 120(3) | W(1) C(15) C(20) 129.5(3) |
| C(7) W(1) C(14) 103.8(2) | C(8) C(7) H(6) 113(2) | C(14) C(15) C(16) 109.0(3) |
| C(7) W(1) C(15) 136.5(1) | C(8) C(7) H(7) 116(3) | C(14) C(15) C(20) 125.7(5) |
| C(7) W(1) C(16) 131.1(1) | H(6) C(7) H(7) 115(4) | C(16) C(15) C(20) 124.6(5) |
| C(8) W(1) C(12) 127.0(1) | W(1) C(8) C(7) 66.3(2) | W(1) C(16) C(12) 72.2(2) |
| C(8) W(1) C(13) 100.5(1) | W(1) C(8) C(9) 92.0(2) | W(1) C(16) C(15) 75.9(2) |
| C(8) W(1) C(14) 103.6(1) | W(1) C(8) H(8) 106(3) | W(1) C(16) C(21) 121.7(2) |
| C(8) W(1) C(15) 133.4(1) | C(7) C(8) C(9) 124.8(4) | C(12) C(16) C(15) 107.7(3) |
| C(8) W(1) C(16) 158.1(1) | C(7) C(8) H(8) 117(3) | C(12) C(16) C(21) 126.9(5) |
| C(12) W(1) C(13) 34.8(2) | C(9) C(8) H(8) 118(3) | C(15) C(16) C(21) 125.2(5) |
| C(12) W(1) C(14) 57.8(1) | W(1) C(12) C(13) 76.1(2) | |
| C(12) W(1) C(15) 57.8(1) | W(1) C(12) C(16) 72.2(2) | |
| C(12) W(1) C(16) 35.6(1) | W(1) C(12) C(17) 121.1(3) | |

**Table A5** Bond Distances (Å) in the Solid-State Molecular Structure Determined for **2.2**

| | | |
|---|---|---|
| W(1) N(1) 1.760(5) | Si(1) C(17) 1.877(9) | C(3) C(8) 1.50(1) |
| W(1) C(1) 2.460(6) | Si(1) C(18) 1.885(9) | C(4) C(5) 1.427(9) |
| W(1) C(2) 2.355(6) | Si(1) C(19) 1.857(9) | C(4) C(9) 1.51(1) |
| W(1) C(3) 2.324(6) | O(1) N(1) 1.237(7) | C(5) C(10) 1.51(1) |
| W(1) C(4) 2.354(7) | C(1) C(2) 1.430(9) | C(11) C(12) 1.46(1) |
| W(1) C(5) 2.458(6) | C(1) C(5) 1.396(9) | C(11) H(11B) 0.98(7) |
| W(1) C(11) 2.182(6) | C(1) C(6) 1.50(1) | C(11) H(11A) 1.03(7) |
| W(1) C(12) 2.433(6) | C(2) C(3) 1.41(1) | C(12) C(13) 1.348(9) |
| W(1) C(16) 2.217(6) | C(2) C(7) 1.49(1) | C(13) C(14) 1.49(1) |
| Si(1) C(16) 1.858(7) | C(3) C(4) 1.40(1) | C(13) C(15) 1.49(1) |

**Table A6** Bond Angles (°) in the Solid-State Molecular Structure Determined for **2.2**

| | | |
|---|---|---|
| N(1) W(1) C(1) 141.3(2) | C(5) W(1) C(11) 85.4(2) | C(4) C(3) C(8) 124.9(9) |
| N(1) W(1) C(2) 107.0(3) | C(5) W(1) C(12) 110.3(2) | W(1) C(4) C(3) 71.4(4) |
| N(1) W(1) C(3) 88.4(2) | C(5) W(1) C(16) 115.2(2) | W(1) C(4) C(5) 76.8(4) |
| N(1) W(1) C(4) 106.1(3) | C(11) W(1) C(12) 36.4(2) | W(1) C(4) C(9) 125.6(5) |
| N(1) W(1) C(5) 140.4(2) | C(11) W(1) C(16) 129.2(2) | C(3) C(4) C(5) 107.8(6) |
| N(1) W(1) C(11) 92.1(3) | C(12) W(1) C(16) 93.7(2) | C(3) C(4) C(9) 126.8(8) |
| N(1) W(1) C(12) 89.0(2) | C(16) Si(1) C(17) 108.9(3) | C(5) C(4) C(9) 124.6(8) |
| N(1) W(1) C(16) 96.7(2) | C(16) Si(1) C(18) 109.7(4) | W(1) C(5) C(1) 73.6(4) |
| C(1) W(1) C(2) 34.5(2) | C(16) Si(1) C(19) 115.7(3) | W(1) C(5) C(4) 68.8(4) |
| C(1) W(1) C(3) 57.2(2) | C(17) Si(1) C(18) 108.2(5) | W(1) C(5) C(10) 130.2(5) |
| C(1) W(1) C(4) 56.7(2) | C(17) Si(1) C(19) 106.6(3) | C(1) C(5) C(4) 108.3(6) |
| C(1) W(1) C(5) 33.0(2) | C(18) Si(1) C(19) 107.4(4) | C(1) C(5) C(10) 125.7(7) |
| C(1) W(1) C(11) 116.2(2) | W(1) N(1) O(1) 170.7(5) | W(1) C(11) C(12) 81.2(4) |
| C(1) W(1) C(12) 129.5(2) | W(1) C(1) C(2) 68.7(3) | W(1) C(11) H(11B) 112(4) |
| C(1) W(1) C(16) 85.6(2) | W(1) C(1) C(5) 73.4(3) | W(1) C(11) H(11A) 118(4) |
| C(2) W(1) C(3) 35.1(3) | W(1) C(1) C(6) 126.3(5) | C(12) C(11) H(11B) 114(4) |
| C(2) W(1) C(4) 57.9(2) | C(2) C(1) C(5) 107.8(6) | C(12) C(11) H(11A) 120(4) |
| C(2) W(1) C(5) 56.6(2) | C(2) C(1) C(6) 124.3(7) | H(11B) C(11) H(11A) 109(6) |
| C(2) W(1) C(11) 138.9(2) | C(5) C(1) C(6) 127.8(7) | W(1) C(12) C(11) 62.4(3) |
| C(2) W(1) C(12) 164.0(2) | W(1) C(2) C(1) 76.8(4) | W(1) C(12) C(13) 94.6(4) |
| C(2) W(1) C(16) 85.2(2) | W(1) C(2) C(3) 71.2(4) | W(1) C(12) H(12) 101(4) |
| C(3) W(1) C(4) 34.9(3) | W(1) C(2) C(7) 126.7(5) | C(11) C(12) C(13) 124.9(7) |
| C(3) W(1) C(5) 57.1(2) | C(1) C(2) C(3) 107.8(6) | C(11) C(12) H(12) 116(4) |
| C(3) W(1) C(11) 113.0(3) | C(1) C(2) C(7) 125.2(8) | C(13) C(12) H(12) 117(4) |
| C(3) W(1) C(12) 149.1(3) | C(3) C(2) C(7) 126.0(8) | C(12) C(13) C(14) 125.6(7) |
| C(3) W(1) C(16) 117.2(3) | W(1) C(3) C(2) 73.7(4) | C(12) C(13) C(15) 120.1(7) |
| C(4) W(1) C(5) 34.4(2) | W(1) C(3) C(4) 73.7(4) | C(14) C(13) C(15) 113.5(7) |
| C(4) W(1) C(11) 82.1(3) | W(1) C(3) C(8) 121.6(5) | W(1) C(16) Si(1) 118.3(3) |
| C(4) W(1) C(12) 117.8(3) | C(2) C(3) C(4) 108.3(6) | |
| C(4) W(1) C(16) 140.7(3) | C(2) C(3) C(8) 126.6(9) | |

**Table A7** Bond Distances (Å) in the Solid-State Molecular Structure Determined for **2.3**

| | | |
|---|---|---|
| W(1) N(1) 1.753(4) | C(2) C(3) 1.413(7) | C(14) C(15) 1.399(8) |
| W(1) C(1) 2.438(4) | C(2) C(7) 1.498(6) | C(14) C(18) 1.520(8) |
| W(1) C(2) 2.390(4) | C(3) C(4) 1.427(6) | C(15) C(16) 1.375(8) |
| W(1) C(3) 2.323(4) | C(3) C(8) 1.501(7) | C(16) C(17) 1.394(7) |
| W(1) C(4) 2.324(5) | C(4) C(5) 1.441(6) | C(16) C(19) 1.508(8) |
| W(1) C(5) 2.419(4) | C(4) C(9) 1.502(7) | C(20) C(21) 1.454(8) |
| W(1) C(11) 2.239(4) | C(5) C(10) 1.501(6) | C(20) H(27) 0.95(6) |
| W(1) C(20) 2.187(5) | C(11) C(12) 1.493(6) | C(20) H(28) 0.94(7) |
| W(1) C(21) 2.391(5) | C(11) H(16) 0.92(6) | C(21) C(22) 1.365(6) |
| O(1) N(1) 1.240(5) | C(11) H(17) 0.96(5) | C(21) H(29) 1.02(5) |
| C(1) C(2) 1.439(6) | C(12) C(13) 1.392(7) | C(22) C(23) 1.491(7) |
| C(1) C(5) 1.414(6) | C(12) C(17) 1.402(7) | C(22) C(24) 1.502(7) |
| C(1) C(6) 1.497(7) | C(13) C(14) 1.393(7) | |

**Table A8** Bond Angles (°) in the Solid-State Molecular Structure Determined for **2.3**

| | | |
|---|---|---|
| N(1) W(1) C(1) 149.4(2) | C(11) W(1) C(21) 89.7(2) | W(1) C(11) H(16) 111(3) |
| N(1) W(1) C(2) 116.1(2) | C(20) W(1) C(21) 36.7(2) | H(16) C(11) H(17) 100(4) |
| N(1) W(1) C(3) 92.3(2) | W(1) N(1) O(1) 171.1(4) | C(11) C(12) C(13) 121.5(4) |
| N(1) W(1) C(4) 102.8(2) | W(1) C(1) C(2) 70.9(2) | C(11) C(12) C(17) 120.9(4) |
| N(1) W(1) C(5) 137.4(2) | W(1) C(1) C(5) 72.3(2) | C(13) C(12) C(17) 117.5(4) |
| N(1) W(1) C(11) 93.6(2) | W(1) C(1) C(6) 124.9(3) | C(12) C(13) C(14) 121.9(5) |
| N(1) W(1) C(20) 94.3(2) | C(2) C(1) C(5) 107.7(4) | C(13) C(14) C(15) 118.7(5) |
| N(1) W(1) C(21) 108.4(2) | C(2) C(1) C(6) 127.3(4) | C(13) C(14) C(18) 120.1(5) |
| C(1) W(1) C(2) 34.7(1) | C(5) C(1) C(6) 124.9(4) | C(15) C(14) C(18) 121.3(5) |
| C(1) W(1) C(3) 58.0(2) | W(1) C(2) C(1) 74.5(2) | C(14) C(15) C(16) 121.1(5) |
| C(1) W(1) C(4) 58.1(2) | W(1) C(2) C(3) 70.0(2) | C(15) C(16) C(17) 119.2(5) |
| C(1) W(1) C(5) 33.9(2) | W(1) C(2) C(7) 128.6(3) | C(15) C(16) C(19) 120.3(5) |
| C(1) W(1) C(11) 109.6(2) | C(1) C(2) C(3) 108.2(4) | C(17) C(16) C(19) 120.5(5) |
| C(1) W(1) C(20) 88.4(2) | C(1) C(2) C(7) 125.3(4) | C(12) C(17) C(16) 121.7(5) |
| C(1) W(1) C(21) 91.7(2) | C(3) C(2) C(7) 125.8(4) | W(1) C(20) C(21) 79.3(3) |
| C(2) W(1) C(3) 34.9(2) | W(1) C(3) C(2) 75.2(3) | W(1) C(20) H(27) 114(4) |
| C(2) W(1) C(4) 58.5(2) | W(1) C(3) C(4) 72.2(3) | W(1) C(20) H(28) 124(5) |
| C(2) W(1) C(5) 57.2(1) | W(1) C(3) C(8) 123.6(3) | C(21) C(20) H(27) 110(4) |
| C(2) W(1) C(11) 141.2(2) | C(2) C(3) C(4) 108.5(4) | C(21) C(20) H(28) 113(4) |
| C(2) W(1) C(20) 79.4(2) | C(2) C(3) C(8) 126.6(4) | H(27) C(20) H(28) 112(5) |
| C(2) W(1) C(21) 102.7(2) | C(4) C(3) C(8) 124.6(5) | W(1) C(21) C(20) 64.0(3) |
| C(3) W(1) C(4) 35.8(2) | W(1) C(4) C(3) 72.1(3) | W(1) C(21) C(22) 100.5(3) |
| C(3) W(1) C(5) 58.3(2) | W(1) C(4) C(5) 75.9(3) | W(1) C(21) H(29) 105(3) |
| C(3) W(1) C(11) 127.5(2) | W(1) C(4) C(9) 128.2(3) | C(20) C(21) C(22) 125.5(5) |
| C(3) W(1) C(20) 106.5(2) | C(3) C(4) C(5) 107.3(4) | C(20) C(21) H(29) 118(3) |
| C(3) W(1) C(21) 136.7(2) | C(3) C(4) C(9) 124.3(4) | C(22) C(21) H(29) 116(3) |
| C(4) W(1) C(5) 35.3(2) | C(5) C(4) C(9) 126.9(4) | C(21) C(22) C(23) 120.8(5) |
| C(4) W(1) C(11) 92.4(2) | W(1) C(5) C(1) 73.8(3) | C(21) C(22) C(24) 123.5(4) |
| C(4) W(1) C(20) 137.9(2) | W(1) C(5) C(4) 68.8(2) | C(23) C(22) C(24) 115.2(4) |
| C(4) W(1) C(21) 148.5(2) | W(1) C(5) C(10) 128.4(3) | W(1) C(11) H(17) 102(3) |
| C(5) W(1) C(11) 84.0(2) | C(1) C(5) C(4) 108.3(4) | C(12) C(11) H(16) 111(3) |
| C(5) W(1) C(20) 121.7(2) | C(1) C(5) C(10) 124.6(4) | C(12) C(11) H(17) 109(3) |
| C(5) W(1) C(21) 114.0(2) | C(4) C(5) C(10) 126.8(4) | |
| C(11) W(1) C(20) 125.0(2) | W(1) C(11) C(12) 120.5(3) | |

**Table A9** Bond Distances (Å) in the Solid-State Molecular Structure Determined for **2.5**

| | | |
|---|---|---|
| W1 N1 1.762(5) | C1 C6 1.504(9) | C12 H12 0.978(10) |
| W1 C16 2.205(6) | C2 C3 1.431(9) | C13 C15 1.499(9) |
| W1 C11 2.235(6) | C2 C7 1.496(9) | C13 C14 1.509(9) |
| W1 C3 2.320(6) | C3 C4 1.423(9) | C16 C17 1.411(9) |
| W1 C2 2.346(7) | C3 C8 1.502(9) | C16 C21 1.422(9) |
| W1 C12 2.363(6) | C4 C5 1.439(9) | C17 C18 1.406(9) |
| W1 C4 2.376(6) | C4 C9 1.497(9) | C17 C22 1.509(9) |
| W1 C1 2.435(6) | C5 C10 1.485(8) | C18 C19 1.381(9) |
| W1 C5 2.456(6) | C11 C12 1.438(9) | C19 C20 1.372(9) |
| O1 N1 1.232(7) | C11 H11A 0.979(7) | C20 C21 1.401(8) |
| C1 C5 1.415(9) | C11 H11B 0.980(8) | C20 C23 1.524(9) |
| C1 C2 1.446(9) | C12 C13 1.371(9) | |

**Table A10** Bond Angles (°) in the Solid-State Molecular Structure Determined for **2.5**

| | | |
|---|---|---|
| N1 W1 C16 98.3(2) | C2 W1 C5 57.8(2) | C1 C5 W1 72.4(3) |
| N1 W1 C11 89.1(2) | C12 W1 C5 109.0(2) | C4 C5 W1 69.7(3) |
| C16 W1 C11 130.9(2) | C4 W1 C5 34.6(2) | C10 C5 W1 131.1(4) |
| N1 W1 C3 88.6(2) | C1 W1 C5 33.6(2) | C12 C11 W1 76.7(4) |
| C16 W1 C3 110.6(2) | O1 N1 W1 168.6(5) | C12 C11 H11A 122(4) |
| C11 W1 C3 118.1(2) | C5 C1 C2 108.4(6) | W1 C11 H11A 116(5) |
| N1 W1 C2 100.5(2) | C5 C1 C6 125.1(6) | C12 C11 H11B 110(5) |
| C16 W1 C2 139.9(2) | C2 C1 C6 126.3(6) | W1 C11 H11B 112(5) |
| C11 W1 C2 84.5(2) | C5 C1 W1 74.0(4) | H11A C11 H11B 114(6) |
| C3 W1 C2 35.7(2) | C2 C1 W1 69.1(3) | C13 C12 C11 124.5(6) |
| N1 W1 C12 104.3(2) | C6 C1 W1 127.0(4) | C13 C12 W1 92.2(4) |
| C16 W1 C12 95.6(2) | C3 C2 C1 107.0(6) | C11 C12 W1 67.0(3) |
| C11 W1 C12 36.3(2) | C3 C2 C7 125.4(6) | C13 C12 H12 118(4) |
| C3 W1 C12 149.0(2) | C1 C2 C7 127.4(6) | C11 C12 H12 117(4) |
| C2 W1 C12 113.3(2) | C3 C2 W1 71.1(3) | W1 C12 H12 106(4) |
| N1 W1 C4 112.4(2) | C1 C2 W1 75.8(4) | C12 C13 C15 119.8(6) |
| C16 W1 C4 81.3(2) | C7 C2 W1 123.0(4) | C12 C13 C14 124.6(6) |
| C11 W1 C4 139.6(2) | C4 C3 C2 108.7(6) | C15 C13 C14 113.8(6) |
| C3 W1 C4 35.3(2) | C4 C3 C8 126.6(6) | C17 C16 C21 116.1(6) |
| C2 W1 C4 58.8(2) | C2 C3 C8 124.5(6) | C17 C16 W1 126.3(4) |
| C12 W1 C4 143.2(2) | C4 C3 W1 74.5(3) | C21 C16 W1 117.3(4) |
| N1 W1 C1 135.4(2) | C2 C3 W1 73.2(3) | C18 C17 C16 119.8(6) |
| C16 W1 C1 119.8(2) | C8 C3 W1 122.1(4) | C18 C17 C22 117.5(6) |
| C11 W1 C1 83.0(2) | C3 C4 C5 107.7(6) | C16 C17 C22 122.7(6) |
| C3 W1 C1 58.2(2) | C3 C4 C9 125.9(6) | C19 C18 C17 122.1(6) |
| C2 W1 C1 35.2(2) | C5 C4 C9 125.9(6) | C20 C19 C18 120.0(6) |
| C12 W1 C1 94.8(2) | C3 C4 W1 70.2(3) | C19 C20 C21 118.7(6) |
| C4 W1 C1 57.4(2) | C5 C4 W1 75.8(3) | C19 C20 C23 121.9(6) |
| N1 W1 C5 145.4(2) | C9 C4 W1 126.1(4) | C21 C20 C23 119.4(6) |
| C16 W1 C5 87.6(2) | C1 C5 C4 108.1(5) | C20 C21 C16 123.3(6) |
| C11 W1 C5 112.6(2) | C1 C5 C10 125.4(6) | |
| C3 W1 C5 57.8(2) | C4 C5 C10 125.8(6) | |

**Table A11** Bond Distances (Å) in the Solid-State Molecular Structure Determined for **3.2**

| | | |
|---|---|---|
| W1 N1 1.761(4) | C1 C7 1.492(7) | C12 H1 0.88(5) |
| W1 C21 2.219(5) | C2 C3 1.427(7) | C13 C14 1.495(7) |
| W1 C11 2.236(5) | C2 C8 1.506(7) | C13 C15 1.503(7) |
| W1 C2 2.313(5) | C3 C4 1.423(6) | C16 C17 1.376(7) |
| W1 C1 2.319(5) | C3 C9 1.507(6) | C16 C21 1.438(7) |
| W1 C16 2.403(5) | C4 C5 1.429(7) | C16 C20 1.508(7) |
| W1 C3 2.405(4) | C4 C10 1.509(7) | C17 C18 1.500(7) |
| W1 C5 2.420(5) | C5 C6 1.496(7) | C17 C19 1.504(8) |
| W1 C4 2.468(5) | C11 C12 1.500(6) | C21 H4 0.96(6) |
| O1 N1 1.220(5) | C11 H2 1.05(6) | C21 H5 1.04(7) |
| C1 C5 1.419(7) | C11 H3 0.92(6) | |
| C1 C2 1.423(7) | C12 C13 1.342(7) | |

**Table A12** Bond Angles (°) in the Solid-State Molecular Structure Determined for **3.2**

| | | |
|---|---|---|
| N1 W1 C21 92.7(2) | C1 W1 C4 57.40(17) | C1 C5 W1 68.7(3) |
| N1 W1 C11 89.7(2) | C16 W1 C4 118.11(16) | C4 C5 W1 74.9(3) |
| C21 W1 C11 129.54(19) | C3 W1 C4 33.93(15) | C6 C5 W1 128.3(3) |
| N1 W1 C2 94.45(18) | C5 W1 C4 33.98(16) | C12 C11 W1 113.3(3) |
| C21 W1 C2 135.0(2) | O1 N1 W1 170.9(4) | C12 C11 H2 105(3) |
| C11 W1 C2 94.88(18) | C5 C1 C2 108.5(4) | W1 C11 H2 103(3) |
| N1 W1 C1 90.61(19) | C5 C1 C7 126.0(5) | C12 C11 H3 112(4) |
| C21 W1 C1 99.89(19) | C2 C1 C7 125.3(5) | W1 C11 H3 115(4) |
| C11 W1 C1 130.49(18) | C5 C1 W1 76.5(3) | H2 C11 H3 108(5) |
| C2 W1 C1 35.79(17) | C2 C1 W1 71.9(3) | C13 C12 C11 130.3(5) |
| N1 W1 C16 86.86(18) | C7 C1 W1 121.0(4) | C13 C12 H1 116(3) |
| C21 W1 C16 35.98(19) | C1 C2 C3 107.5(4) | C11 C12 H1 114(3) |
| C11 W1 C16 94.05(18) | C1 C2 C8 125.0(5) | C12 C13 C14 121.4(5) |
| C2 W1 C16 170.99(18) | C3 C2 C8 126.5(5) | C12 C13 C15 124.1(4) |
| C1 W1 C16 135.40(18) | C1 C2 W1 72.3(3) | C14 C13 C15 114.4(4) |
| N1 W1 C3 127.35(18) | C3 C2 W1 75.9(3) | C17 C16 C21 119.9(5) |
| C21 W1 C3 130.7(2) | C8 C2 W1 126.5(4) | C17 C16 C20 121.2(5) |
| C11 W1 C3 83.32(18) | C4 C3 C2 108.3(4) | C21 C16 C20 118.8(5) |
| C2 W1 C3 35.14(16) | C4 C3 C9 124.1(4) | C17 C16 W1 86.5(3) |
| C1 W1 C3 58.20(17) | C2 C3 C9 126.9(5) | C21 C16 W1 65.0(3) |
| C16 W1 C3 145.54(17) | C4 C3 W1 75.5(3) | C20 C16 W1 115.1(3) |
| N1 W1 C5 119.59(19) | C2 C3 W1 68.9(3) | C16 C17 C18 124.3(5) |
| C21 W1 C5 79.73(19) | C9 C3 W1 128.8(4) | C16 C17 C19 121.7(5) |
| C11 W1 C5 139.49(18) | C3 C4 C5 107.7(4) | C18 C17 C19 111.1(5) |
| C2 W1 C5 58.29(18) | C3 C4 C10 124.8(4) | C16 C21 W1 79.0(3) |
| C1 W1 C5 34.77(17) | C5 C4 C10 126.6(5) | C16 C21 H4 125(4) |
| C16 W1 C5 113.43(17) | C3 C4 W1 70.6(3) | W1 C21 H4 109(3) |
| C3 W1 C5 57.03(17) | C5 C4 W1 71.2(3) | C16 C21 H5 113(4) |
| N1 W1 C4 147.72(18) | C10 C4 W1 131.8(4) | W1 C21 H5 112(3) |
| C21 W1 C4 96.78(19) | C1 C5 C4 107.9(4) | H4 C21 H5 113(5) |
| C11 W1 C4 107.19(18) | C1 C5 C6 124.5(5) | |
| C2 W1 C4 57.68(17) | C4 C5 C6 127.1(5) | |

**Table A13** Bond Distances (Å) in the Solid-State Molecular Structure Determined for **3.3**

| | | |
|---|---|---|
| W1 N1 1.795(4) | P1 C16 1.826(5) | C11 C12 1.437(7) |
| W1 C12 2.149(5) | P1 C17 1.826(5) | C11 H1 0.91(5) |
| W1 C11 2.205(4) | C6 C1 1.509(6) | C11 H2 1.12(6) |
| W1 C4 2.339(5) | C10 C5 1.505(6) | C13 C12 1.324(7) |
| W1 C3 2.356(5) | C9 C4 1.496(7) | C7 C2 1.495(6) |
| W1 C5 2.365(5) | C5 C1 1.419(6) | C2 C1 1.412(6) |
| W1 C2 2.405(4) | C5 C4 1.429(7) | C2 C3 1.442(6) |
| W1 C1 2.416(4) | C14 C13 1.517(7) | C4 C3 1.438(7) |
| W1 P1 2.4660(12) | C15 C13 1.502(7) | C8 C3 1.501(6) |
| P1 C18 1.826(5) | N1 O1 1.224(5) | |

**Table A14** Bond Angles (°) in the Solid-State Molecular Structure Determined for **3.3**

| | | |
|---|---|---|
| N1 W1 C12 108.62(18) | C12 W1 P1 85.84(13) | C1 C2 C3 108.3(4) |
| N1 W1 C11 90.99(18) | C11 W1 P1 117.14(14) | C1 C2 C7 125.6(4) |
| C12 W1 C11 38.50(18) | C4 W1 P1 127.27(12) | C3 C2 C7 125.7(4) |
| N1 W1 C4 95.98(17) | C3 W1 P1 96.04(12) | C1 C2 W1 73.4(3) |
| C12 W1 C4 142.06(17) | C5 W1 P1 152.70(12) | C3 C2 W1 70.5(3) |
| C11 W1 C4 115.53(18) | C2 W1 P1 95.94(11) | C7 C2 W1 127.8(3) |
| N1 W1 C3 110.16(16) | C1 W1 P1 124.97(12) | C5 C4 C3 107.9(4) |
| C12 W1 C3 140.97(17) | C18 P1 C16 101.5(3) | C5 C4 C9 126.2(5) |
| C11 W1 C3 143.42(18) | C18 P1 C17 99.5(3) | C3 C4 C9 125.7(4) |
| C4 W1 C3 35.68(16) | C16 P1 C17 102.9(3) | C5 C4 W1 73.3(3) |
| N1 W1 C5 116.03(17) | C18 P1 W1 110.4(2) | C3 C4 W1 72.8(3) |
| C12 W1 C5 106.73(17) | C16 P1 W1 113.90(17) | C9 C4 W1 123.1(4) |
| C11 W1 C5 85.31(18) | C17 P1 W1 125.32(18) | C13 C12 C11 134.0(5) |
| C4 W1 C5 35.37(16) | C1 C5 C4 108.1(4) | C13 C12 W1 149.2(4) |
| C3 W1 C5 58.84(16) | C1 C5 C10 126.1(4) | C11 C12 W1 72.9(3) |
| N1 W1 C2 145.14(16) | C4 C5 C10 125.0(5) | C2 C1 C5 108.7(4) |
| C12 W1 C2 105.72(16) | C1 C5 W1 74.7(3) | C2 C1 C6 125.1(4) |
| C11 W1 C2 120.35(17) | C4 C5 W1 71.3(3) | C5 C1 C6 126.1(4) |
| C4 W1 C2 58.42(16) | C10 C5 W1 127.9(3) | C2 C1 W1 72.5(3) |
| C3 W1 C2 35.25(15) | O1 N1 W1 175.0(4) | C5 C1 W1 70.8(3) |
| C5 W1 C2 57.67(16) | C12 C11 W1 68.6(3) | C6 C1 W1 125.4(3) |
| N1 W1 C1 150.43(17) | C12 C11 H1 122(3) | C4 C3 C2 107.0(4) |
| C12 W1 C1 89.19(16) | W1 C11 H1 120(3) | C4 C3 C8 125.7(4) |
| C11 W1 C1 88.84(17) | C12 C11 H2 120(3) | C2 C3 C8 126.7(4) |
| C4 W1 C1 57.98(16) | W1 C11 H2 112(3) | C4 C3 W1 71.5(3) |
| C3 W1 C1 57.96(15) | H1 C11 H2 109(4) | C2 C3 W1 74.2(2) |
| C5 W1 C1 34.52(16) | C12 C13 C15 124.3(5) | C8 C3 W1 126.4(3) |
| C2 W1 C1 34.05(15) | C12 C13 C14 121.8(5) | |
| N1 W1 P1 80.87(13) | C15 C13 C14 113.9(5) | |

# APPENDIX B

## Kinetic Data and Statistical Analysis Consulting Report

**Table A15 Kinetic Data: Integral of Npt $CMe_3$ signal vs internal standard signal of $^1H$ NMR spectrum ($C_6D_6$) showing decomposition of 1.1**

| Time (s) | Integral | Ln (I(t)/I(0)) |
|---|---|---|
| 0 | 1.257862 | 0 |
| 312 | 1.176471 | -0.06689 |
| 612 | 1.111111 | -0.12405 |
| 912 | 1.010101 | -0.21936 |
| 1212 | 0.943396 | -0.28768 |
| 1512 | 0.884956 | -0.35163 |
| 1812 | 0.813008 | -0.43643 |
| 2112 | 0.775194 | -0.48406 |
| 2412 | 0.714286 | -0.56589 |
| 3012 | 0.628931 | -0.69315 |
| 3612 | 0.534759 | -0.85535 |
| 4212 | 0.480769 | -0.96178 |
| 4812 | 0.421941 | -1.0923 |
| 5412 | 0.363636 | -1.24101 |
| 6012 | 0.314465 | -1.38629 |
| 7212 | 0.245098 | -1.63551 |
| 8412 | 0.194932 | -1.86452 |
| 9612 | 0.151057 | -2.11951 |
| 10812 | 0.112233 | -2.41659 |
| 12012 | 0.088183 | -2.65775 |
| 13212 | 0.069204 | -2.90011 |
| 15012 | 0.049652 | -3.23212 |

**Significance Testing of Carbon-Hydrogen Bond in an Organometallic Complex**

**Natalie Thompson**

**STAT 551 PROJECT, 2002**

## 1 Introduction

The following describes a method to determine the hydrogen loss in an organometallic complex; and it describes how to determine the relative proportion of times the loss comes from the central allyl instead of from the allyl Me's.

The dimethylallyl ligand (allyl) is combined with benzene ($C_6H_6$) as the control group. And then the dimethylallyl ligand is combined with deuterated benzene ($C_6D_6$). Deuterium (D) is essentially the same as hydrogen (H) but it is not detected by NMR Spectroscopy. As such, the benzene and d-benzene (deuterated benzene) will undergo the same reactions with the allyl, but when $C_6D_6$ combines with the allyl instead of a $C_6H_6$ hydrogen the 6 D molecules will be undetected.

The benzene or deuterated benzene bond to either the central allyl or the allyl Me by dropping one of their hydrogen or deuterium molecules, respectively. This loss will herein be referred to as the hydrogen loss. The presence of a single hydrogen loss would indicate a particular molecular structure as the outcome of the reaction with benzene. The total loss of greater than one hydrogen atom would imply a more complicated outcome.

There were five repetitions of each of the two reactions. The hydrogen mass was recorded at four locations of the molecular structure. These are labeled central allyl H, term allyl H, allyl Me 1, and allyl Me 2. Both allyl Me's are structurally indiscernible from each and are thus combined as one outcome. And the term allyl H is used to calibrate the NMR Spectroscopy (NMRS).

In the control group, the number of hydrogen molecules is known. The deuterium group will reveal where and how many hydrogen molecules originated from the benzene. The questions addressed in this paper are the following:

- How to test the hypothesis that only one hydrogen is replaced by benzene in the reaction.
- How to determine the relative frequency of times the hydrogen loss occurs at the central allyl instead of from one of the two allyl Me's.

**2 Analysis**

The number of hydrogen atoms is known for the control group. As such, due to the relative error in the NMRS rescale the results for the five repetitions so that the average of the trials is equal to the known expected hydrogen mass.

For the central allyl obtain the average before scaling. Since the expected mass for this group is one, this average is the also the scale for this group. Divide the mass for each

trial for the central allyl by this scale. The average of the scaled masses will be 1. Use this scale for the deuterium trials for the central allyl group. Obtain the average for this group.

For the Me1 group the known expected mass is 3. Obtain the average of the masses for the trial for the un-scaled readings. Divide the average mass by 3 to obtain the scale factor. Then divide the mass for each trial for the Me Group by this scale factor. The average of the scaled masses will be 3. Apply this scale factor to each of the trials for Me 1 for the deuterium trials as well.

Follow the same scaling procedure for Me 2 as was carried out for Me 1, in the last paragraph.

Sum the central, Me 1 and Me 2 mass for each of the ten trials, label them $x_{1c}$ to $x_{5c}$ for the control group and $x_{1d}$ to $x_{5d}$ for the deuterium group. Compare the means of the two groups with a paired t-test using the following estimates for the expected values and the standard deviations.

$\mu_c = [\Sigma^5_{i=1} (x_{ic})] \div 5$

$\mu_d = [\Sigma^5_{i=1} (x_{id})] \div 5$

$\sigma_c = [\ \Sigma^5_{i=1} (x_{ic} - \mu_c)^2 \div 4\ ]^{1/2}$

$\sigma_d = [\ \Sigma^5_{i=1} (x_{id} - \mu_d)^2 \div 4\ ]^{1/2}$

The standard deviation for the difference of the means $\delta = \mu_c - \mu_d$ is:

$\sigma = [\sigma_c^2 + \sigma_d^2]^{1/2}$.

A confidence interval for the overall hydrogen loss is:

$\delta \pm t_{4,\alpha/2} * \sigma$.

Under the assumption that only one hydrogen molecule is lost, the following describes a method to determine the relative frequency of hydrogen molecules lost from the central allyl instead of from either the Me 1 or Me 2 locations.

Take the average of the scaled masses for the central allyl for the control group and the deuterium group. Label these, $\Pi_c$ and $\Pi_d$ respectively. Let the difference of the two be

$\varpi = \Pi_c - \Pi_d$ .

This is the proportion of times the hydrogen is lost from the central allyl. In order to obtain a confidence interval for this proportion, use the following as an estimate for standard deviation:

$\tau = [\tau_c^2 + \tau_d^2]^{1/2}$, where $\tau_c$ and $\tau_d$ are the standard deviations for $\Pi_c$ and $\Pi_d$ respectively. $\tau_c$ and $\tau_d$ are obtained using a similar equation used to calculate $\sigma_c$, replacing the $x_{ic}$ with the individual masses for each trial at the central allyl, and using the appropriate mean.

A confidence interval for the proportion of times the hydrogen loss occurs at the central allyl is:

$\varpi \pm t_{4,\alpha/2} * \tau$.

**3. Discussion**

It is easiest to calculate the standard deviation for the net hydrogen mass loss, δ, by first combining the masses for the central, Me 1 and Me 2 since it avoids the cumbersome and possibly impossible calculation of the correlation between the masses of different locations on the same molecule.

The proportion of times the hydrogen loss occurs at the central allyl can be obtained directly without rescaling since it was shown that only one hydrogen loss occurred in the reaction. If more or less hydrogen was lost, the loss from the central allyl would need to be divided by this amount, to get the proportion.

**Table A16 Deuterium incorporation $^1$H NMR integral data:**

**Control Cp*W(NO)($C_6H_5$)($\eta^3$-1,1-$Me_2C_3H_3$) (2.1)**

| Central allyl H | Allyl Me1 | Allyl Me2 | Terminal allyl H |
|---|---|---|---|
| 1.0700 | 3.0431 | 3.7851 | 1.0000 |
| 0.9922 | 2.9677 | 3.6561 | 1.0000 |
| 1.0539 | 2.9566 | 3.6249 | 1.0000 |
| 1.0201 | 2.9819 | 3.6763 | 1.0000 |
| 1.0049 | 2.9386 | 3.5610 | 1.0000 |

**Table A17 Deuterium incorporation $^1$H NMR integral data:**

**Experimental Cp*W(NO)($C_6D_5$)($\eta^3$-1,1-$Me_2$-allyl-$d_1$) (2.1-$d_6$)**

| Central allyl H | Allyl Me1 | Allyl Me2 | Terminal allyl H |
|---|---|---|---|
| 0.3600 | 2.6633 | 3.5217 | 1.0000 |
| 0.3679 | 2.6743 | 3.4541 | 1.0000 |
| 0.3508 | 2.5945 | 3.6116 | 1.0000 |
| 0.3581 | 2.6096 | 3.4118 | 1.0000 |
| 0.3589 | 2.6140 | 3.5607 | 1.0000 |